



SP-1193

ERS-1 SAR Sea Ice Catalogue

GEN43



SP-1193

March 1997

ERS-1 SAR Sea Ice Catalogue

**O.M. Johannessen, S. Sandven, Å. Drottning,
K. Kloster & T. Hamre**

Nansen Environmental & Remote Sensing Centre
Bergen, Norway

***European Space Agency
Agence spatiale européenne***

Title:

Serial Number:

ESA SP-1193

O.M. Johannessen, S. Sandven, Å. Drotning, K. Kloster & T. Hamre
Nansen Environmental and Remote Sensing Center
Bergen, Norway

Technical Coordinator:

Juerg Lichtenegger ESA, ESRIN

Published and distributed by:

ESA Publications Division, ESTEC, Noordwijk, The Netherlands

Printed in:

The Netherlands

Edited by:

W.R. Burke

Cover design by:

C. Haakman

International Standard Serial Number:

ISSN 0379 6566

International Standard Book Number:

ISBN 92-9092-371-7

Price: 50 Dutch Guilders

Copyright:

© 1997 European Space Agency

Summary

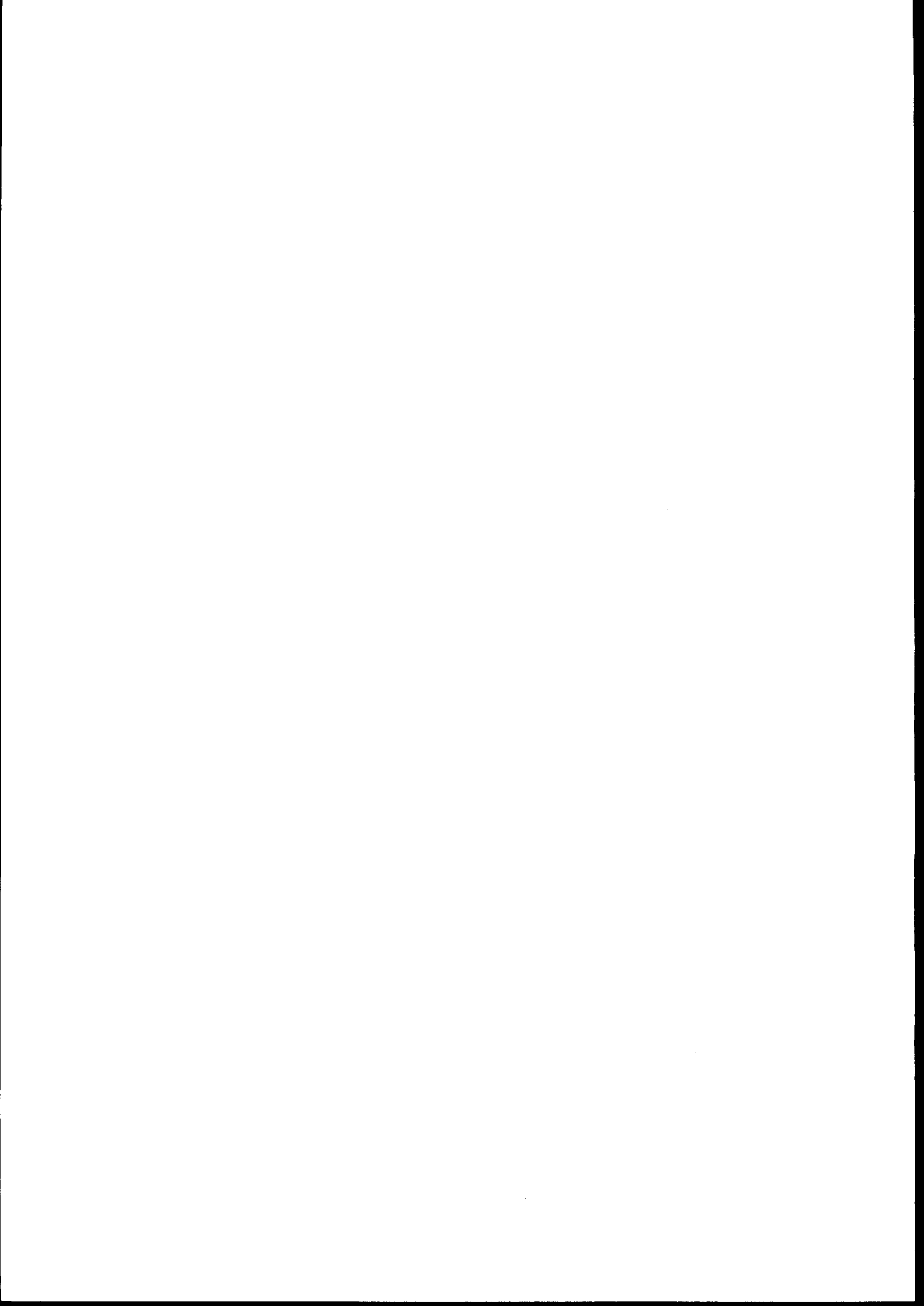
This catalogue contains a selection of ERS-1 synthetic aperture radar (SAR) images to illustrate various sea-ice conditions and phenomena and to demonstrate their characteristic SAR signatures.

Most of the images were obtained by the Tromsø Satellite Station and cover the European sector of the Arctic, from the eastern coast of Greenland to the Kara Sea; the other images are from the Baltic Sea, North America and Antarctica. The images are taken at various times of the year and during various weather conditions in order to demonstrate both long-term and short-term variability in ice characteristics.

The images include examples of the most important types of ice, such as multi-year ice, first-year ice, various stages of young ice, new ice, grease ice and ice bergs. Processes in the ice-edge region, such as wave penetration, eddies, ice-tongue and vortex pair formation and freezing — as well as compaction and relaxation of the ice edge due to wind variation — are also illustrated. The catalogue includes examples of phenomena observed near coasts, such as land-fast ice, shear zones and polynyas and processes that take place in the interior of pack-ice fields, such as leads, ice motion and break-up of floes.

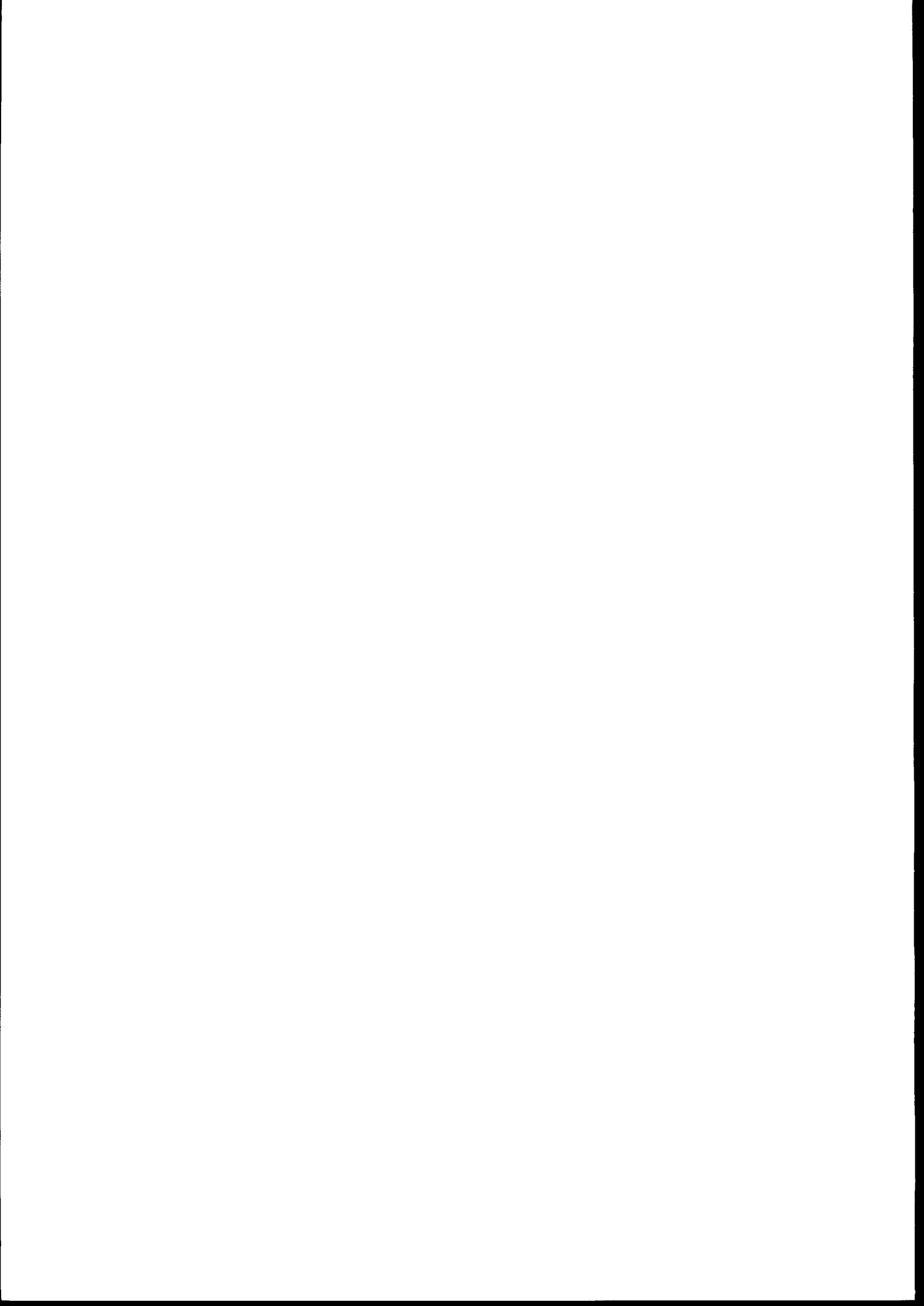
Products derived from SAR images, such as ice-classification maps, ice-concentration estimates and interpretations of ice kinematics are demonstrated, and applications of SAR imagery as an aid to ice navigation and other marine operations in the Arctic are described. Examples are given of products based on SAR images combined with SSM/I or AVHRR data.

The purpose of the catalogue is to promote the use of SAR imagery in sea-ice research and operational monitoring and to encourage its use both as an aid in the theoretical education of students and as a practical tool for the training of personnel responsible for sea-ice monitoring. It is also hoped that the catalogue will be useful to those engaged in environmental monitoring in the Arctic as well as to those planning and implementing offshore operations in ice-covered areas.



Contents

1. Introduction	1
2. ERS-1 Synthetic Aperture Radar (SAR)	5
3. East Greenland Coast	9
4. Greenland Sea	17
5. Barents Sea	29
6. Kara Sea	43
7. Baltic Sea	59
8. North America	63
9. Arctic, Scatterometer	75
10. Antarctica	77
Acknowledgements	82
References	83
Appendix: Ice Glossary	85



1. Introduction

This catalogue was produced by the Nansen Environmental and Remote Sensing Centre, supported by the European Space Agency and the Norwegian Space Centre.

The **European Space Agency (ESA)** is an international organisation whose task is 'to provide for and to promote, for exclusively peaceful purposes, cooperation among European States in space research and technology and their space applications'. ESA's contribution to the monitoring of the environment in the nineties is a series of Earth-observation satellites, of which ERS-1 was the first. ERS-2 followed in 1995 and Envisat is planned to be launched in 1999. Through its Prodex programme, ESA has contributed to the development of applications of data from the SAR sensor aboard ERS-1, for utilisation in coastal waters and in ice-infested regions of the European Arctic.

The **Norwegian Space Centre (NSC)** is an independent organisation, established by Ministry of Industry decree on 5 June 1989. NSC works in accordance with governmental guidelines, for the benefit of – and in cooperation with – industry, research institutes, official agencies and Norwegian interests in general. One of the priorities of NSC is Earth observation. Based on user requirements, NSC has supported a national programme for developing near-real-time marine applications of radar data from satellites. A national infrastructure has been developed for this purpose, in which the Tromsø Satellite Station plays an important role.

The **Nansen Environmental and Remote Sensing Centre (NERSC)** is an independent non-profit environmental and climate-research institute affiliated with the University of Bergen. NERSC plans and performs basic and applied research programmes and projects funded by governmental agencies, research councils and industry. Among the research topics are ice and ocean monitoring, climate modelling and the application of remote-sensing techniques in Earth observation. NERSC is responsible for the compilation and analysis of the SAR data in this catalogue.

The sea ice in the European sector of the Arctic has many important effects, climatologically, on human habitation, exploration and exploitation of marine resources, and sea transportation. The East Greenland coast is to a large extent inaccessible and unhabited owing to the sea ice, which is transported southwards by the ocean currents. The west coast of Svalbard, on the other hand, is practically ice-free throughout the year, owing to the warm West Spitzbergen Current (Johannessen 1986). The Barents and Kara Seas, which are large areas with considerable economic activities including sea transportation, have restricted access because of the seasonal ice cover.

The need for real-time sea-ice information in the Arctic is growing owing to increased activity in fisheries, offshore oil exploitation, ship traffic, research and monitoring of pollution and the environment in these regions. In the Barents Sea and the region around Svalbard, a rich marine life forms the base for extensive fisheries for several countries. Additionally, oil and gas exploitation is moving further north into the seasonal ice zone, and eastwards on the Siberian shelf. The sea-ice conditions impose severe restrictions on these activities. Regular access to high-quality, weather-independent satellite observations will improve the ice mapping and contribute to safer operations in the Arctic.

Ice mapping by satellites has been important in these regions for more than two decades. Visual and infrared observations from the AVHRR on the NOAA satellites have been used by meteorological institutes and ice centres, but the frequent cloud cover

inhibits regular and reliable ice maps based on these data. Therefore, ice mapping institutions have also used low-resolution, passive microwave data from Nimbus-7 SMMR and DMSP SSM/I, which are independent of cloud cover, in addition to the AVHRR data. SSM/I data provide daily ice extent and concentration maps of the whole Arctic and Antarctic at a resolution of about 30 km. An example of maximum and minimum ice extent in the Arctic is shown in Figure 1. Passive microwave data such as SSM/I have been obtained regularly for nearly 20 years, providing useful climatological ice data both regionally and globally. The main limitation of the SSM/I data is their coarse resolution. Ice features and ice processes with spatial scales of less than about 30 km cannot be mapped with the SSM/I data.

Synthetic Aperture Radar (SAR) imagery from satellites as well as aircraft combines high spatial resolution and independence of daylight and cloud cover. Consequently, the SAR has proved to be the most useful tool for regular and detailed mapping of sea ice on regional and local scales. The first series of SAR images from satellites was obtained by Seasat during a three-month period in 1978, some of which were from ice-covered areas. Airborne SAR images have also been obtained during many campaigns and in operational ice monitoring of the east coast of Canada. ERS-1 was the first radar satellite to provide a large number of SAR scenes of sea ice in various parts of the world. The ERS-1 SAR has operated successfully from its launch in July 1991 until 1996, while its successor ERS-2 was launched in 1995.

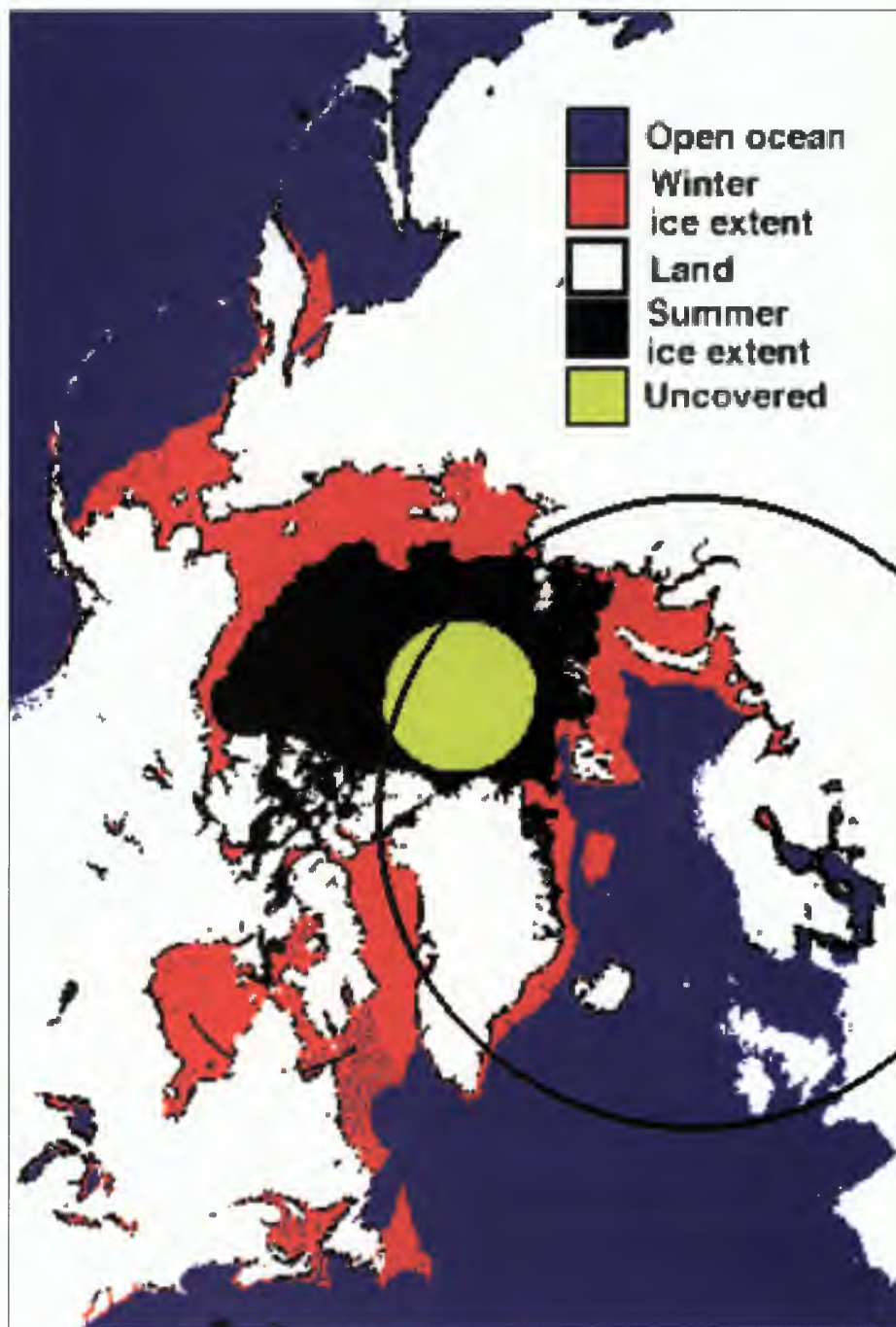


Figure 1. Maximum and minimum ice extent in the Arctic for a typical late winter and late summer situation. This map is based on passive microwave data from the Special Sensor Microwave Imager (SSM/I) of the Defence Meteorological Satellite Programme (DMSP). The black circle indicates the area covered by the SAR-antennae of Tromsø Satellite Station. SAR data from ERS-1 have been obtained from many sea ice areas of the Arctic Ocean. In this catalogue, examples of SAR ice images and analysed products from the European sector are presented.

The infrastructure for downlinking, processing and distributing SAR images in near-real-time from the European sector of the Arctic has been developed in Norway. The Tromsø Satellite Station currently has the fastest SAR processing and distribution system in Europe, and is capable of delivering SAR scenes to users in near-real-time (Johannessen et al. 1992; Johannessen et al., 1994; Sandven et al., 1994). This infrastructure has enabled the Nansen Environmental and Remote Sensing Centre to perform several pre-operational demonstrations where interpreted SAR scenes and other SAR products have been delivered to various types of Arctic operations including research expeditions. The area covered by Tromsø Satellite Station is shown in Figure 1.

The SAR images obtained from ERS-1 have been used by many researchers in the study of sea ice. These studies have provided new insight into many sea-ice processes and phenomena, examples of which are presented in this catalogue. Several SAR satellites are planned for operation in the next few years, and SAR images are expected to become one of the most important data sources in ice research as well as in ice monitoring and forecasting.

2. ERS-1 Synthetic Aperture Radar (SAR)

The SAR instrument is a side-looking imaging radar operating from moving platforms such as satellites, the Space Shuttle and aircraft. SAR images of the Earth's surface represent the spatial pattern of reflected microwave energy. A series of electromagnetic pulses is transmitted towards the Earth in a direction perpendicular to the platform track; these illuminate an elliptical footprint on the Earth's surface due to the directional properties of the antenna (Fig. 2). The strength of the signal which is returned from the surface depends upon the physical characteristics of that surface. The amount of reflected energy for a point target is given by the radar cross-section (RCS), defined as the projected area (πr^2) of a metal sphere with radius r ($r \gg \lambda$) which returns the same echo signal as the target. For a diffuse target, such as the ocean and ice, σ^0 is used. The latter is defined as the mean RCS divided by the illuminated projection area, and is expressed in dB. By quantifying the cross-sectional values, it is possible to relate the returned energy to the physical properties of the scene.

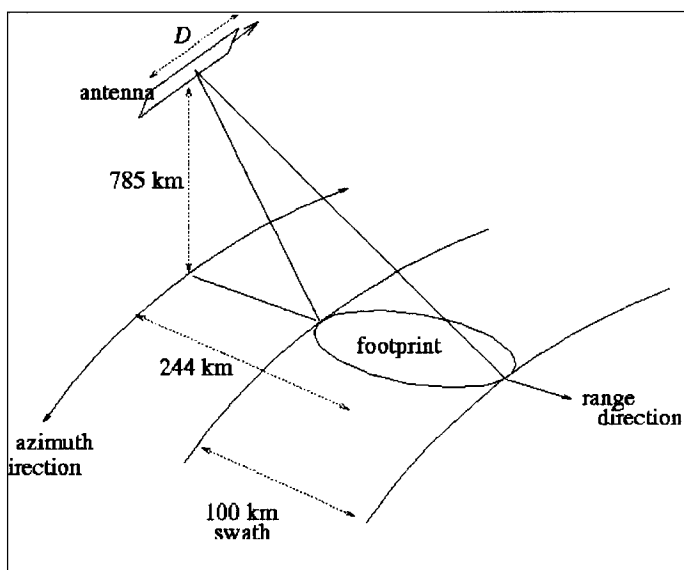


Figure 2. Illustration of the ERS-1 SAR coverage. D is the length of the SAR antenna (10 m).

In the high-resolution imaging mode, the ERS-1 SAR provides three-look, noise-reduced images with a spatial resolution of 26 m in range (across-track) and 30 m in azimuth (along-track). Image data are acquired for a maximum duration of approximately 12 minutes per orbit, and data are transmitted to ground receiving stations within line-of-sight.

The rectangular antenna of the SAR is aligned along the satellite's line of flight to direct a narrow beam sideways and downwards onto the Earth's surface (Fig. 2) to obtain strips of high-resolution imagery about 100 km in width (cross-track direction). The high-resolution range is achieved by the time delay of the returned signals. The high resolution is achieved by synthesizing a much larger antenna, taking into account also the phase of the received signal. Some characteristics of the ERS-1 SAR are listed in Table 1.

Table 1. Characteristics of the ERS-1 SAR system and high-resolution products.

Parameter	Values
Satellite altitude (nominal)	785 km
Radar frequency	5.3 GHz \pm 0.2 MHz
Radar wavelength (C-band)	0.056 m
Spatial resolution (three looks)	along-track \leq 30 m; across-track \leq 26.3 m*
Radiometric resolution (speckle noise at three looks)	2.5 dB below mean value
Dynamic range	$\sigma^0 \leq$ 25 dB
Swath width	100 km
Localisation accuracy	along-track \leq 1 km; across-track \leq 0.9 km*
Antenna dimensions	10 m long, 1 m wide
Incidence angle	23° - 26° from vertical at mid-swath
Polarisation	linear vertical, transmit and receive
Maximum operating time	about 12 minutes per orbit

*Resolution, noise and accuracy are dependent on the SAR product

2.1. Sea-Ice Imaging

For given radar parameters (frequency, polarisation and incidence angle), the intensity of backscattered signals to the antenna depends on the surface and upper-layer characteristics of sea ice, such as snow cover, surface roughness and dielectric properties of the target. If the dielectric constant is large, as is the case with the ocean, the radar signals do not penetrate into the media, and surface roughness alone determines the backscatter. If the surface consists of an asymmetric pattern of similar length scale to the radar wavelength, resonance with intensification of the backscatter occurs. This so-called 'Bragg scattering' is illustrated in Figure 3.

For targets with low dielectric constants, such as dry snow and ice, the signal will penetrate the medium. Because of inhomogeneities within the medium (air bubbles or crustal structures in sea ice), volume scattering will occur at these discontinuities (Fig. 4).

Differences in type and age of the ice, surface roughness and snow cover will modify the backscatter intensity of the microwaves and produce images with variable sigma zero. Multi-year ice with a low salinity in the upper layer reflects more of the microwaves, owing to a combination of volume scattering from the upper layer of the ice and surface scattering from the top of the ice. First-year ice, on the other hand, has a higher salinity in the upper layer, which impedes the penetration of microwaves into the ice. Therefore the sigma zero of first-year ice is dominated by surface scattering, and the surface roughness will to a large extent determine the strength of the return signal. For the average surface roughness found in the interior of the ice pack, multi-year ice will produce higher backscattering than the first-year ice. This difference can be used to classify the two types of ice by simple histogram segmentation. The difference in backscatter between the two types of ice will depend on incidence angle, frequency and polarisation. The dependency of sigma zero on incidence angle is illustrated in Figure 5. It is noticeable that the difference between first-year and multi-year sigma zero is much less in summer than in winter at all incidence angles.

In the marginal ice zone, where the ice is often broken into many small floes with rough edges, the average backscatter from large areas of first-year ice can be similar to or higher than that from the multi-year ice. New ice types, such as grease ice and frazil ice dampen the short surface waves and produce low backscatter values. As the ice grows thicker (nilas and grey ice) the backscatter stays low as long as the ice is level. But as soon as frost flowers start to build up and pancake ice with characteristic edge forms, the sigma zero increases rapidly (Fig. 6).

The temperature of the ice and snow cover is an important

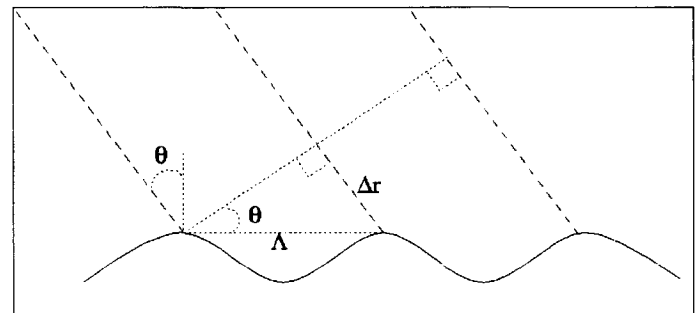


Figure 3. Bragg scattering from two adjacent crests will interfere positively if the excess distance $2\Delta r$ equals an integer number of radar wavelengths Λ is the surface wavelength.

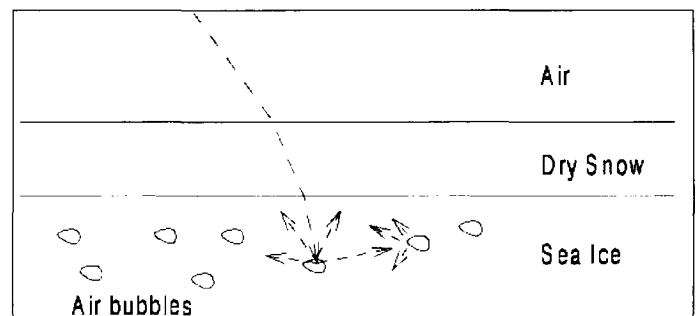


Figure 4. Volume scattering. Radar signal is scattered at the discontinuities inside the medium.

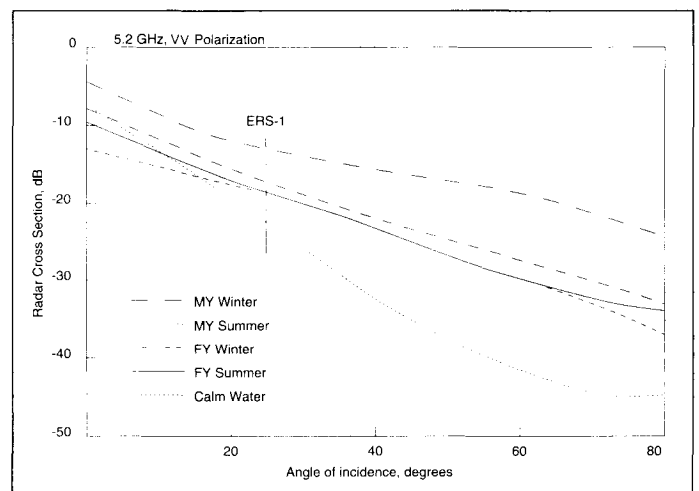
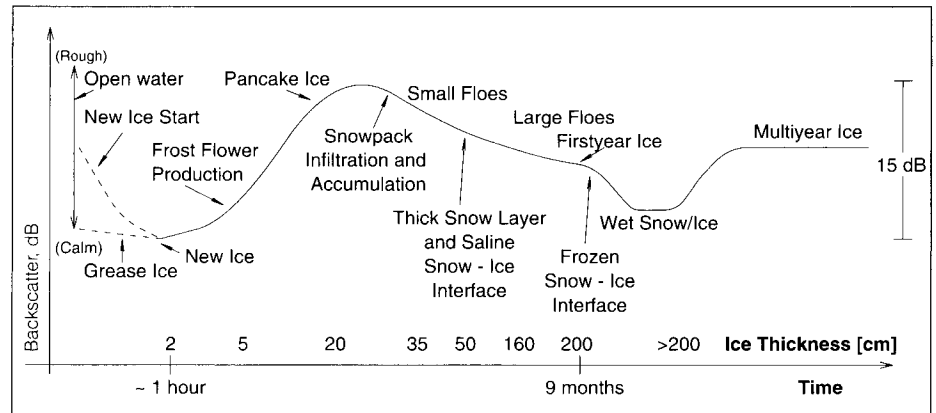


Figure 5. Backscatter coefficient versus incidence angle for different ice types and calm water (from Onstott, 1992). MY is multi-year ice and FY is first-year ice.

Figure 6. Time evolution of backscatter from sea ice (from Onstott, 1992)



modifying parameter which, especially in the melt season, changes the backscatter characteristics of the ice and snow significantly. Dry snow on multi-year ice has little effect on backscatter, while dry snow on first-year ice can have an important effect in some cases, depending on the SAR parameters and the snow characteristics. Moist

snow has considerable effect on the backscatter because dry and wet snow have very different electrical properties. The most pronounced effect of temperature is to moisten the snow cover so that the backscatter of multi-year ice is lowered to a level similar to that of the first-year ice, which makes discrimination between the two types of ice difficult in the melt season. Also, melt ponds on top of the ice have strong effect on the backscatter because they act as 'no return' areas comparable to open calm water between floes. The main features of the time evolution of the backscatter for different stages in the ice growth are shown in Figure 6, but more research is needed before the relationship between the backscatter and the various types of ice can be fully understood. An overview of the ERS-1 SAR scenes presented in this catalogue is provided in Table 2.

Table 2. Overview of SAR scenes

Area	Year	Month	Id	Topic
East Greenland Coast	1993	Oct	AA	New ice along the East Greenland coast
	1993	Oct	AB	Icebergs off the East Greenland coast
	1993	Oct	AC	Enlargement of iceberg in AB
	1993	Nov	AD	Pack-ice off the Greenland coast
	1994	Apr	AE	Ice conditions across the Denmark Strait
Greenland Sea	1992	Jan	CA-CE	Dynamics of the ice edge
	1992	Feb	CF	From Greenland coast towards Jan Mayen
	1992	Feb	CG	The Odden ice tongue
	1994	Feb	CH	Combined SAR and SSM/I data
	1992	Jan	CI	Fram Strait winter ice
	1993	Aug	CJ	Deep-sea drilling on the Yermak Plateau
	Barents Sea	1992	Mar	GA
1992		Mar	GB	North coast of Svalbard
1992		Jan	GC	West coast of Svalbard
1994		Dec.	GC2	Shrimp trawling north of Svalbard
1992		Mar	GD-GK	Rapidly changing ice edge in the Hopen area
1992		Feb	GL-GM	Ice dynamics inside the ice edge
1992		Mar	GN	Classification of winter ice
1992		Mar	GO	Northeastern Barents Sea
1992		Mar	GP	Glaciers of Franz Josef Land
1992		Mar	GQ	Enlargement of calving glacier in GP
Kara Sea	1994	Mar	FA	Ice-breaker route on Yenesei river
	1994	Feb	FB-FC	Ice motion in Ob river estuary
	1993	Nov	FE-FF	Freeze-up in Baydratskaya Bay
	1993	Oct/Nov	FG-FH	New ice in the Kara Gate and the Jugor Strait
	1993	Nov	FH	New ice in the Kara Gate and Jugor Strait
	1993	Apr	FI	Novaya Zemlya east coast
	1991	Aug	FJ-FK	L'Astrolabe through the Northeast Passage
	1993	Nov	FL	Eddy currents in Pechora Sea
	1993	Nov	FM	Ice-breaker navigation in Mathiessen Strait
	1993	Nov	FN	Ice conditions in the Vilkitskogo Strait
	1994	Mar	FO	The northernmost islands off the Siberian coast
	1993	Sep	FP	The interior of the Arctic pack ice

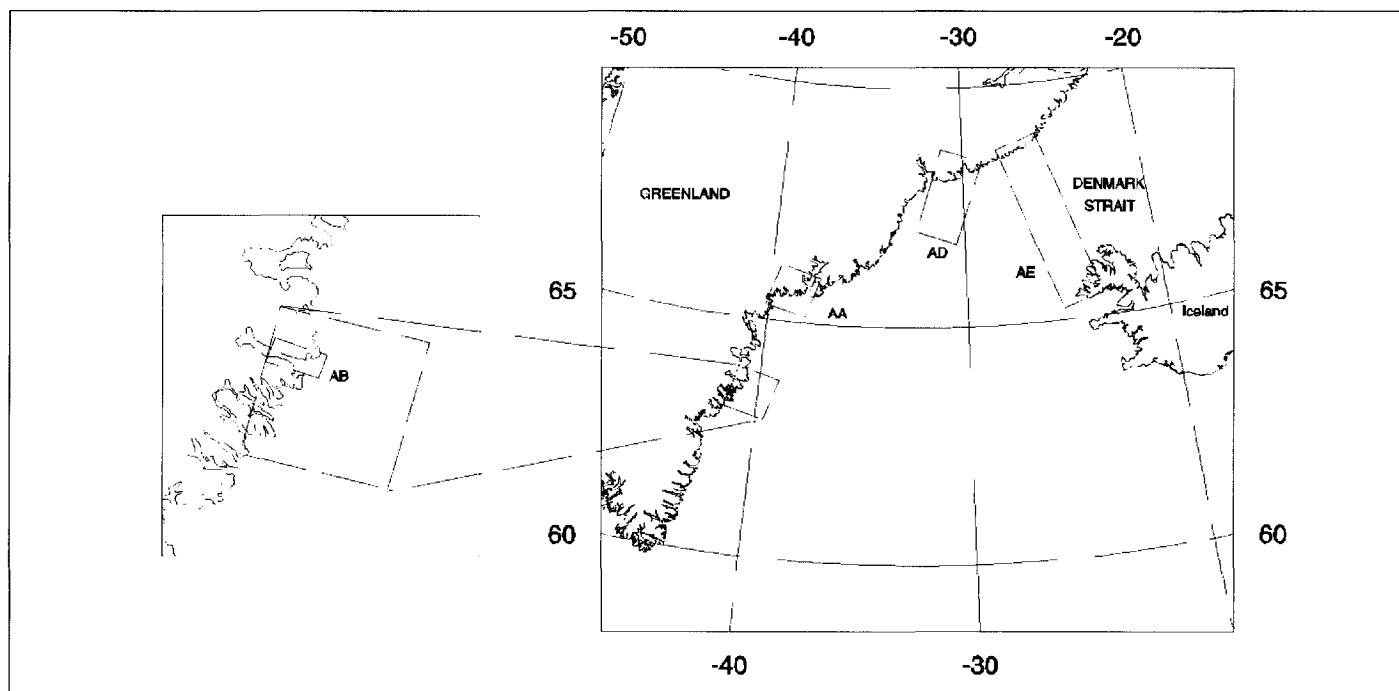
3. East Greenland Coast

The coasts of Greenland are severely influenced by drifting sea ice and icebergs, restricting ship traffic to and from Greenland. To assist these and other marine activities, in particular in the southern part of Greenland, an ice-monitoring service for Greenland has been operated by the Danish Meteorological Institute for more than 30 years (Hansen & Valeur, 1994). This service is based on aircraft reconnaissance flights, satellite data and other observations. The usefulness of radar data from satellites, including SAR images, is currently being tested in this region. It is expected that SAR data will be used operationally when they are regularly available.

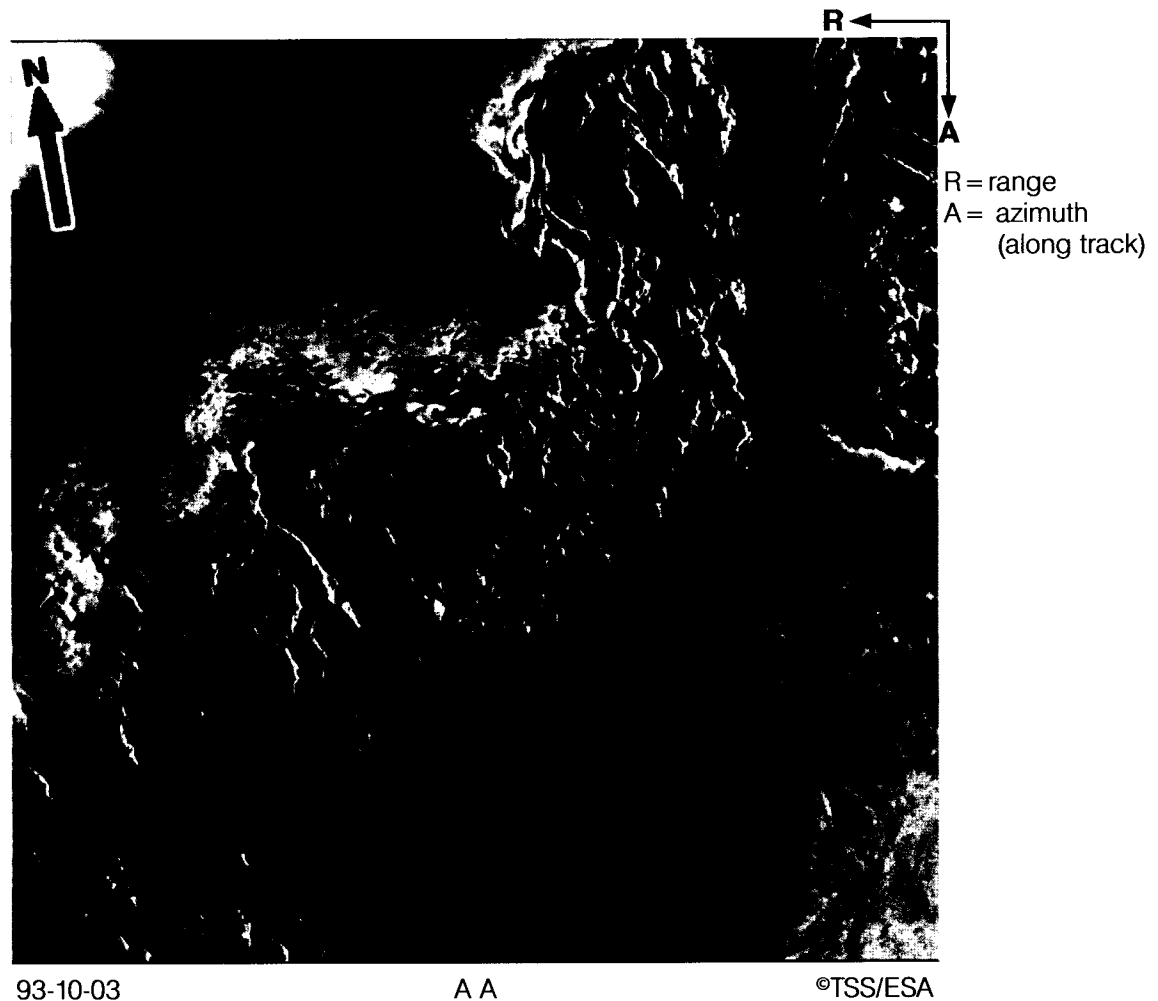
Several types of ice, including icebergs, are to be found around Greenland's coasts throughout the year. Minimum ice cover occurs in August–October when the southern part can be ice-free (Fig. 1). Multi-year ice from the Arctic Ocean is transported by the East Greenland Current along the whole eastern continental shelf (Wadhams, 1981). This ice is 2–5 m thick and the floes can be tens of kilometres in horizontal extent. The large floes are broken into smaller pieces during the southward drift, but in the winter clusters of ice floes can freeze together and form large areas of compact ice cover. South of Scoresby Sound (70°N, 20°W), most of the floes are less than 1 km in diameter. During the winter, land-fast ice is formed along most of the eastern coast. In the summer, this land-fast ice and large parts of the multi-year ice melt. In the Kap Farvel area, where most of the ship traffic occurs, icebergs and small multi-year floes can be dangerous to ships because this ice is difficult to monitor. Even high-resolution SAR images have limited ability to identify ice with a horizontal extent of 100 m or less.

In the Denmark Strait, between Greenland and Iceland, sea ice can occur in important fishing areas. It can even be found along the north coast of Iceland in some years. The Icelandic Meteorological Institute is responsible for sea-ice monitoring in this region based on various observations from ships and aircraft. Although satellite data are not used routinely, in the Denmark Strait their potential there has been demonstrated by NERSC using ERS-1 SAR data in near-real-time.

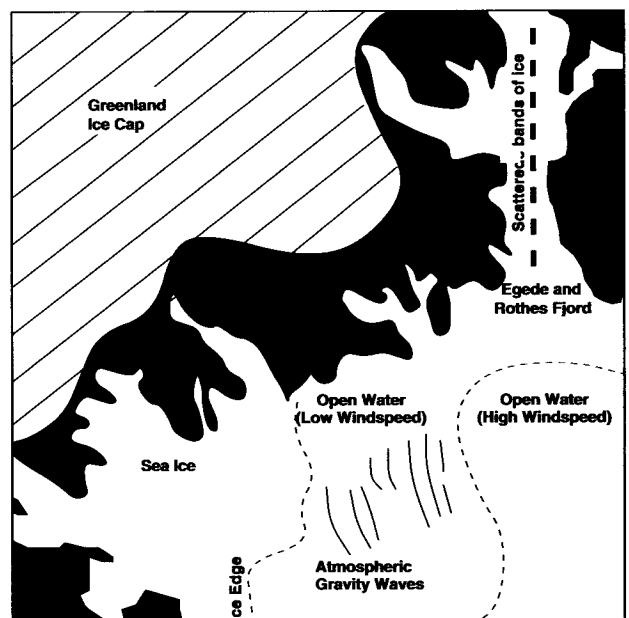
Figure 7. Location of SAR images used in this section



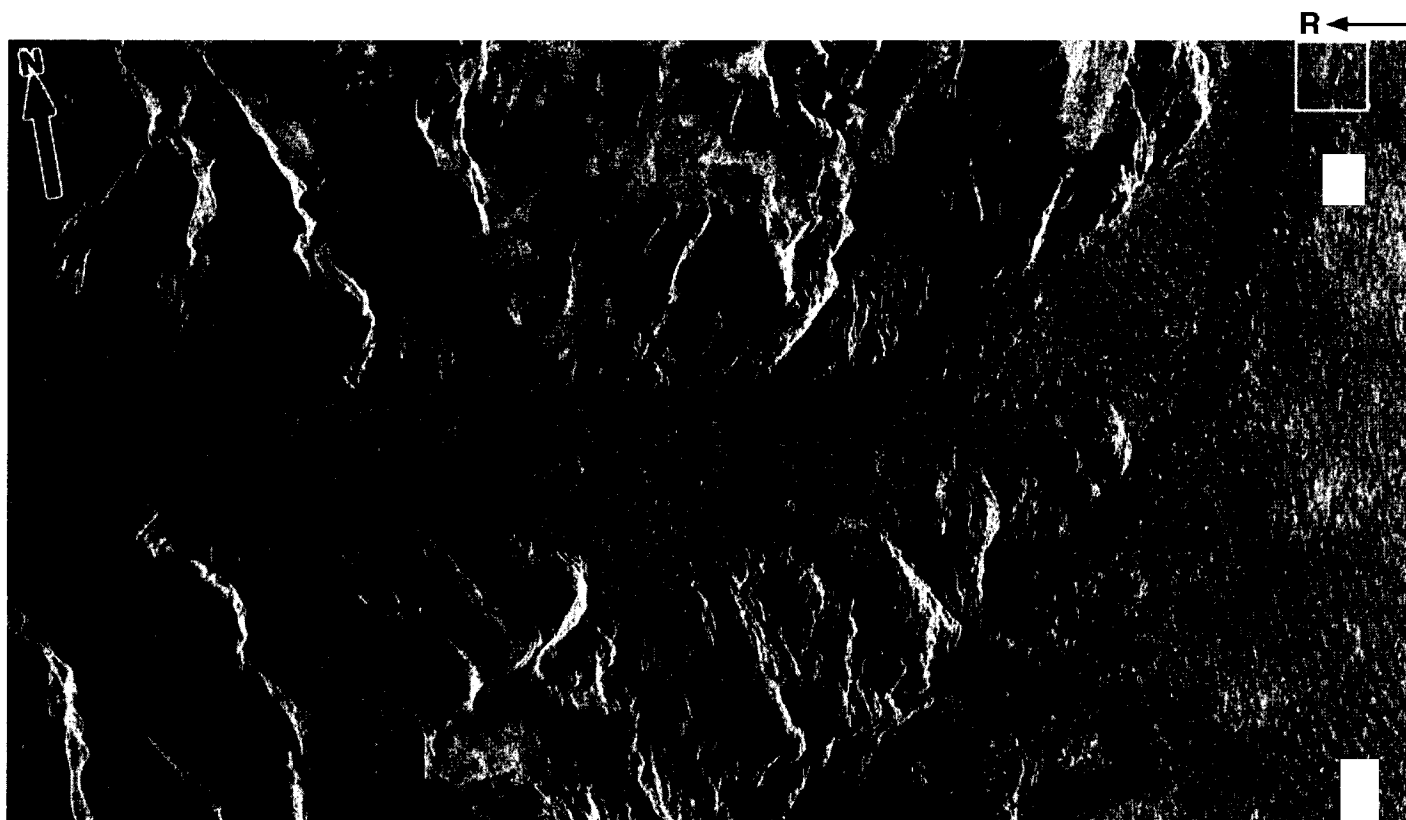
Formation of New Ice along the Greenland Coast in October



This SAR image (upper figure) covers a part of the Greenland Ice Cap, some fjords, and the open ocean at about 66°N. A simplified interpretation of the image is shown to the right. It was obtained on 3 October 1993 when the first new ice had formed in the fjords in the lower left-hand part of the image (grey signature). The fjords further north are almost ice-free (dark signature except for some scattered bands of ice in the Egede and Rothes Fjord). The difference in open-water backscatter (between the area near land and further east) is caused by small changes in wind speed. The ice cap has a varying signature reflecting differences in wetness, snow structure and roughness of the surface. In the summer, wet snow tends to give low backscatter from glaciers, while in the winter the backscatter is high. Atmospheric gravity waves are sometimes observed in SAR images due to oscillations of the surface wind speed. This phenomenon has been studied in detail by Vachon et al. (1994).



Icebergs off the East Greenland Coast



93-10-03

AB

©TSS/ESA

The image covers about 20x40 km of a fjord at 63°40'N, where several icebergs were observed off the coast on 3 October 1993. The image is full-resolution (16x20 m) and shows waves propagating towards the coast. The waves are about 300 m long and are attenuated as they enter shallow water. The fjord is covered with new ice and at its mouth a cluster of icebergs can be observed.



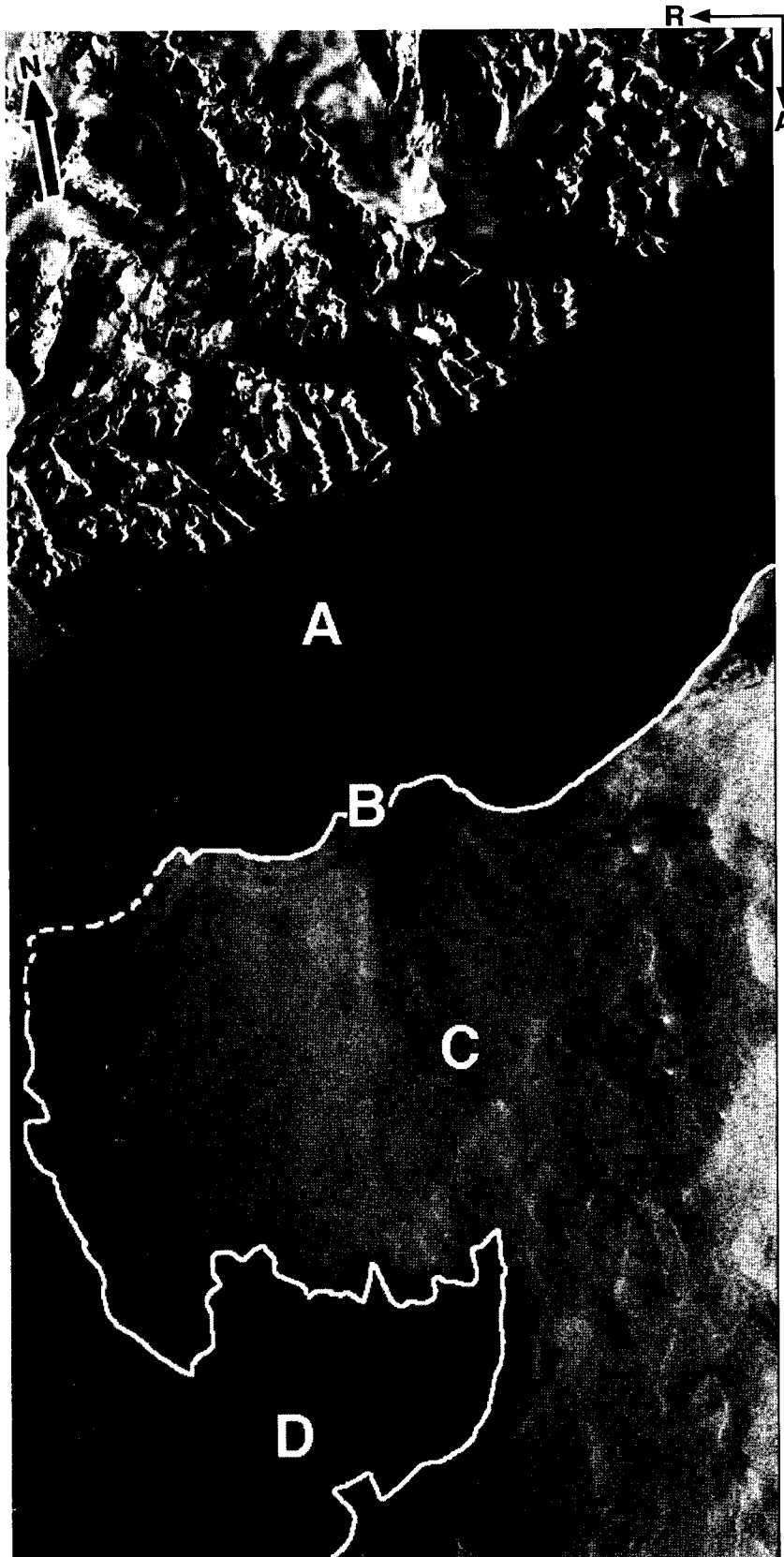
93-10-03

AC

©TSS/ESA

One of the icebergs in the upper right-hand corner was also observed from a ship in the area; a zoomed and enlarged 3x3 km subimage is shown to the left. The iceberg is about 500 m long and 50–100 m wide, and is characterised by a very bright signature. It is surrounded by open water, and the dark area to the west of it is assumed to be an area of fresh-water released by the iceberg, or grease ice formation. Smaller icebergs, with horizontal extents of less than 200 m, are often difficult to identify in ERS-1 SAR images. The icebergs are difficult to detect even after noise filtering of the full-resolution image, because iceberg signals can be similar to the speckle noise.

Pack Ice off the Greenland Coast in November



Later in the autumn and further north on the Greenland coast, the pack ice was more developed. On 11 November 1993, a 40–50 km wide zone of mostly new and young ice types 10–30 cm thick, is observed at about 67°30'N. The open water signature is slightly brighter than the ice signature. In cases of low wind speed (2–4 m/s), open water and ice can give similar backscatter levels, making discrimination of ice from water difficult. In the lower part of the image, a large tongue of ice extends outwards more than 100 km from the coast.

- A = Small floes and newly frozen ice
- B = Ice edge
- C = Open water
- D = Ice tongue.

93-11-11

AD

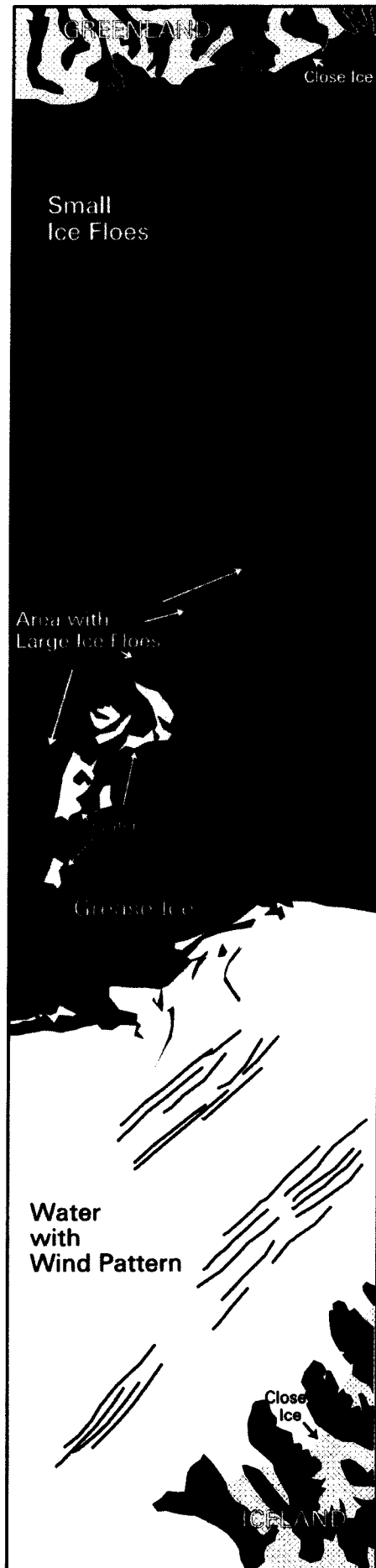
©TSS/ESA



94-04-18

AE

©TSS/ESA



94-04-18

Ice Conditions across the Denmark Strait

The ice in the Denmark Strait and along the north coast of Iceland is important for the fisheries and other marine activities in the area. The Icelandic Meteorological Office produces ice maps in this region based mainly on direct observations, not satellite data. Their ice maps, which show ice concentration and ice edge position, are somewhat less detailed than SAR image maps. The SAR strip is 100 km wide and 400 km long and covers the 300 km wide strait between Greenland and Iceland. The image was taken in late winter (18 April 1994) when the ice extent can be at a maximum. The ice cover extends 200 km from the Greenland coast, and several individual floes can be observed. The large floes, which can be more than 10 km in diameter, are multi-year floes which usually have a brighter signature than the surrounding ice. In this image, some multi-year floes appear dark, probably owing to wet snow on top of the ice. A manually interpreted ice map derived from the ERS-1 SAR data is shown on the right.

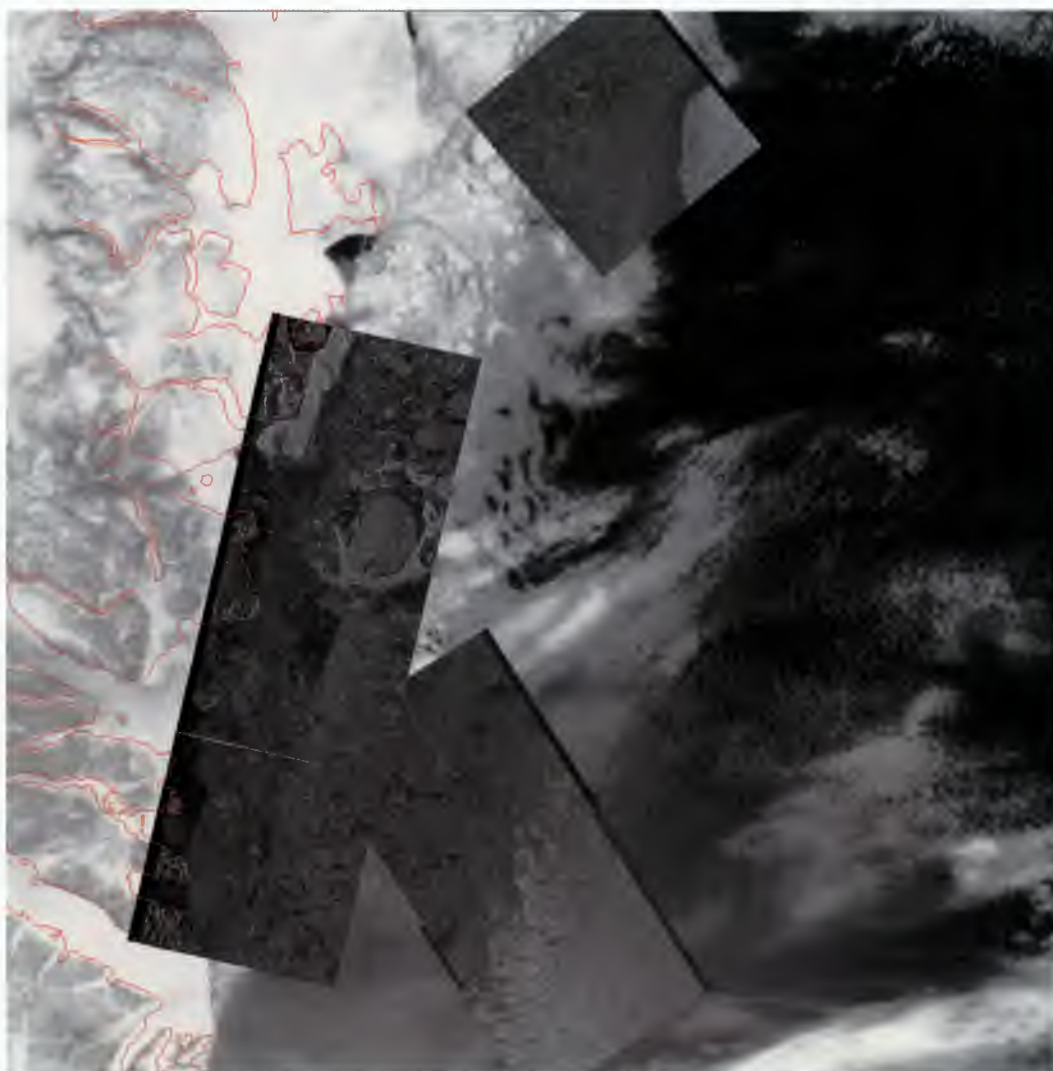
AVHRR and SAR Scenes from Greenland



94-01-19



94-01-26



NOAA/AVHRR and ERS-1/SAR superimposed

(Courtesy H. Valeur & K. Hansen, DMI, Denmark)

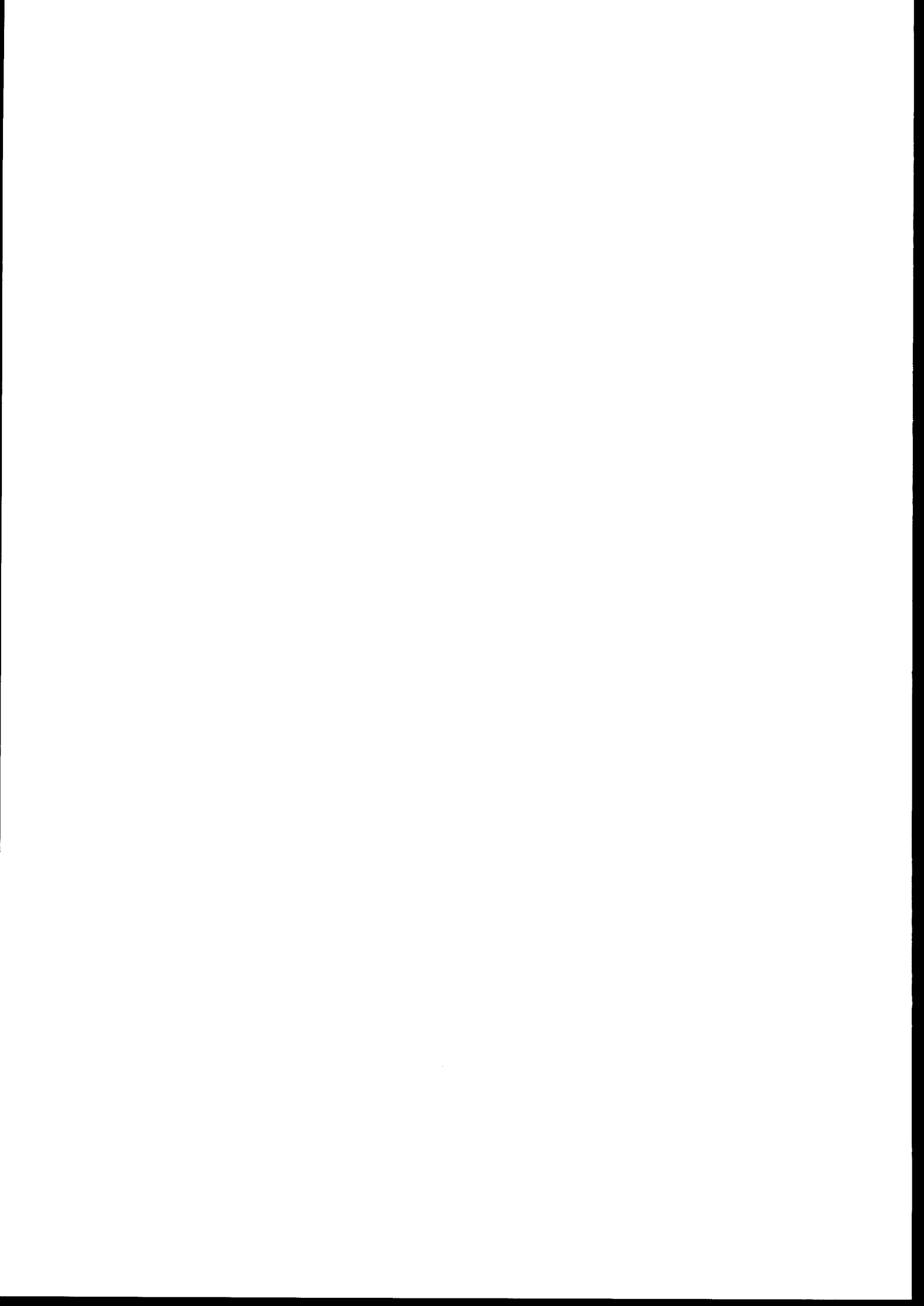
The Greenland Coast: Combined Mapping with SAR and AVHRR Data

The coasts of Greenland are strongly influenced by drifting sea ice and icebergs. To assist shipping, particularly in the southern part of Greenland, an ice-monitoring service has been operated by the Danish Meteorological Institute for more than 30 years. This service is based on aircraft reconnaissance flights, satellite data, and other observations. Radar data from satellites including SAR images are currently being tested in this region and there are plans to use them operationally in the future.

Several ice types are found along the Greenland coasts, and ice is present throughout the year. Minimum ice cover occurs in August–October. Multi-year ice from the Arctic Ocean is transported by the East Greenland Current along the whole eastern continental shelf. This ice is 2–5 m thick and a floe can be tens of kilometres in horizontal extent. The large floes are broken into smaller pieces during the southward drift, but in winter clusters of ice floes can freeze together and form large areas of compact ice cover. South of Scoresby Sound, most of the floes are less than 1 km in diameter. During the winter, landfast ice is formed along most of the eastern coast. In the summer, the landfast ice and large parts of the multi-year ice melt. The most hazardous ice in the Kap Farvel area, where most of the ship traffic is found, are icebergs and small multi-year floes.

The image is a NOAA AVHRR image, from January 1994, covering the east Greenland coast between Shannon and Scoresby Sound (71 to 75°N). Because of clouds and haze, the ice is very diffuse in the AVHRR image. The SAR images, which are superimposed on the AVHRR image, are independent of cloud cover and provide a much more detailed picture of the ice cover and the ice edge. All images were obtained within a 10 day period in January 1994.

4. Greenland Sea



As one moves north in the East Greenland Current, the thicker and more frequent multi-year ice floes become. The Fram Strait between Greenland and Svalbard is an important route for the outflow of ice from, and the inflow of warm water masses into, the Arctic Ocean (Wadhams, 1991, Johannessen, 1986). The Greenland Sea between 70° and 75°N is also an important area for the formation of deep water, which plays a global role in ocean circulation and climate (Johannessen et al., 1992). North of Jan Mayen, a characteristic ice tongue called the 'Odden' often occurs in the winter. This tongue consists of young ice. Another characteristic feature off the coast of Greenland at 80°–82°N is the Northeast Polynya (not shown here). This consists of open water or thin/young ice and can be found even in the winter. The polynya is caused by a divergence of the ice cover away from the coast, and has been documented by AVHRR images as well as field observations.

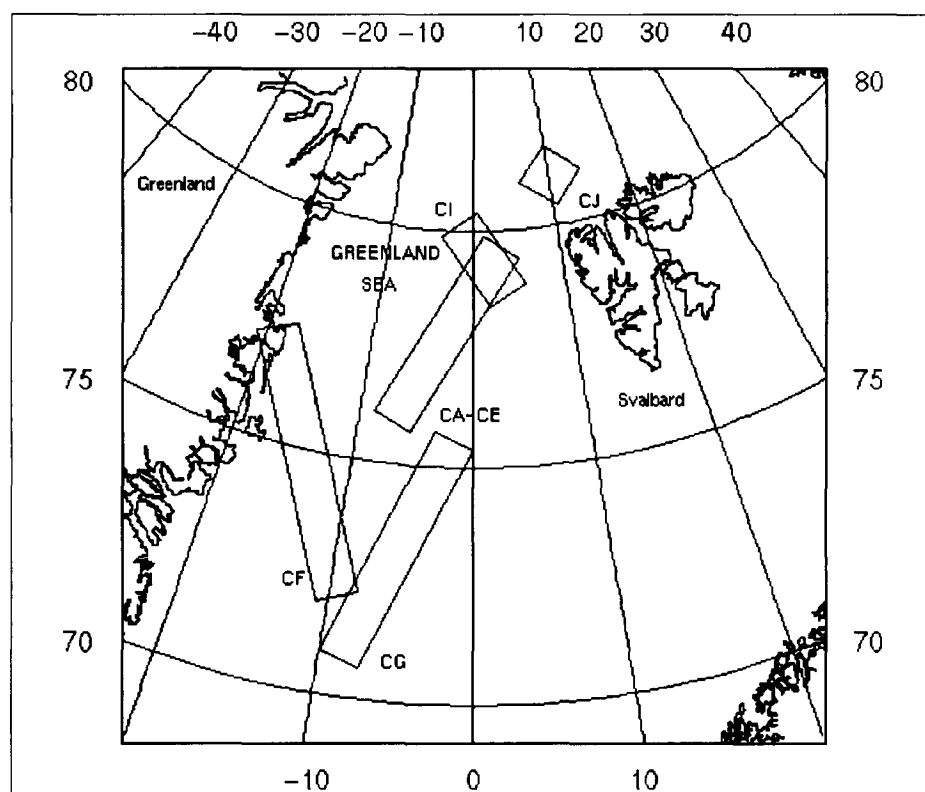


Figure 8. Location of SAR images used in this section.

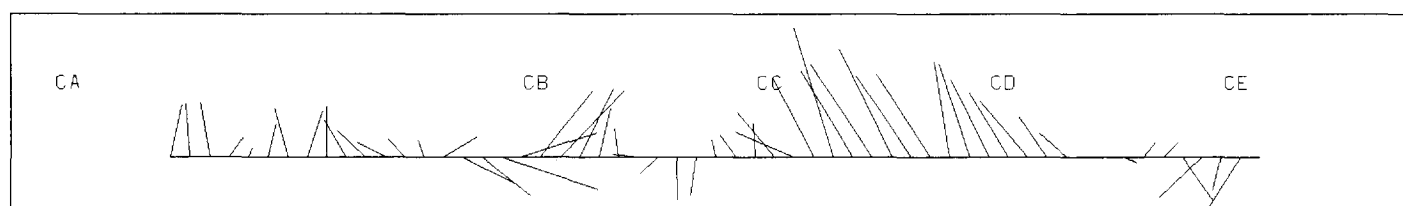
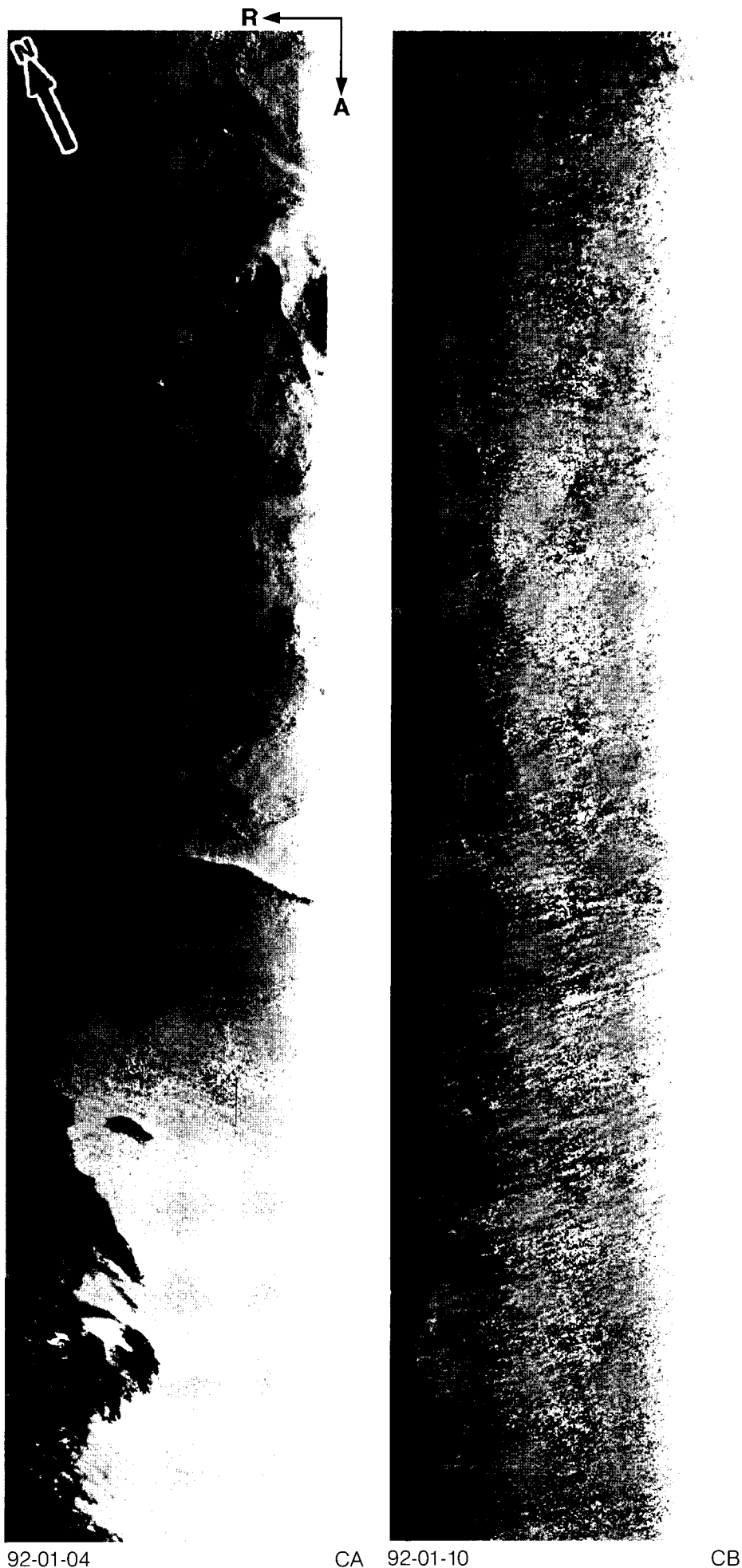


Figure 9. Wind vectors every 6 hours from 6 to 19 January 1992. CA-CE denote times when the SAR images were obtained. The line segments indicate the wind direction and speed. For example, between 13 and 16 January 1992 (images CC and CD), the winds were from the NNW at about 20 m/s.

Dynamics of the Ice Edge

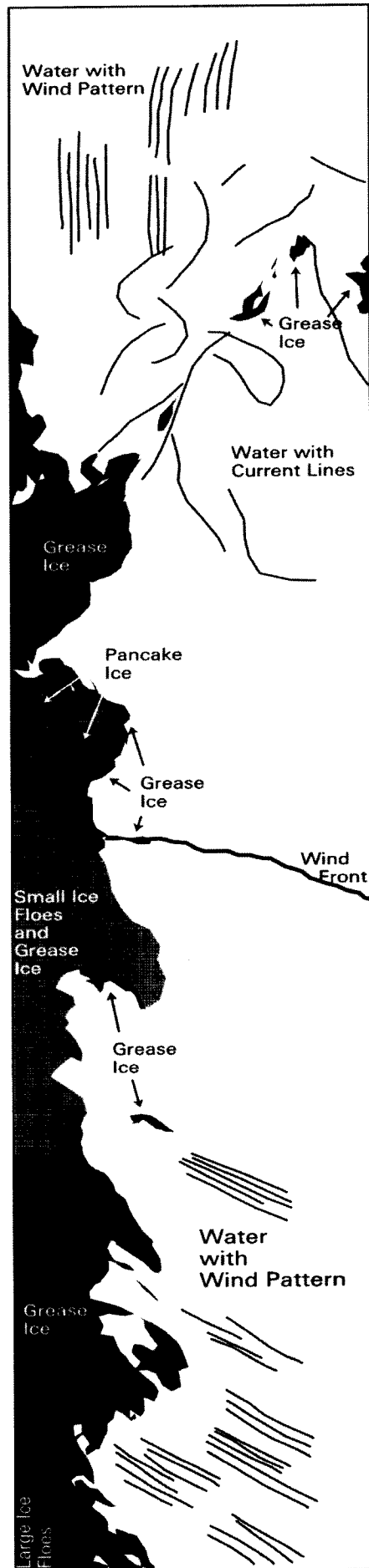
Each SAR strip, which is 500 km long and 100 km wide, covers the same geographical area in the ice-edge region between 76° and 80°N (see Fig. 8). This series of five images and corresponding interpretation maps shows how the ice-edge location and features changed in the period from 4 to 19 January 1992. During this period, the R/V Håkon Mosby undertook oceanographical investigations in the area (Johannessen et al., 1994). SAR images were the only data capable of providing accurate ice-edge location in a period of almost no daylight. SAR images transmitted to the ship in near-real-time were therefore used to plan the ship's course near the edge of the ice. Without SAR imagery, the R/V Håkon Mosby would not have been able to operate close to the edge of the ice as the wind conditions were variable (see Fig. 9), including storm events with wind speeds of more than 25 m/s. During southeasterly winds, the ice edge was pushed towards the west. On 10 January, the wind was 20 m/s from the southeast and most of the edge was located west of the image. From 10 to 13 January the wind was northerly and then southerly, resulting in a more eastward location of the edge. On 16 January, a NNW wind direction is made visible in open ocean by streamers oriented parallel to the wind. Three days later, westerly winds had made the ice edge very diffuse. The rapid change in edge location and detailed ice features which is characteristic of this area, could only be observed from a time series of SAR images.



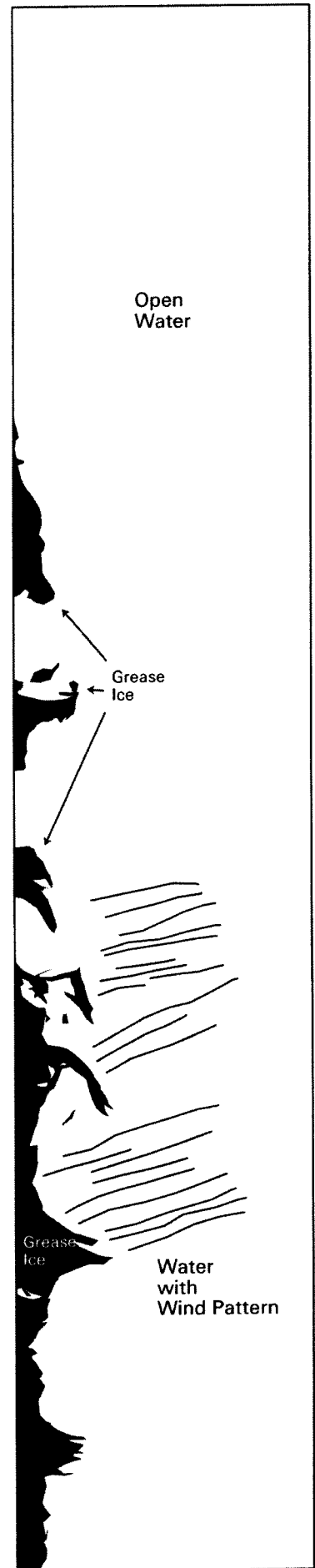
92-01-04

CA 92-01-10

CB



92-01-04

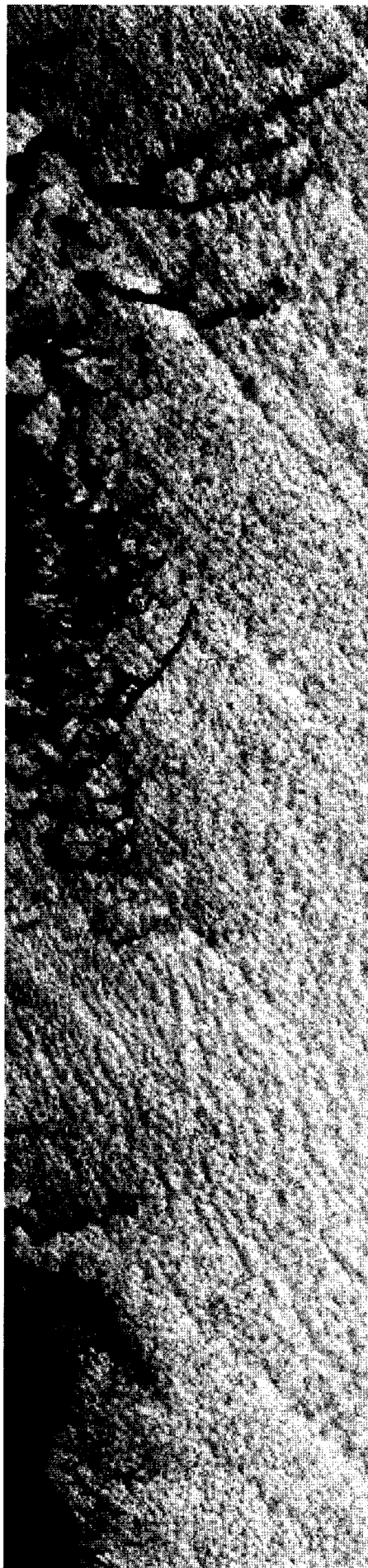


92-01-10



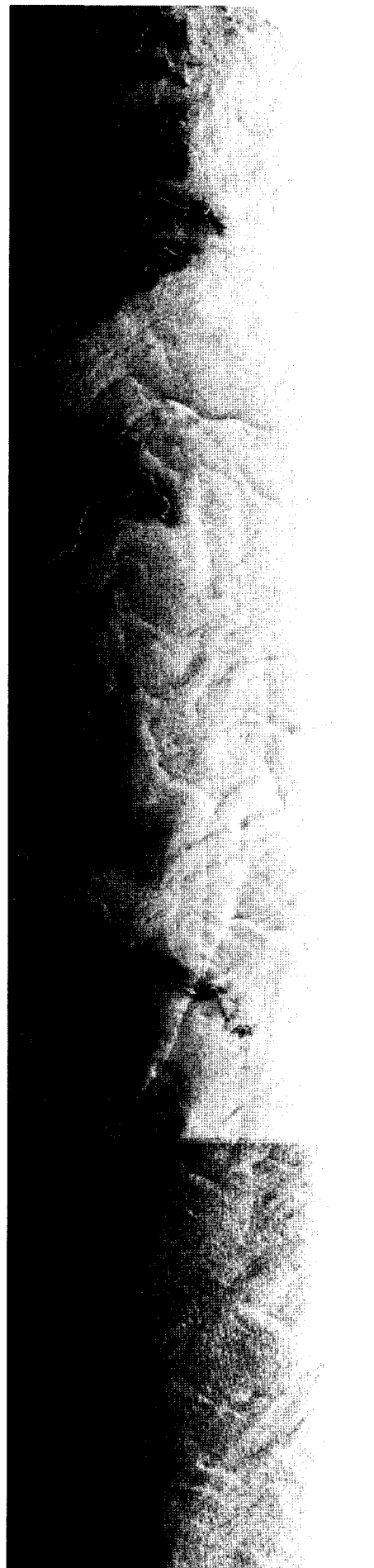
92-01-13

CC



92-01-16

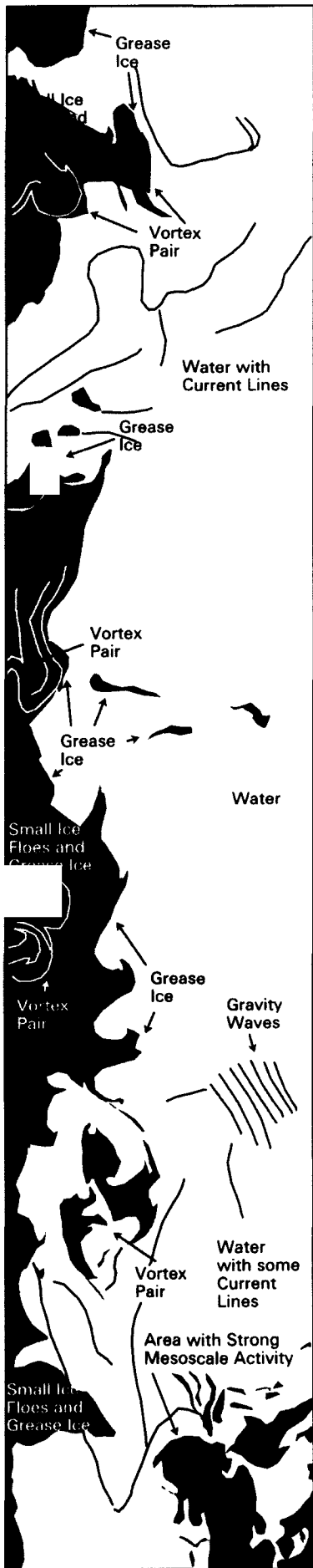
CD



92-01-19

CE

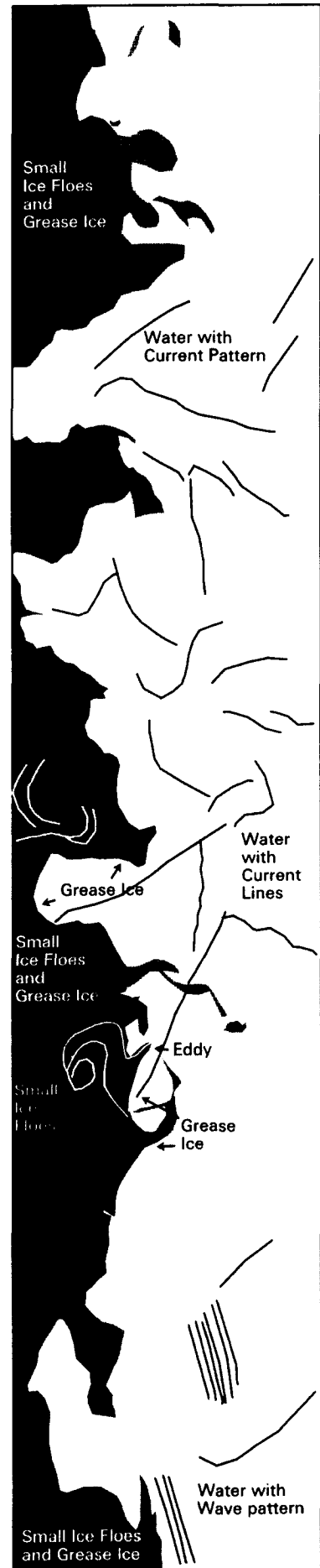
©TSS/ESA



92-01-13



92-01-16

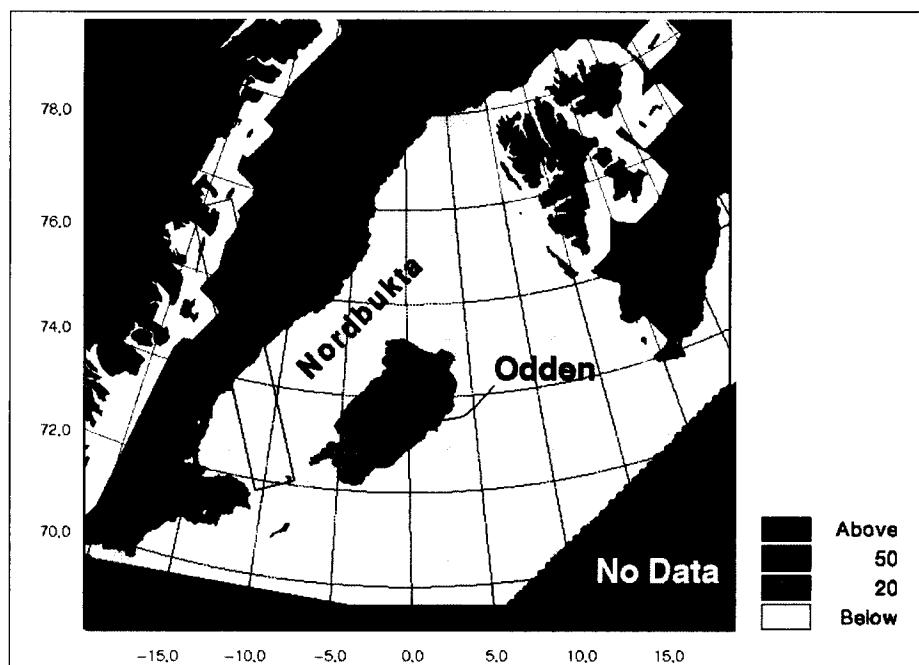


92-01-19

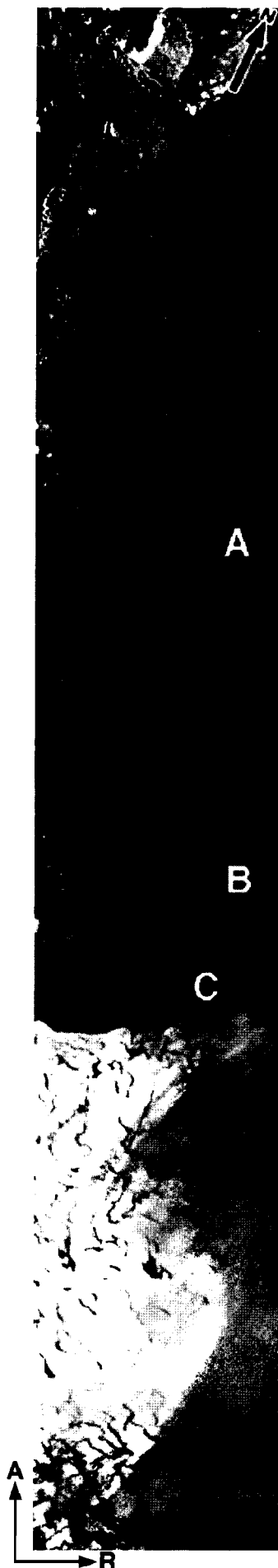
From the Greenland Coast towards Jan Mayen

In February 1993, R/V Håkon Mosby operated in the central Greenland Sea (75°N, 2°W) where deep water formation occurs in winter time. SAR images from ERS-1 as well as SSM/I data were used to map the sea-ice extent, especially the Odden ice tongue and the bay of open water between Odden and the main pack ice (Nordbukta). The ice tongue was well developed in this period, as can be seen in the SSM/I map. The SAR strip to the left, which is 700 km long, was taken on 13 February and extends from the Greenland Coast at about 77°N, in a southeasterly direction into the ice tongue. The SAR strip covers several ice types and the open water in Nordbukta. In the interior of the ice pack, most of the ice consists of large multi-year floes which can be up to several tens of kilometres in diameter. Between the large floes, young ice and first-year ice with lower backscatter are seen in the SAR strip.

- A = Large multi-year floes
- B = Small floes broken up by waves
- C = Ice edge
- D = Mostly open water (less than 20% ice concentration)
- E = Formation of bands of new ice in the Odden ice tongue



Ice concentration (percent) from SSM/I data on the same day as the SAR strip. The rectangle indicates the location of the SAR strip. White areas are due to masking of land effects.



The Odden Ice Tongue

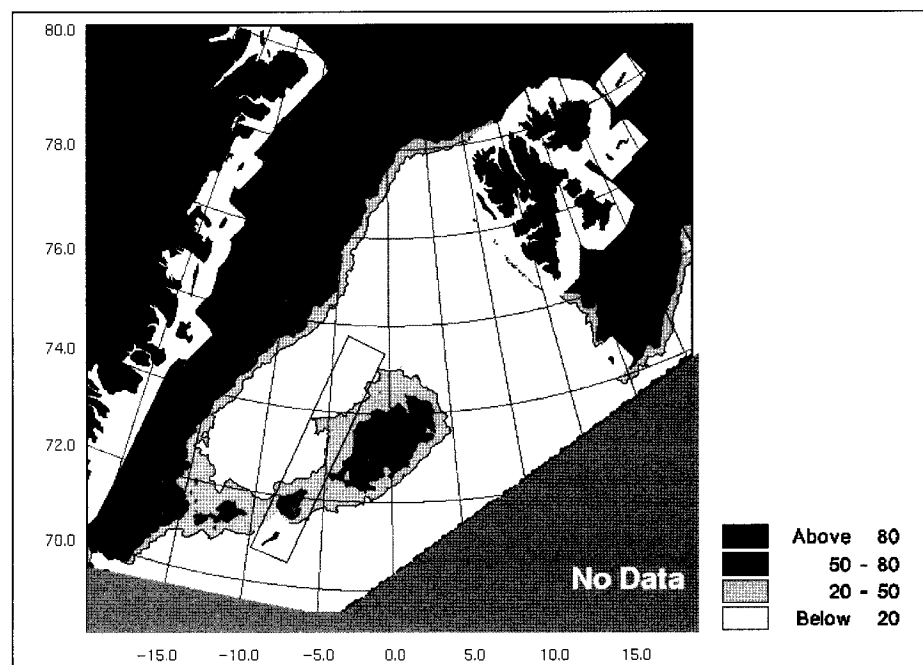
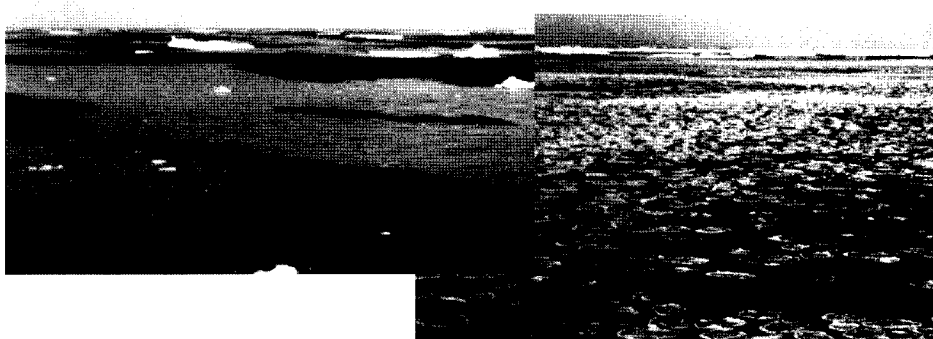
The SAR strip is from 16 February 1993 and cuts across the Odden ice tongue, which consists mainly of pancake ice and grease ice. These types of ice were documented by observations from R/V Håkon Mosby, which operated in the northern part of the ice tongue (see photographs below). The ice tongue usually develops in December and lasts until April, but does not occur every year. Passive microwave data since 1978 from SMMR and SSM/I show that the ice tongue is absent during some winters, as was the case in 1994., 1995 and 1996.

A = Open water

B = Photos from R/V Håkon Mosby on 19 February 1993

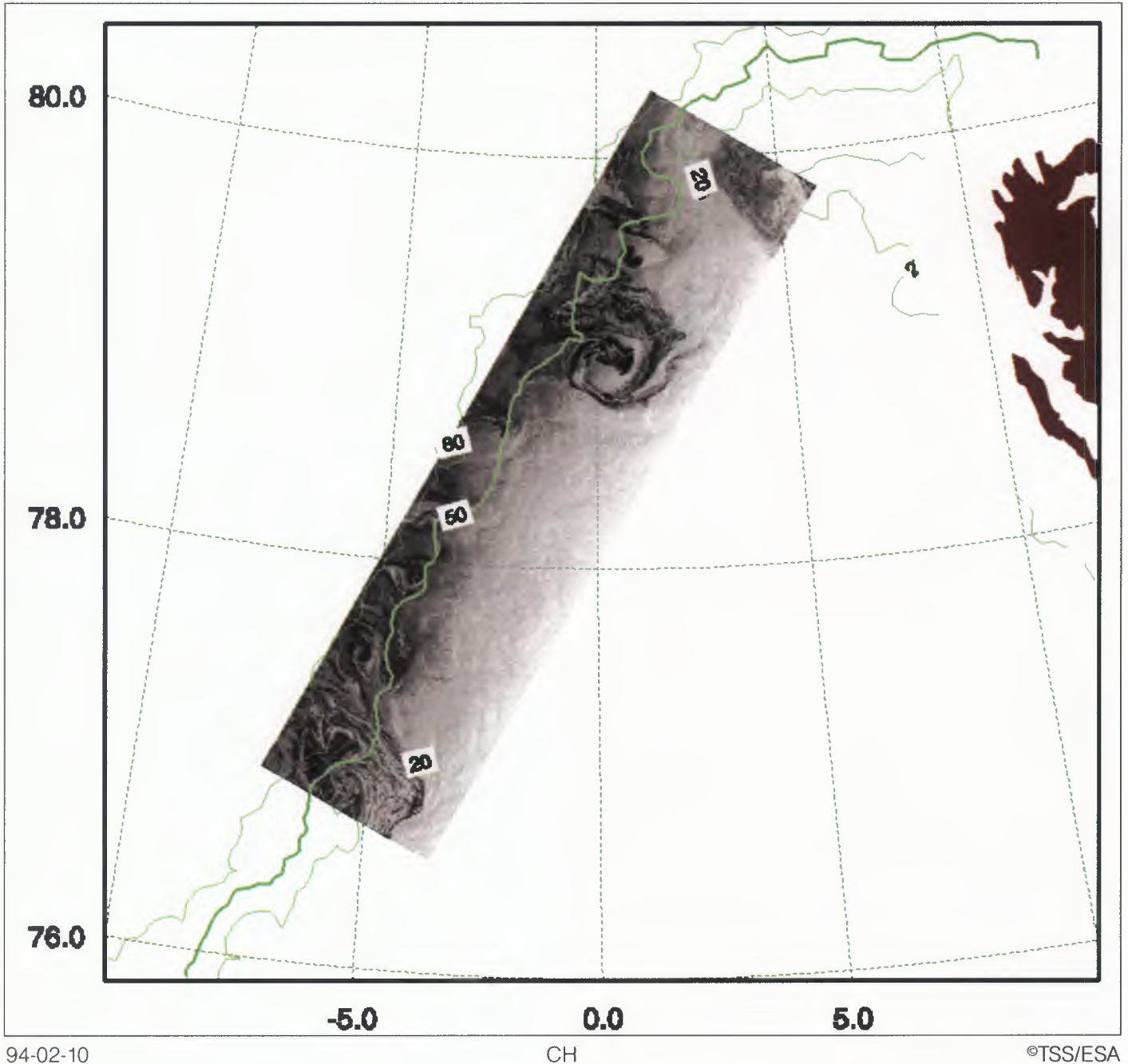
C = Grease ice and pancake ice

D = Jan Mayen island.



Ice concentration in % from SSM/I data on the same day as the SAR strip. The rectangle indicates the location of the SAR stripe. White areas are due to masking of land effects.

Combined SAR and SSM/I Data

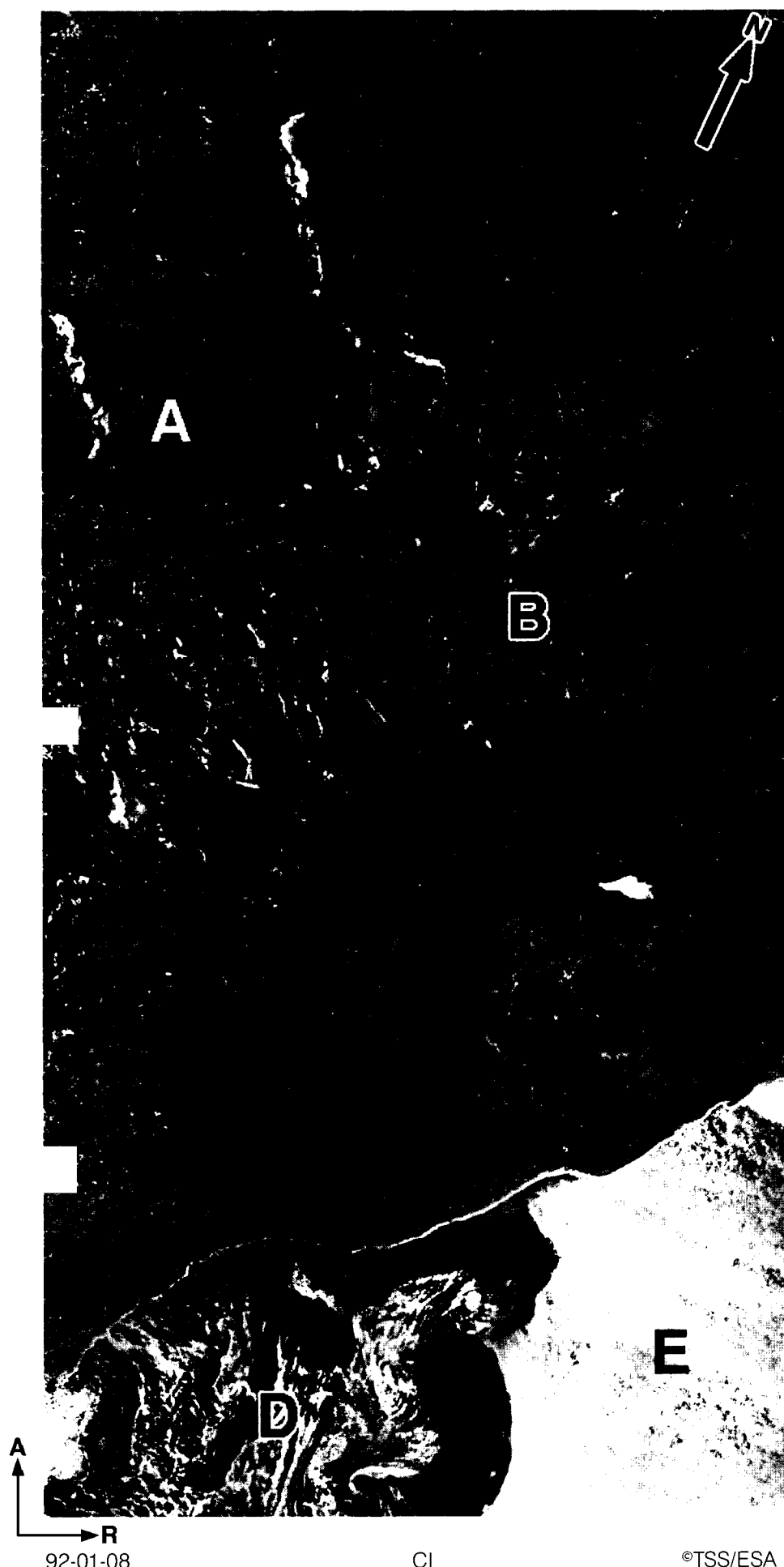


94-02-10

CH

©TSS/ESA

In regional ice mapping, ERS-1 SAR imagery on a given day only covers a limited area. To obtain daily ice maps of regions which are typically 500 km x 500 km in extent, it is useful to combine SAR imagery with other satellite data such as ERS-1 ATSR, NOAA/AVHRR or SSM/I data. Since ice-edge regions are cloud-covered most of the time, visible satellite images are not useful on a daily basis. Therefore SSM/I ice-concentration maps are suitable for combining with the SAR image, as shown in the above example. The SAR image is superimposed on a map and enhanced to distinguish ice from open water. Isolines for ice concentration (20%, 50% and 80%) from SSM/I data, taken on the same day as the SAR image (10 February 1994) are plotted for the whole region and superimposed on the SAR image.



Fram Strait Winter Ice

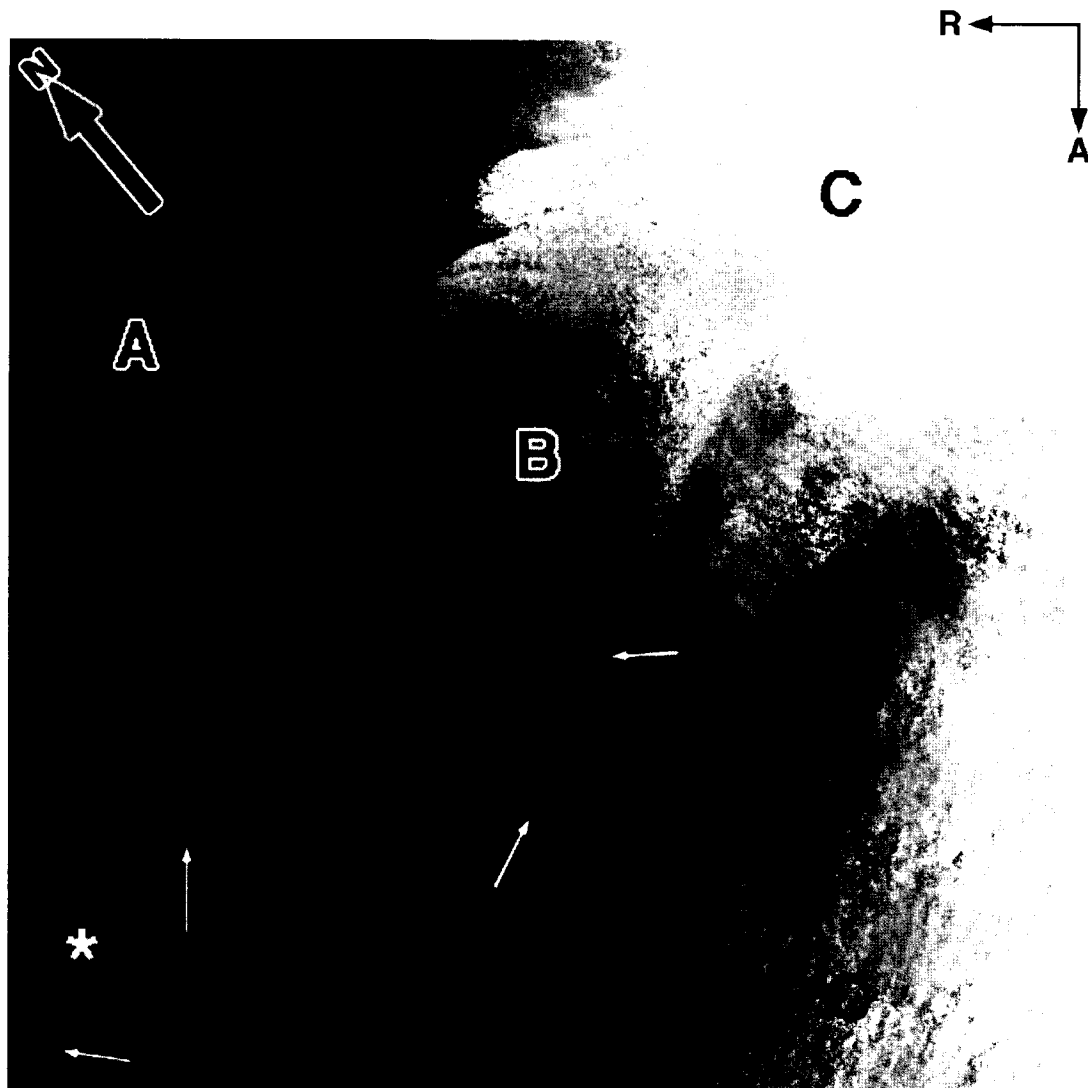
The SAR image to the left was obtained on 8 January 1992 in the Fram Strait and shows characteristic winter conditions with refrozen leads (A), multi-year ice in the interior of the ice pack (B), small multi-year ice floes broken up by wave action (C), first-year ice, grease and pancake ice (D), and open water (E) beyond the ice edge. Time series of such images, taken at 3–6 day intervals, are useful for calculating ice motion in the Fram Strait, which is important for the estimation of ice outflow from the Arctic Ocean to the Greenland Sea. The grease and pancake ice show the eddy circulation which is characteristic for the ice-edge region in the Fram Strait. During several field experiments from 1983 to 1989, the edge processes were intensively investigated using airborne SAR in combination with in-situ observations (Johannessen et al., 1987a; Johannessen et al., 1987b; Johannessen et al., 1992).

92-01-08

CI

©TSS/ESA

Deep-Sea Drilling on the Yermak Plateau (81°N, 7°E)



93-08-22

CJ

©TSS/ESA

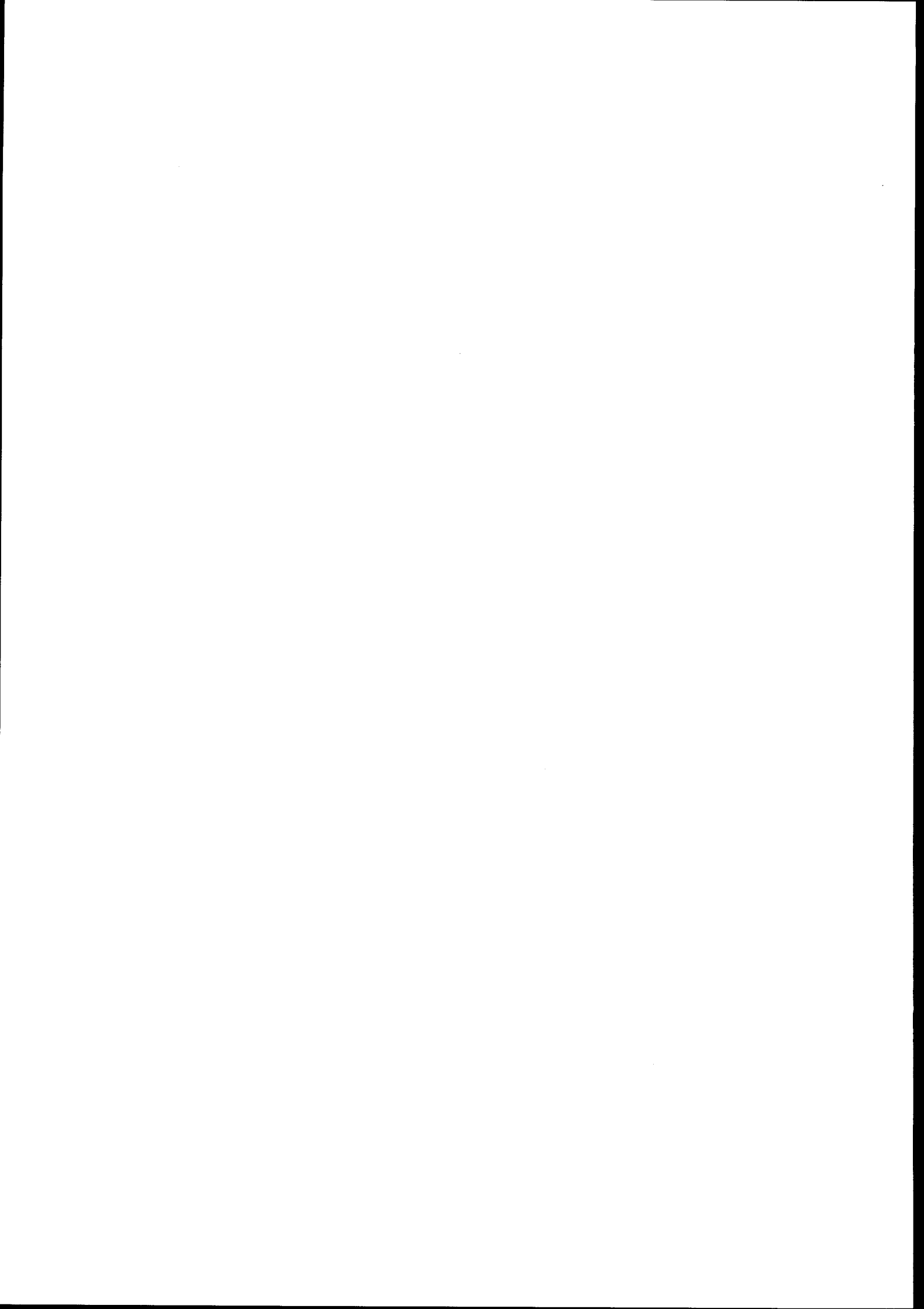
A special deep-sea drilling vessel was operating in the Fram Strait in August and September 1993, during Leg 151 of the Ocean Drilling Programme (ODP). Some of the drill sites were in the ice-edge region north of 80°N, and accurate ice maps available in real time were important for the planning and implementation of the drilling operations. Therefore, ERS-1 SAR images were used whenever they were available in this area. These SAR images were interpreted for ice-edge location, ice concentration and ice motion. The image taken on 22 August showed a clear and compact ice edge (B and arrows) between the compact pack ice (A) and the open water (C). In other cases, the edge was more diffuse and not always easy to identify in SAR images. In addition, SSM/I and AVHRR data were used to fill in gaps between the SAR coverage and map the ice edge on a larger scale, as shown in image CH.

The position of the drill site Y1 (81.05°N, 7°E) is marked. This location was ice-covered most of the time in August and September. The successful use of satellite data in the ODP, especially ERS-1 SAR images, has been reported in *Offshore Engineer* (Wagner, 1994) and in articles by Sandven et al. (1994a and 1994b).



The icebreaker MSV Fennica was used to support the JOIDES Resolution in the Greenland Sea and Fram Strait in August/September 1993. This area is one of the most difficult and challenging for deep-sea drilling because of the sea ice, which imposes severe restrictions on the drilling. MSV Fennica's role was to patrol and monitor the ice-edge region in the vicinity of the drilling sites, and to serve as a rescue vessel in the event of an emergency. ERS-1 SAR images were used onboard the ice breaker as well as the drilling ship to monitor the ice edge. MSV Fennica is one of the newest and most advanced icebreakers belonging to the Finnish National Board of Navigation.

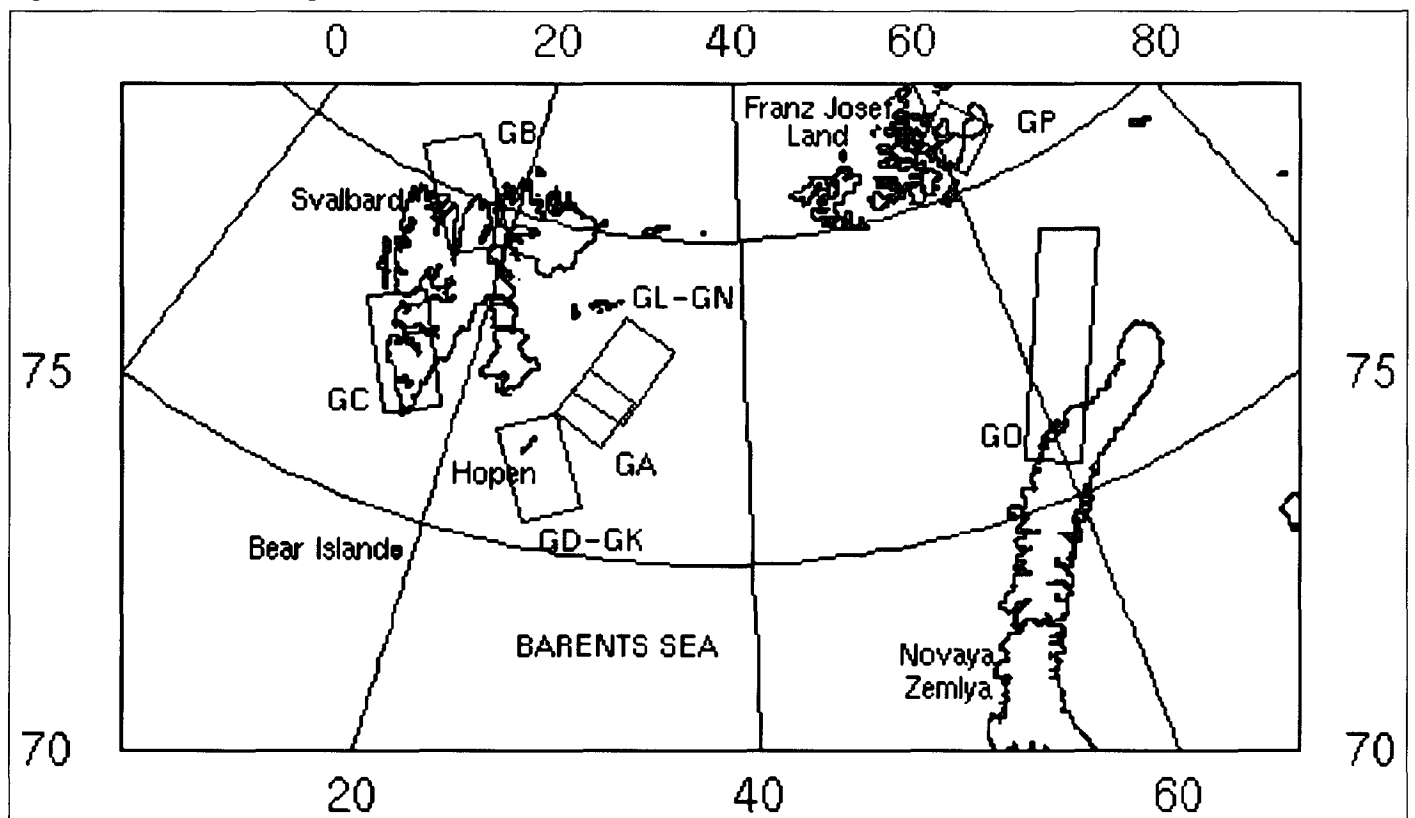
(Courtesy of the Finnish National Board of Transportation)



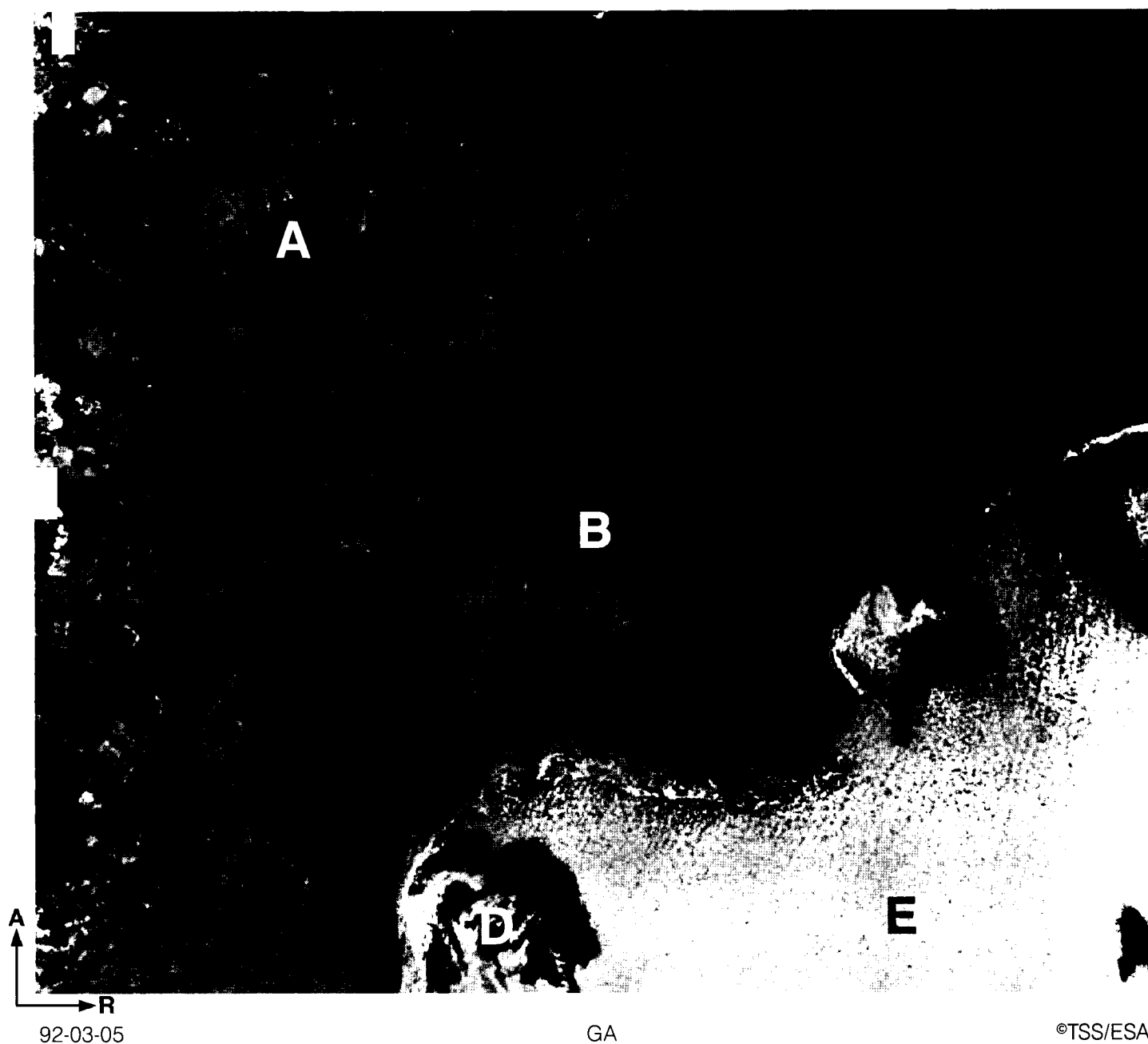
5. Barents Sea

The Barents Sea is a shallow sea located between the north of Norway, Svalbard, Franz Josef Land and Novaya Zemlya (Fig. 10). It covers an area of about 1.4 million km², most of which is within the economic zones of Norway and Russia. The Barents Sea has large potential oil/gas fields and the fishery resources are among the most important in Europe. However, the exploitation of both fish and, in the future, oil/gas resources is severely restricted by the presence of sea ice and icebergs. During the winter, more than 70% of the Barents Sea can be covered with ice 1–3 m thick. Only the southwesterly part, between Bear Island, the Kola peninsula and the north of Norway, is ice-free throughout the year. During the summer, only the northern part of the Barents Sea is covered with ice. However, there is a large inter-annual variability in the maximum ice extent, in both summer and winter, associated with a varying inflow of warm Atlantic water from the south and outflow of cold, dense bottom water. Short-term variability of the ice conditions is significant due to wind forcing, eddy circulation, tidal currents and wave activity. Investigations of ice conditions by airborne SAR were carried out during field experiments in 1987 and 1989 (Sandven & Johannessen, 1993). Since the launch of ERS-1, several hundred SAR scenes have been obtained in the area around Svalbard and in the western Barents Sea. Many of these were analysed and validated during the Seasonal Ice Zone Experiment (SIZEX 92) reported by Sandven et al. (1993).

Figure 10. Location of SAR images used in this section.



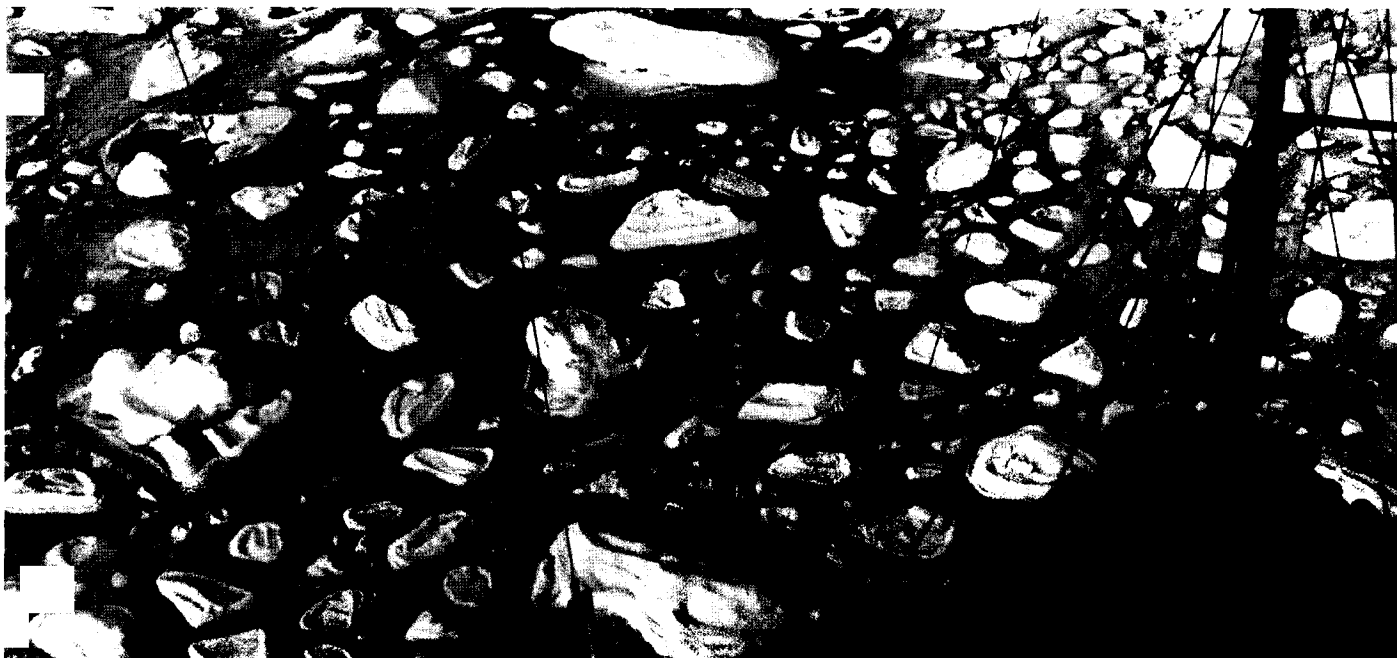
The SIZEX 92 Experiment



The SAR image of 5 March 1992 is one of a series of images obtained in the western Barents Sea where the SIZEX 92 experiment was carried out during the winter of 1992. SIZEX 92 was a sea-ice validation experiment for ERS-1 SAR, whereby in-situ observations of different ice types were made using a specially strengthened vessel (R/V Polarsyssel), helicopter and aircraft. The image, which is from the area northeast of Hopen, shows all of the most important ice types found in the Barents Sea during winter time, such as multi-year ice, consolidated first-year ice, broken-up first-year ice in the marginal ice zone, refrozen leads, pancake ice and grease ice. Numerous small icebergs some 100 m in size were also observed in the area, some of which were also identified in the SAR-images.

A = Large multi-year floes
 B = Broken up first-year ice
 C = Ice edge
 D = Pancake ice and grease ice
 E = Open water.

Photographs of Sea Ice in the Barents Sea



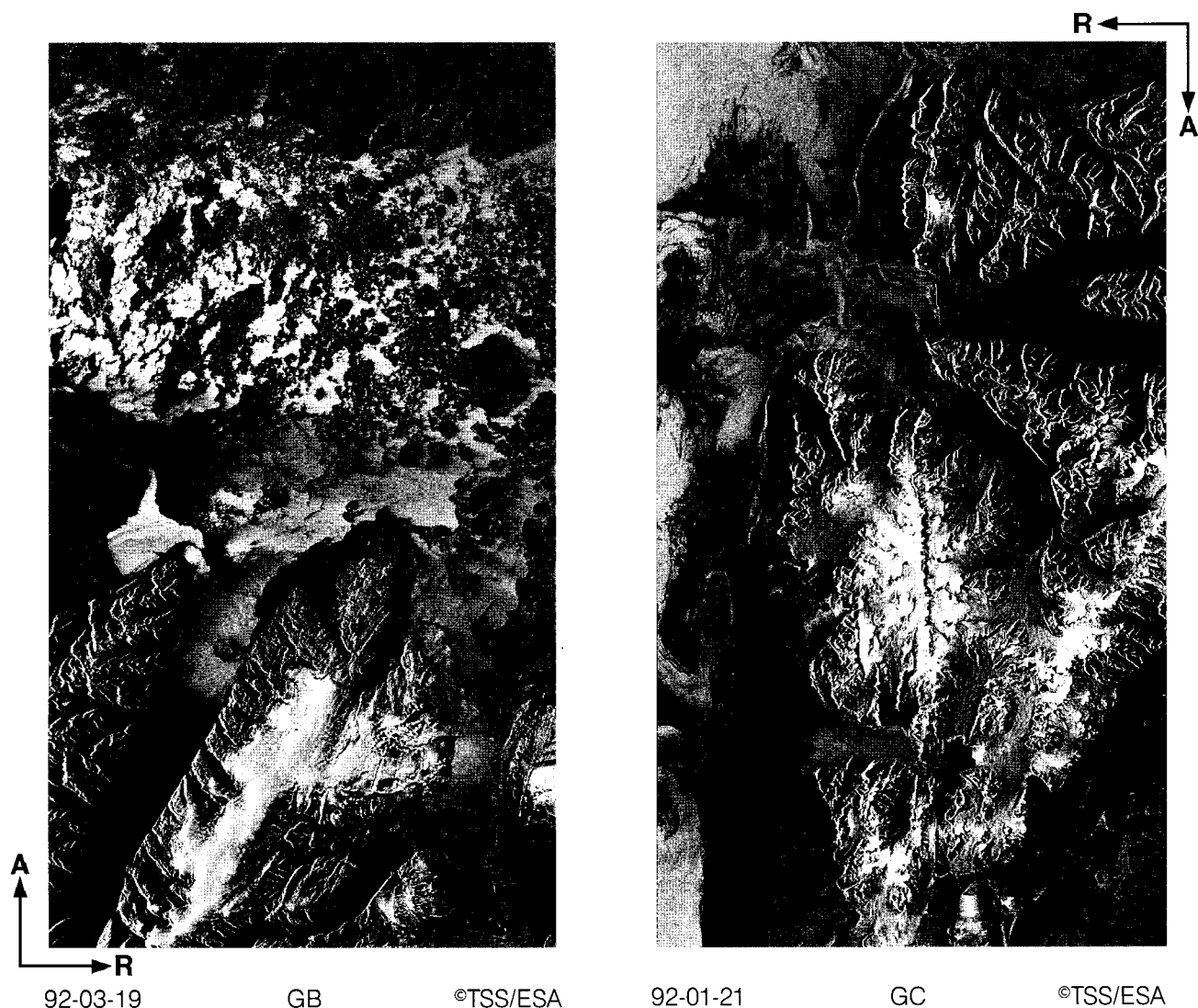
Photograph A. Compact pancake ice and brash ice observed from Polarsysssel



Photograph B. Drifting multi-year floe observed from helicopter

Numerous photographs of the ice were taken during the SIZEX 92 experiment. Photograph A shows compacted pancake ice and brash ice, which was found 100 m inside the ice edge after a period of strong on-ice winds. The floe size is 1–2 m and the thickness 30–50 cm. Photograph B shows part of a 10 km-sized multi-year floe (to the right) which was investigated by helicopter during SIZEX 92. The multi-year floe is characterised by a smooth surface covered with a 50 cm layer of snow. The floe thickness varied from 2.0 to 4.5 m. The ice to the left of the multi-year floe is mainly first-year ice with ridges and some refrozen leads.

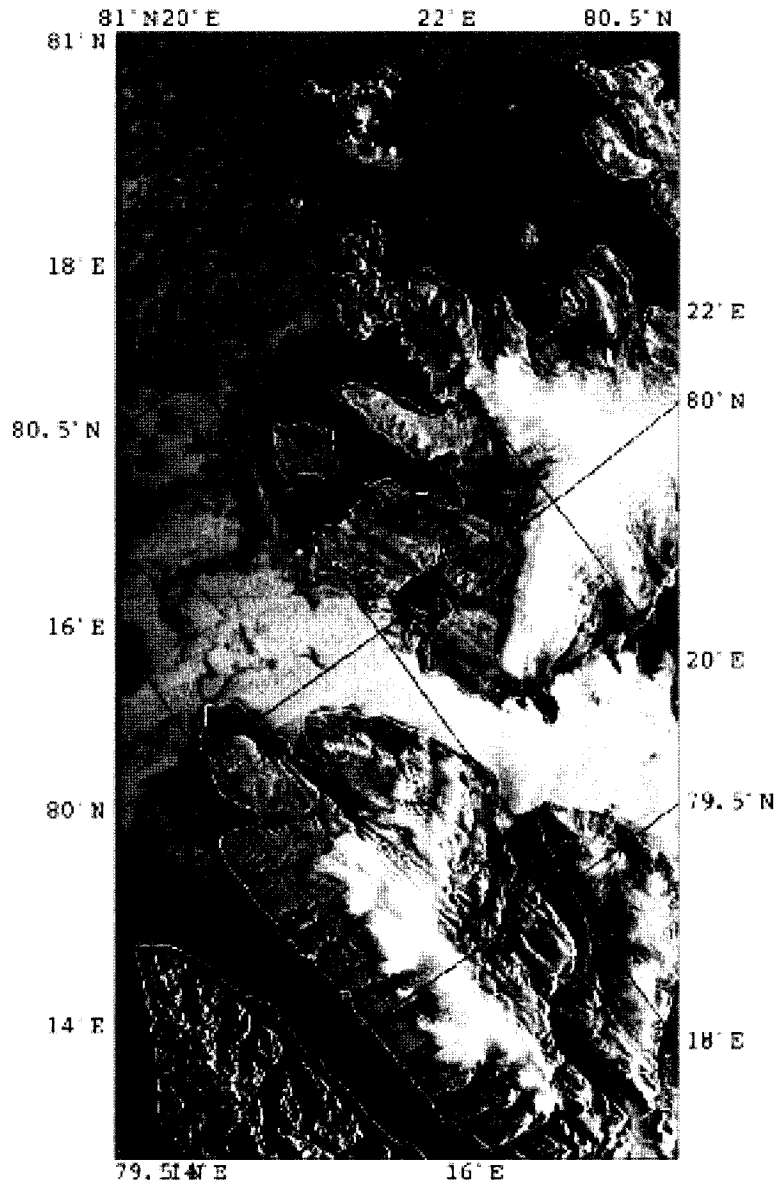
The North and West Coasts of Svalbard



The area north of Svalbard can be ice-free even in the winter due to the West Spitzbergen Current, which transports warm water to the area. The image of 19 March 1992 shows multi-year ice in the upper part of the image, which is present throughout the year. Further south, an area of scattered ice (ice concentration of 50%) is to be found, where open water is identified by the bright areas in the image. This bright signature of open water suggests that the wind speed is more than 6–8 m/s. The ice edge was found just to the left of the image in this period. Some fjords and a glacier on northern Svalbard are seen in the lower part of the image.

The image obtained over the southwestern coast of Svalbard (21 January 1992) shows a band of compact first-year ice along the west coast in the lower part of the image. This ice originates east of Svalbard and is transported along the coast by the ocean currents. Further north, newly frozen ice, especially grease ice, is identified as dark patches off the coast. Also, the fjords are covered with ice which is usually formed locally. Isfjorden, in the upper part of the image, has some scattered ice and patches of open water. The ice conditions in Isfjorden are important for the ship traffic to and from Longyearbyen, the main port of Svalbard.

Shrimp Trawling North of Svalbard

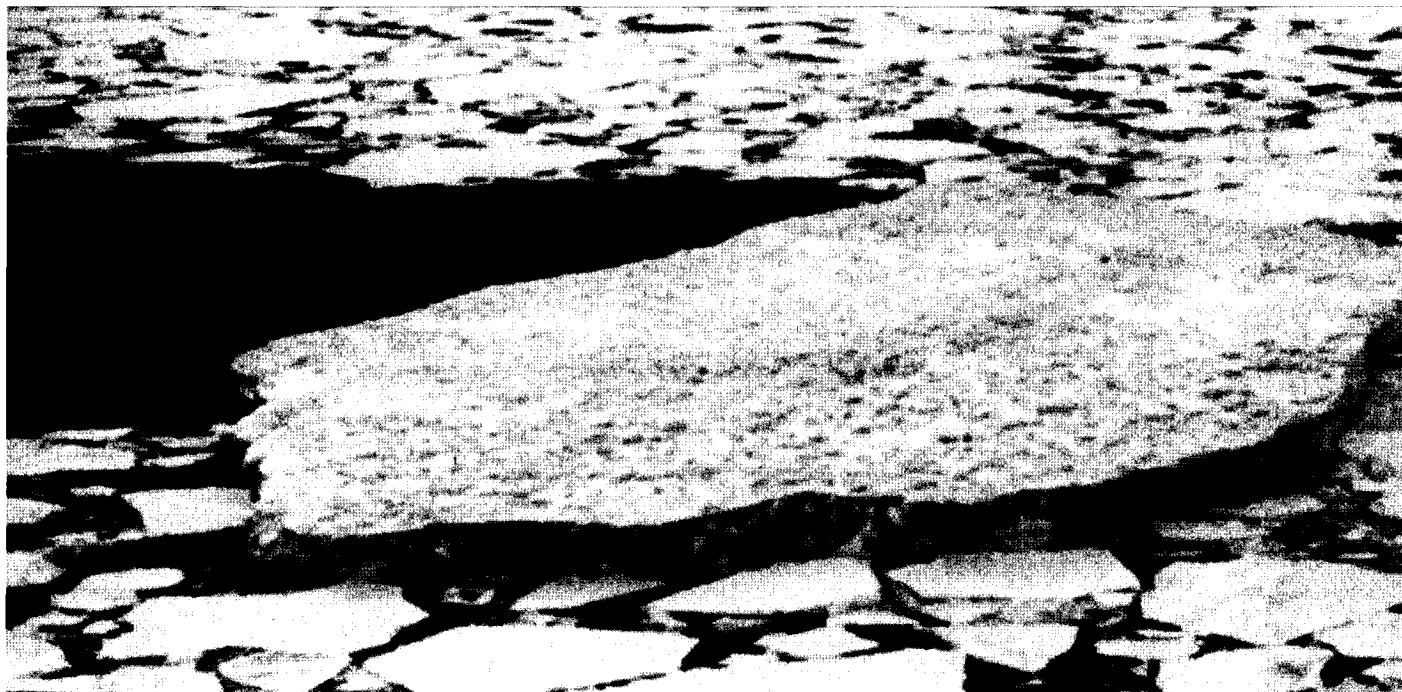


The shallow banks on the north coast of Svalbard are an important fishing area, especially for shrimp trawling. The area is affected by ice for most of the year. In the summer, the ice edge is usually located north of 81°N, keeping the fishing banks ice-free. In the wintertime, the north coast is usually ice-covered, but during southeasterly winds it can become ice-free, allowing fishing vessels to enter the area.

Detailed ice mapping by SAR has been demonstrated several times for shrimping vessels such as the Ocean Trawler. SAR imagery obtained in near-real-time, as shown in this example, has been used by the Ocean Trawler to decide if she should enter the area. Particularly in the dark winter season, no other data can provide reliable ice maps in the area.

This SAR image, from 2 December 1994, also shows areas of open water (bright signature) in the Hinlopen Strait and along the north coast of Svalbard.

Photograph of Drifting Iceberg



The photograph shows a drifting iceberg about 60 m long and rising 6 m above the surface. It was located about 10 km inside the ice edge and was surrounded by a 90–95% concentration of broken-up first-year ice.

Rapidly Changing Ice Edge in the Hopen Area (next pages)

A time series of eight SAR images obtained at three-day intervals in February and March 1992 shows how the ice edge changes with varying winds in the Hopen area. The wind data from this area are shown below in Figure 11. In the period from 21 to 24 February, southeasterly winds prevailed and pushed the ice edge northwards. From 24 to 27 February, the winds were weak and no displacement of the main ice edge was observed, but formation of grease and pancake ice is clearly seen image GF. In the next three days more southeasterly winds pushed the ice edge north of Hopen. From 1 to 4 March, a northerly wind displaced the ice edge back to the south of Hopen, where it remained for the next 9 days. In all images, areas of new ice formation can be seen outside the main ice edge, caused by low air temperatures ranging from -10 to -25°C . Areas of open water around the island also show how the ice moved in different directions 1 to 2 days prior to each image.

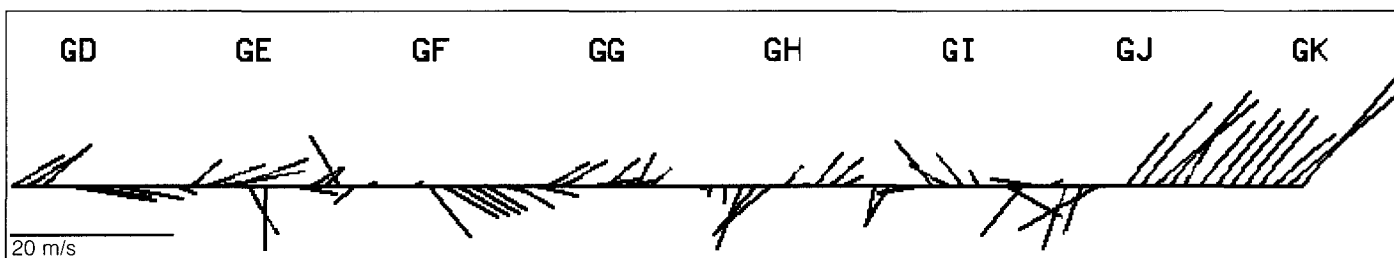


Figure 11. Wind vectors in the Hopen area every 6 hours from February 21 to March 13, 1992. GD-GK denote times when the SAR images were obtained.



92-02-21

GD



29-02-24

GE



92-02-27

GF



92-03-01

GG



92-03-04

GH



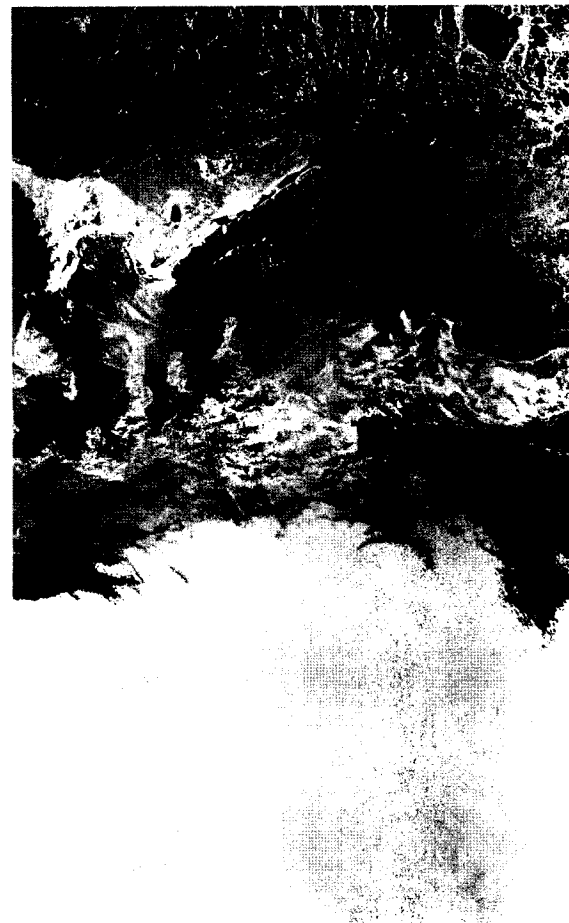
92-03-07

GI



92-03-10

GJ



92-03-13

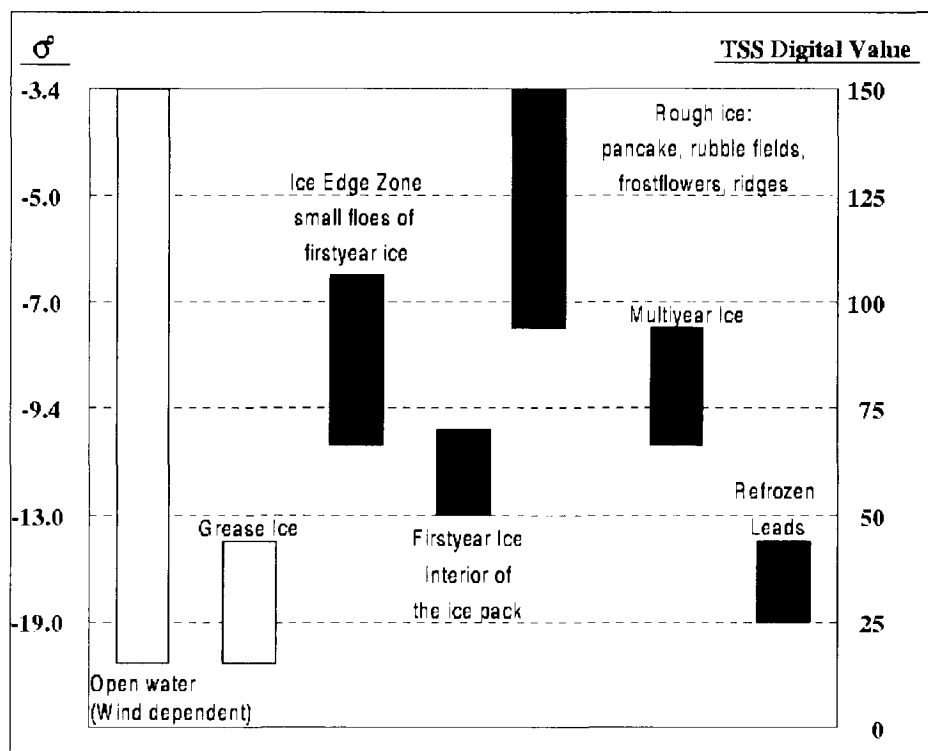
GK

©TSS/ESA

Sea Ice Classification

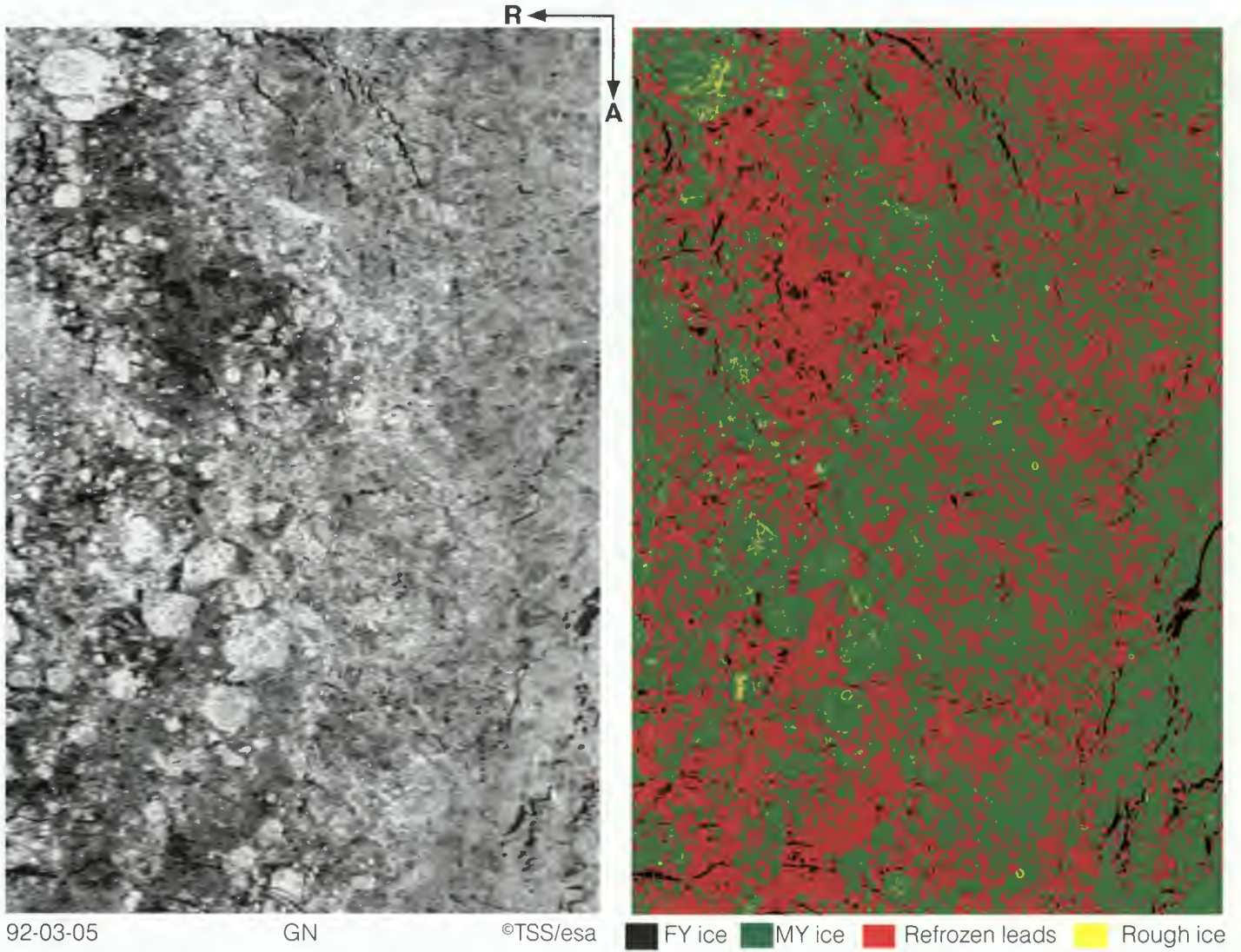
Since the SAR backscatter varies with type of ice, snow cover, surface roughness and other ice characteristics, it is possible to classify SAR imagery into several ice types. Two principles can be applied: one is to use calibrated backscatter values for each individual pixel, and the other is to use textural information in the image. The first principle requires knowledge about the relationship between SAR backscatter value and ice type/surface characteristics. Such relations have been established through a series of validation experiments. Textural classification can be used as a supplement to backscatter levels. None of these methods is fully automatic and reliable classification requires manual analysis by an expert.

During the ERS-1 experiments in the Greenland and Barents Seas, SAR signatures of water and different types of ice were studied during winter conditions. The diagram below shows the range of SAR backscatter versus surface type established from the validation experiments. This diagram was used in combination with textural information to classify the SAR image (GN) on the following page.



Backscatter versus surface type in winter conditions.

Classification of Winter Ice



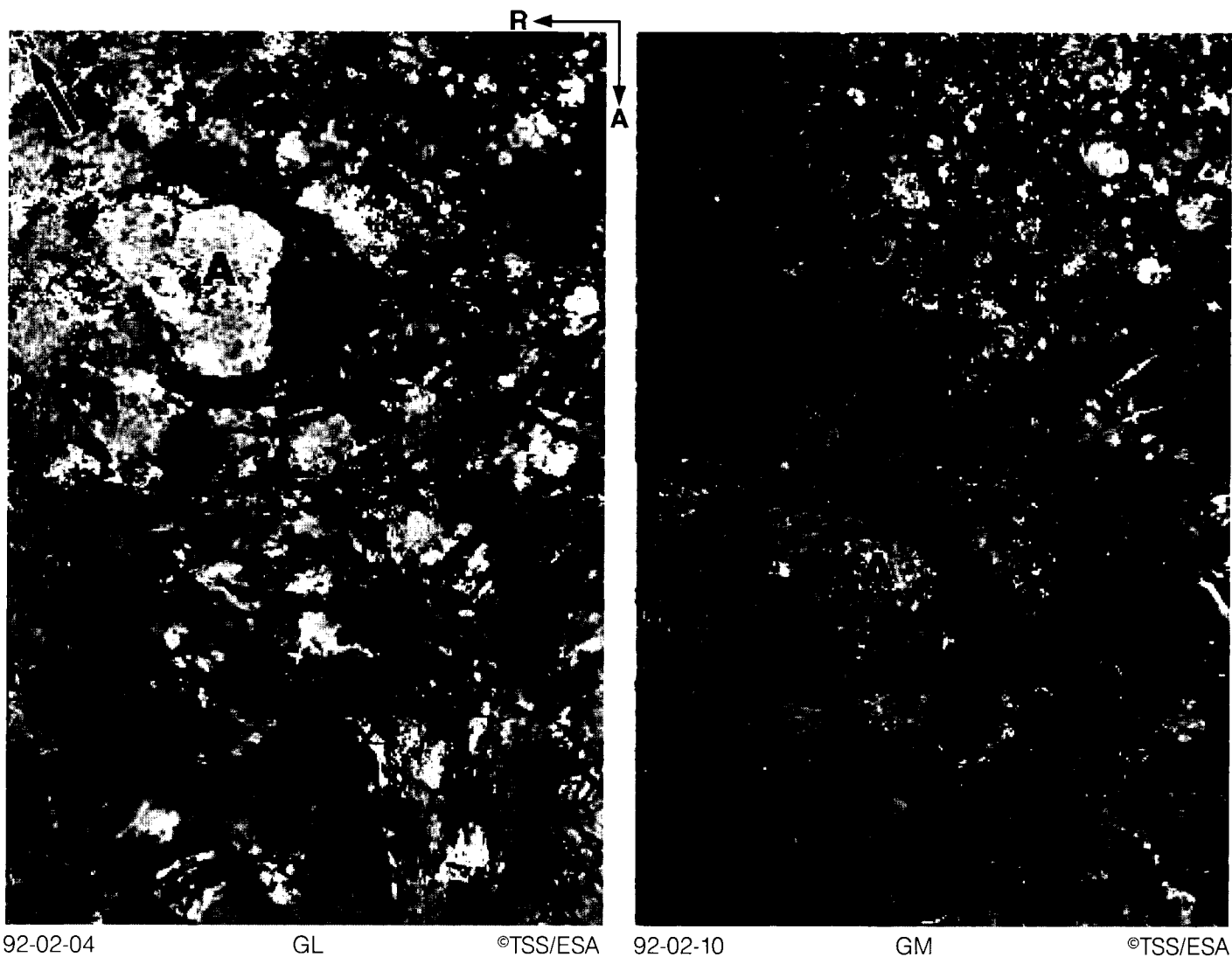
92-03-05

GN

©TSS/esa

■ FY ice ■ MY ice ■ Refrozen leads ■ Rough ice

Ice Dynamics inside the Ice Edge



In the area east of Svalbard, multi-year ice from the Arctic is transported southwards by the East Spitsbergen Current. The multi-year ice is identified as the brighter floes or cluster of floes in the SAR images above. The two images were taken 6 days apart in February 1992 and cover the same geographical area. The ice pack was drifting southwestwards at a speed of about 10 km per day. The largest floe (marked A) in the image to the left is a 40 km long multi-year floe. After 6 days, this floe had moved 60 km and had broken into several pieces. Another interesting observation is the occurrence of several leads orientated in an east-west direction in the left image, to the left. The leads are characterised by a dark signature, indicating thin ice. These leads had disappeared 6 days later owing to a compaction of the ice field.



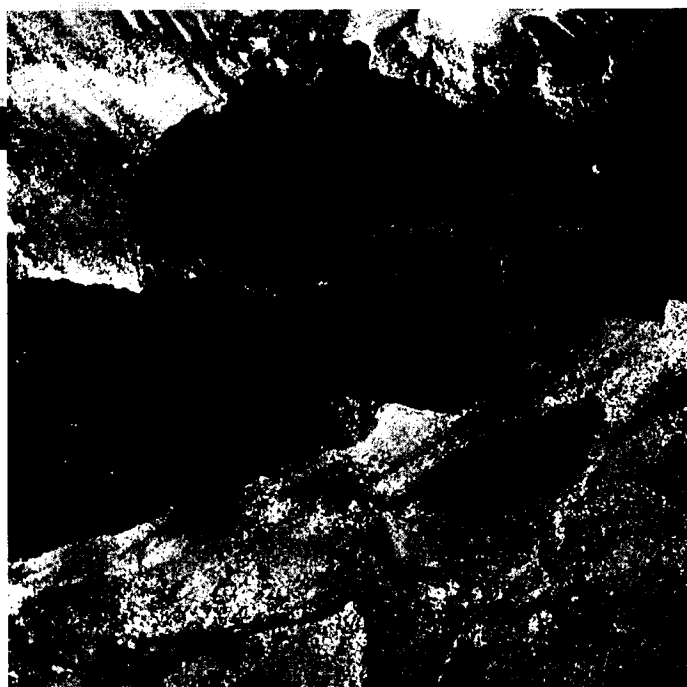
92-03-28

GP

©TSS/ESA

Glaciers of Franz Josef Land

This image shows some of the islands of Franz Josef Land covered by glaciers, which have bright SAR signatures in winter. The sea ice is represented by the dark areas of the image, indicating level first-year ice. In the lower part of the image, the greyish signatures represent rough ice outside the archipelago where the ice motion is more dynamic. The lower image, which covers about 25 x 25 km, is a subimage of the full scene above. It is an enlargement of an area where icebergs are produced and can be recognised in the SAR image. Many of the icebergs which drift away from Franz Josef Land are transported to the area between Hopen and Bear Island (Vinje, 1985). Repeated SAR images over several years can be useful in the monitoring of iceberg production.



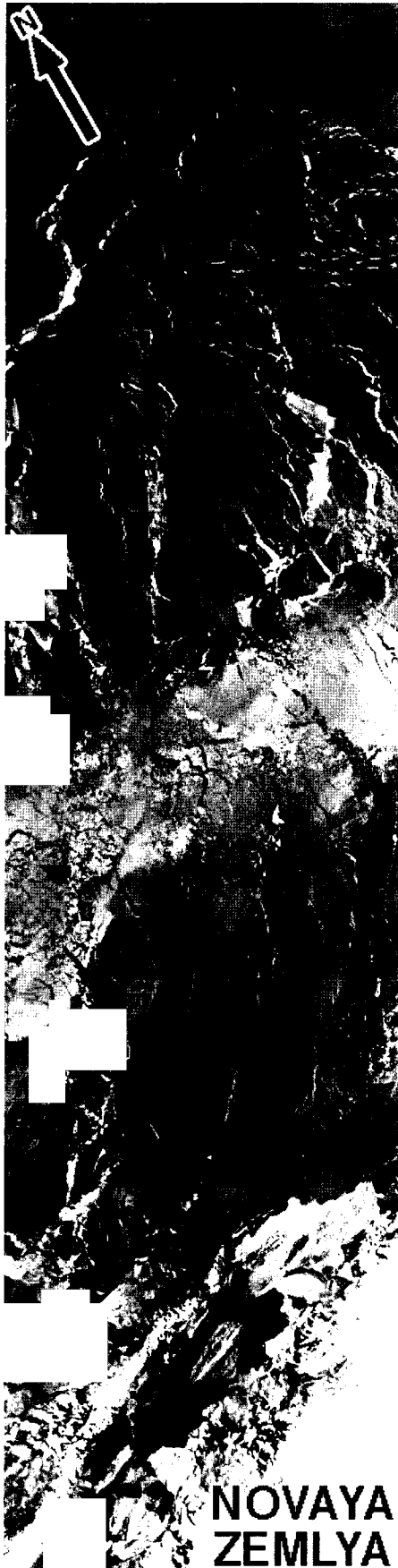
92-03-28

GQ

©TSS/ESA

The Northeastern Barents Sea

This SAR swath, obtained on 30 March 1992, covers part of the strait between Novaya Zemlya and Franz Josef Land in the northeastern part of the Barents Sea, where sea ice is present throughout the year. The ice in this image is primarily first-year. There is no influence from ice-edge eddies and surface waves from the open ocean as in the western Barents Sea. The ice cover is therefore characterised by consolidated ice broken up by shear zones and leads formed as a result of the ice motion. Dark leads indicate that thin ice has formed, whereas bright leads suggest that either open water or ice with high surface roughness is present. In the southern part of the image, land-fast ice and shore leads off the coast of Novaya Zemlya can be seen.



92-03-30

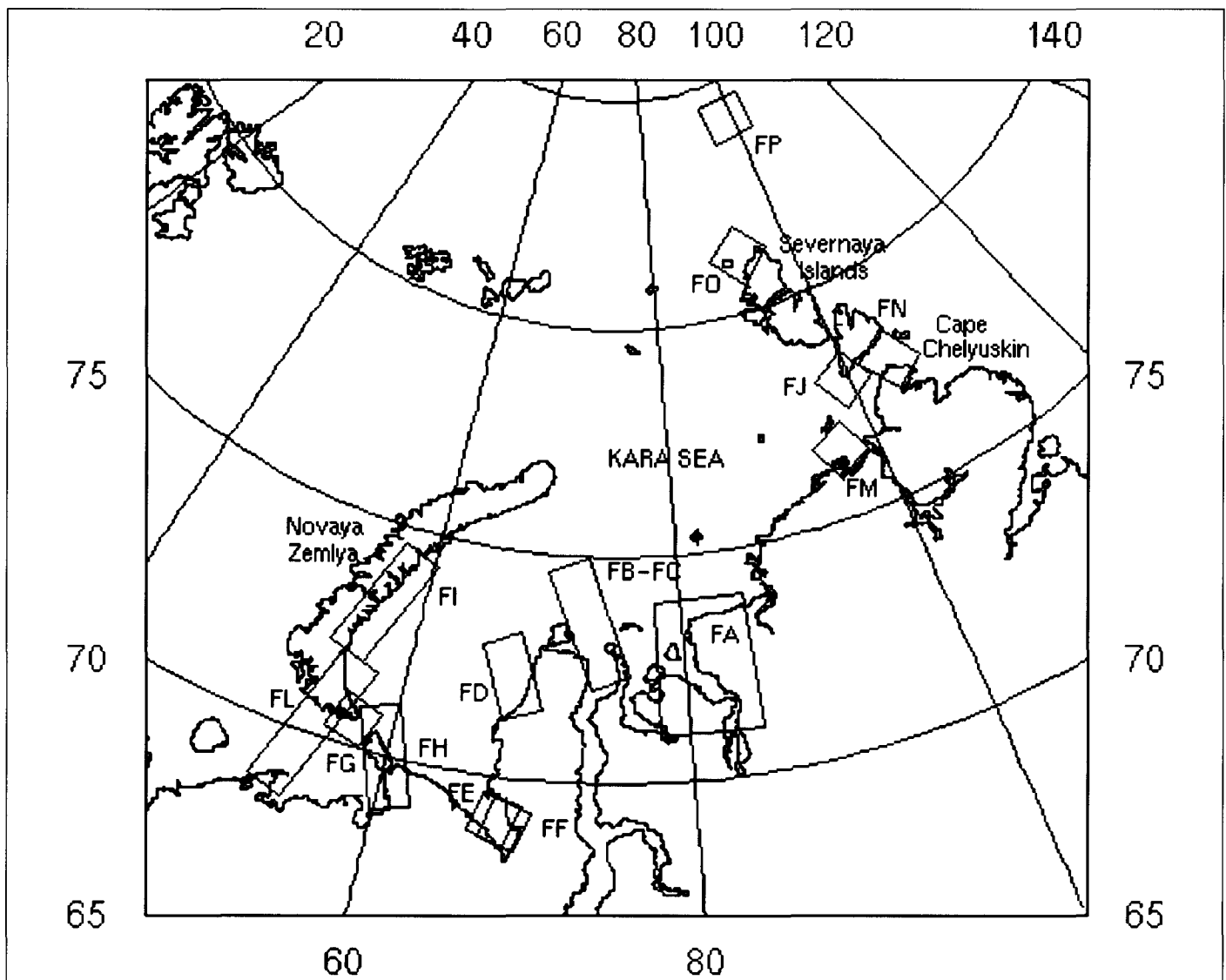
GO

©TSS/ESA

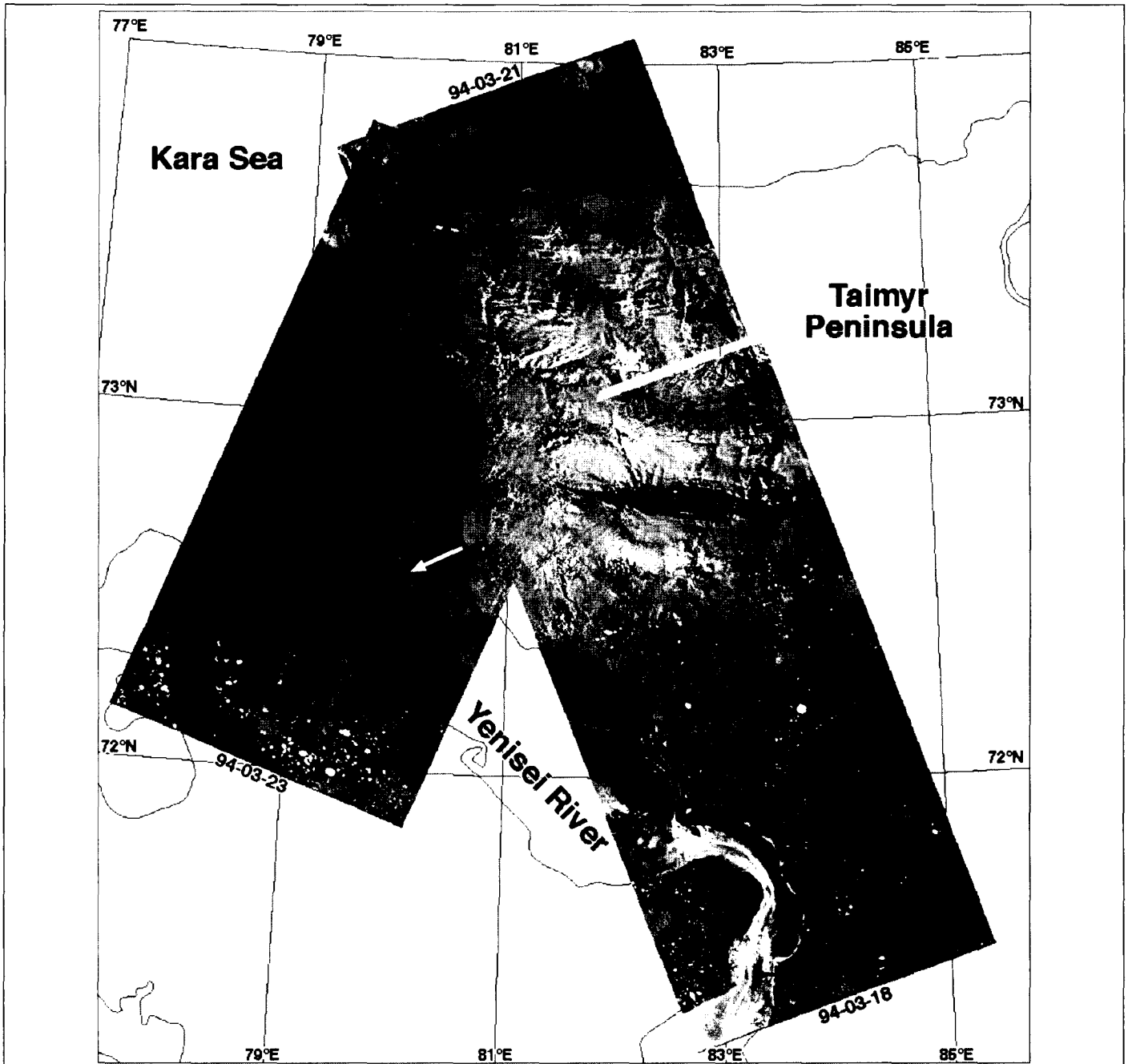
6. Kara Sea

The ice conditions in the Kara Sea are strongly influenced by the freshwater discharges of two large rivers, the Ob and the Yenisei. The Kara Sea is a shallow sea bounded by Novaya Zemlya in the west and Severnaya Zemlya in the east. Warm Atlantic water masses, which keep the southern Barents Sea ice-free in the winter, do not enter the Kara Sea. It is therefore totally covered with ice in the winter season, usually from November to June. The Kara Sea is also characterised by land-fast ice along a major part of the coast, which can be identified and mapped by SAR images. The river discharge causes the formation of fresh-water ice at the river outlets during winter. The characteristics of fresh-water ice are different from those of saline ice. In the river estuaries, different types of ice can be observed by SAR and the identification of fresh-water ice in SAR imagery is possible, but has not been documented yet. In the northeastern part of the Kara Sea, multi-year ice is present throughout the year. At the northernmost point of the Eurasian continent, Cape Chelyuskin, the ice conditions can be severe and may hamper ice-breaker navigation. This section presents ERS-1 SAR images from various parts of the Kara Sea, which are used for ice research and navigation.

Figure 12. Locations of SAR images used in this section



Icebreaker Route on Yenisei River



03-94

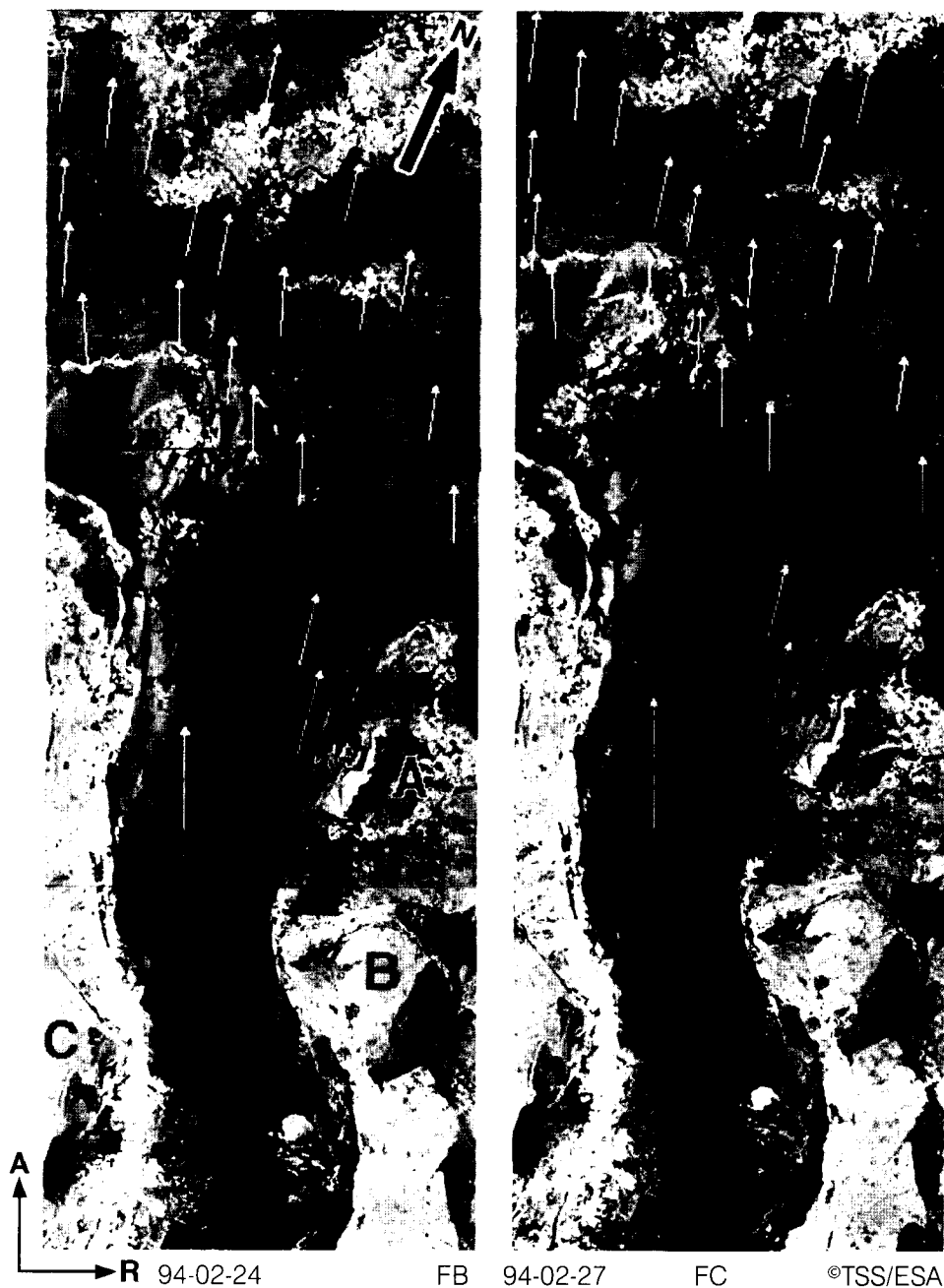
FA

©TSS/ESA

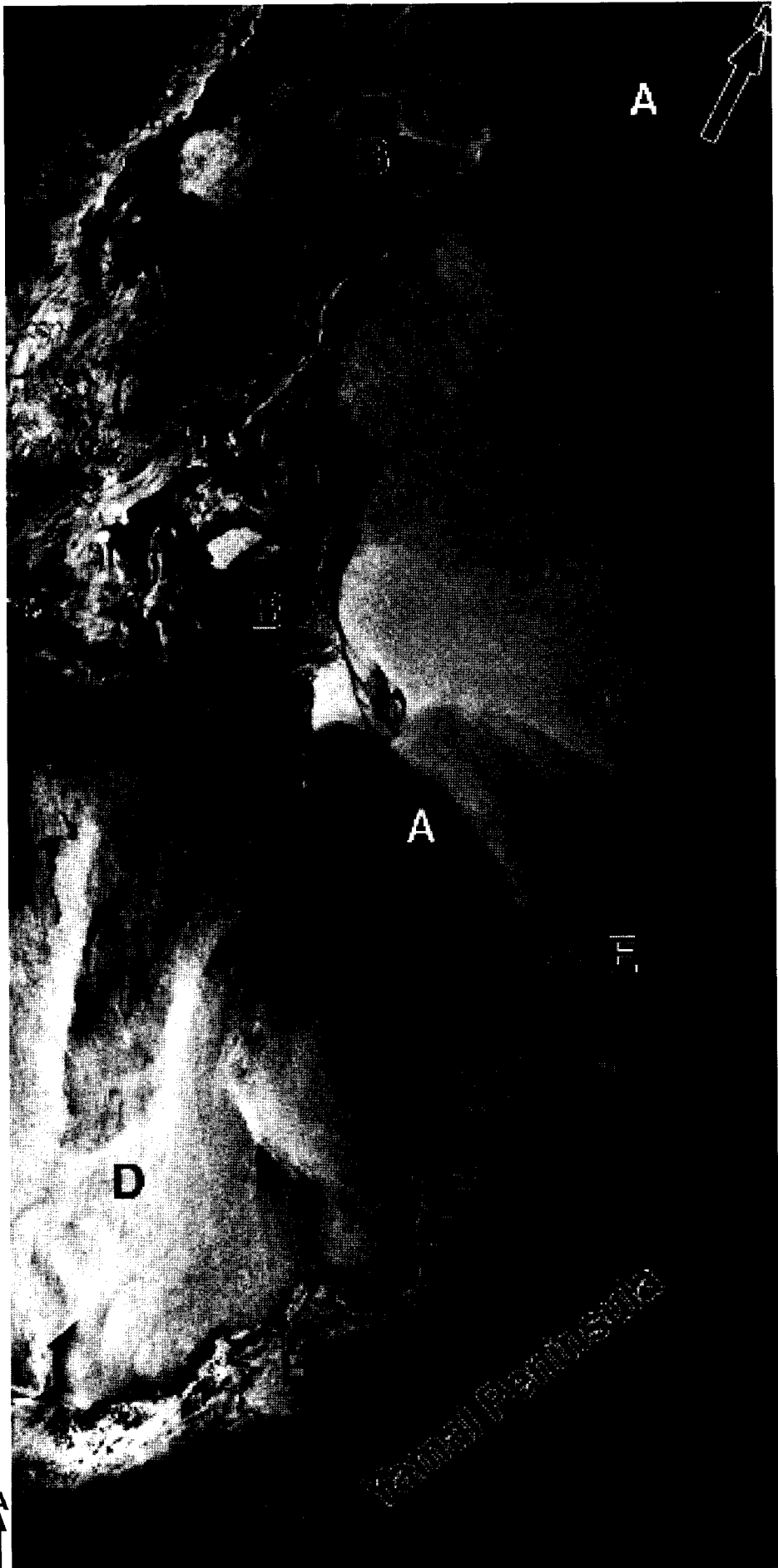
Ice monitoring using SAR images from ERS-1 has been shown to assist Russian icebreakers navigating the Kara Sea. SAR images have been obtained for some of the important sailing areas and sent out to icebreakers by telefax. Ship transportation on the Yenisei River occurs throughout the year although the river is ice-covered for more than half the year. The SAR image mosaic above is from the mouth of the Yenisei River and shows the ice conditions on 18 to 23 March 1994. The track in the ice made by icebreakers going up the river to the ports in Dudinka and Igarka is clearly shown in the image (see arrows). The SAR image also shows individual ice floes and areas of thin ice that are only a few days old.

Ice Motion in the Ob River Estuary

- A Landfast ice
- B Island
- C Yamal Peninsula



The Ob River releases large amounts of fresh water into the Kara Sea, which freezes in the winter season. Some of this ice is land-fast along the coasts, as can be seen in this pair of SAR images from 24 and 27 February 1994. In this period, southerly winds prevailed, causing the drifting ice to move towards the north. The ice displacement has been calculated from the two images using an ice kinematics algorithm and the velocity vectors are superimposed on the images. The mean displacement is 16 km in three days, which is equivalent to a mean ice speed of 6 cm/s. The dark signature is thin newly frozen ice which has formed as the thicker pack ice moved northwards. Some of the ice in this region is fresh-water ice, which is harder and more difficult for ice breakers to penetrate.



New Ice in the Kara Sea

This image is from late October 1993 when ice started to form in the southern Barents Sea. The darker areas (A) are grease ice, while the brighter areas in the upper left part of the image and along the Yamal peninsula (B) are grey-white ice 15-30 cm thick, which had formed in the previous two weeks. It is noteworthy that ice forms close to land before it forms in deeper water (D). There are several ice tongues and meanders along the coast (E) which reflect mesoscale ocean currents. The ice pack in the northern Kara Sea (upper left), advances southwards during the autumn, and by late November the Kara Sea is usually completely ice-covered.

93-10-29

FD

©TSS/ESA



93-11-01

FE

©TTS/ESA



93-11-17

FF

©TSS/ESA

Freeze-up in Baydaratskaya Bay

Estimation of the freezing period in Baydaratskaya Bay is based on statistical data, especially the continuous series of satellite data starting in 1979. These data show that the most important freezing period in the bay is from week 42 to 45 (mid-October to early November). In some years, the freezing period was 3–4 weeks later. Russian observations, which started in 1920, show that freezing can start as early as week 40 (first week of October). In 1993, SAR images from ERS-1, combined with meteorological data, were used to monitor the freeze-up period more accurately. The images on the opposite page show a characteristic behaviour of the freezing process. During southwesterly winds, ice is formed first on the eastern coast. On 1 November, most of the bay is open water with strips of grease ice oriented parallel to the wind direction. The ice accumulates in the down-wind direction and in the next two weeks the ice cover grows towards the west. On 17 November only a narrow band of open water (bright signature) is still present.

The freeze-up of the bay can be delayed if the trajectory of the low-pressure systems in November goes from the Svalbard area towards Severnaya Zemlya, causing warm southwesterly winds to flow over the bay. The ice edge in the Kara Sea is pushed towards the northeast and the cooling of the water and the associated ice formation is delayed. This situation can be monitored with the aid of ice maps based on meteorological satellite data. The ocean temperature data will show a delay of the cooling in the water column. The low-pressure trajectories, as soon as they have been established, tend to follow the route from Svalbard and head eastwards for some weeks, especially if a strong high-pressure area is settled over central Russia. This was the case in November 1993, when the western side of the bay was kept ice-free for several weeks.

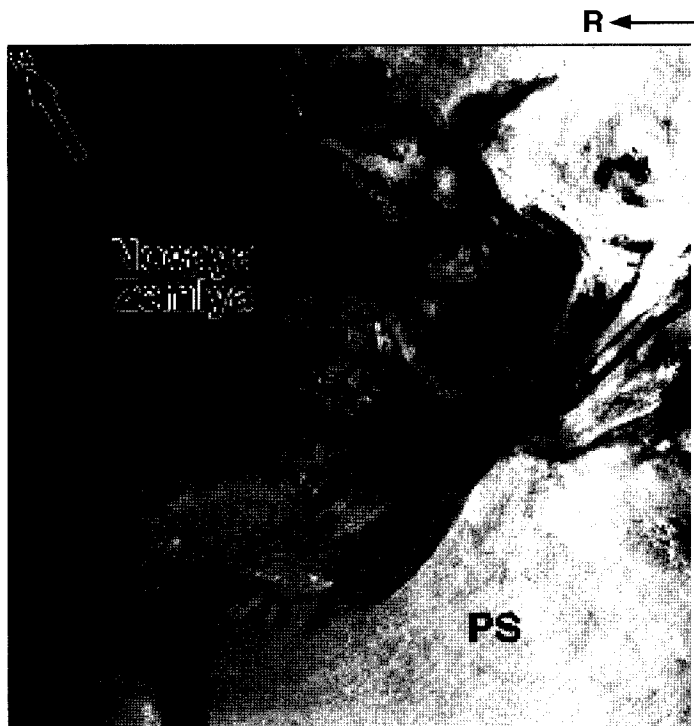
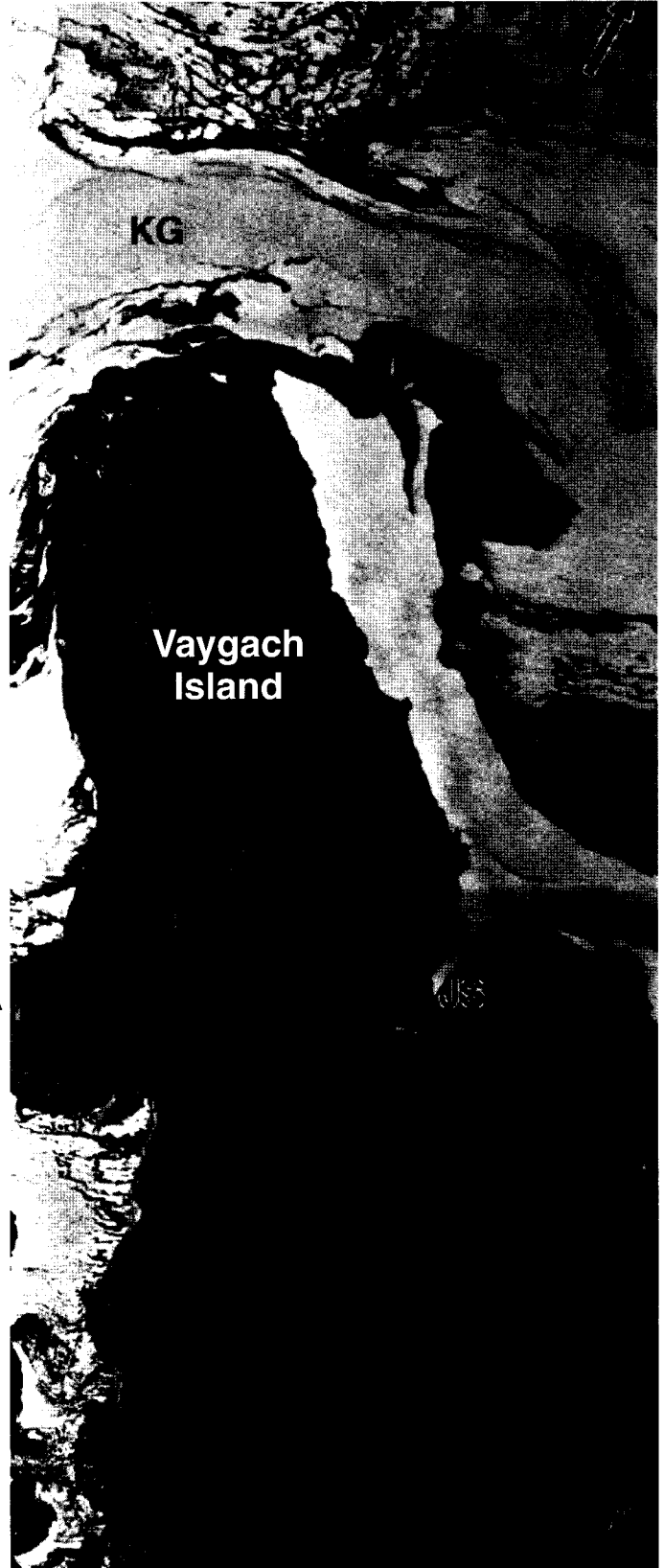
Early freeze-up has not been observed in the last 15 years. A situation which will encourage early freeze-up is that of a high-pressure area settled over the Kara Sea and Barents Sea region during September and the beginning of October. The high pressure will generate cold air masses, which cool the water column to freezing point within a couple of weeks. Ice formation can then start in early October. However, if early freezing occurs, there is some probability that the ice concentration only reaches 60–80%, or if it goes up to 90–100% it will be reduced again after a few weeks. This will be the case if the high pressure over the Kara Sea disappears and is replaced by a series of eastward-moving low-pressure areas.

New Ice in the Kara Gate and Jugor Strait

The new ice observable in SAR images is useful for studying surface currents and ice drifts in the Kara Gate (KG) and the Jugor Strait (JS), which are the main links between the Barents Sea/Pechora Sea (PS) and the Kara Sea. The image below (21 October 1993) shows the southern tip of Novaya Zemlya and strips of grease ice which indicate that the surface current transports ice from the east coast of Novaya Zemlya, through the Kara Gate and into the Pechora Sea.

The image on the right was taken four weeks later (on 19 November 1993) and shows that there was still much open water in the Kara Gate. The westerly winds are driving the surface current, including bands of new ice, from the Pechora Sea into the Kara Sea. The winds also cause ice to accumulate on the west coast of Vaygach Island and the mainland, and drive a band of ice through the narrow Jugor Strait.

The Kara Gate and Jugor Strait are important sailing routes in which the sea ice can cause difficulties when combined with strong currents. SAR images can provide detailed maps of the ice conditions which are useful for shipping.



93-10-21

FG

©TSS/ESA

93-11-19

FH

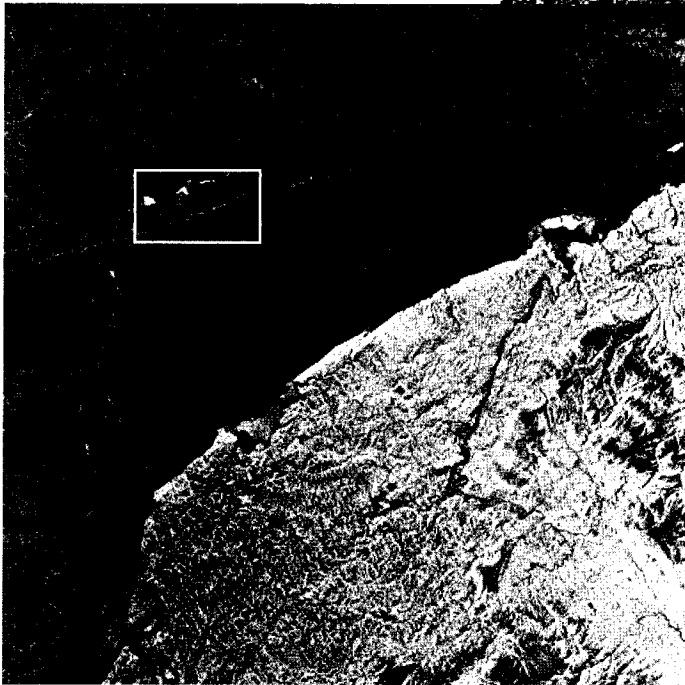
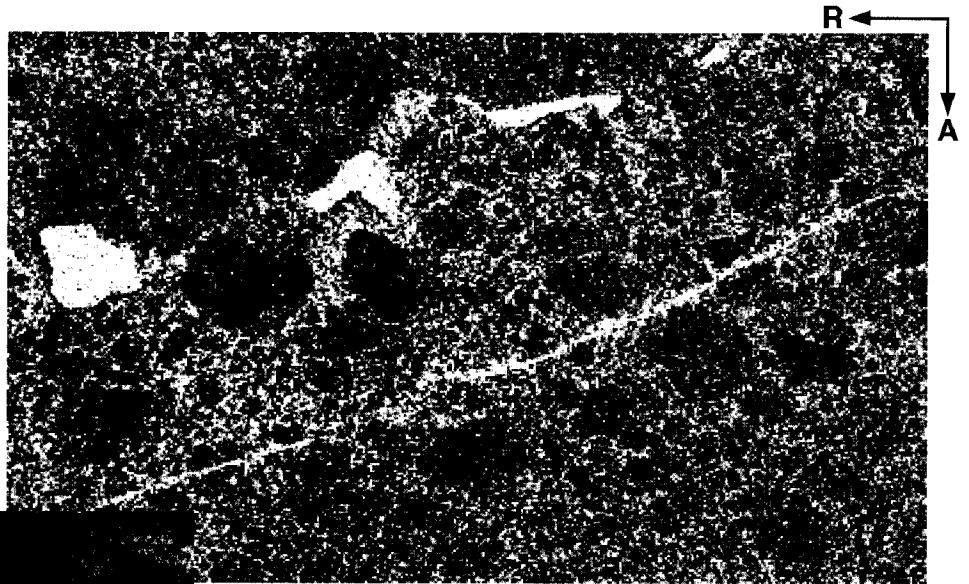
©TSS/ESA



East Coast of Novaya Zemlya

During westerly winds in the winter, the ice off the east coast can drift away from the coast, leaving a polynya of open water which refreezes. The SAR strip of 19 April 1993 shows a refrozen polynya as a band with a dark signature along the whole image. The refrozen polynya consists of young ice, 10–30 cm thick, with a smooth surface which produces low SAR backscatter signals. The Novaya Zemlya coastal polynya with a cover of young ice is a preferred sailing route for icebreakers in east–west transit, if the ice conditions further south are difficult. An icebreaker track is observed in the image as a bright line through the dark young ice. The image also shows open leads (bright linear features) oriented southeast–northwest, caused by a differential motion of the ice pack.

The L'Astrolabe Expedition through the Northeast Passage



FJ

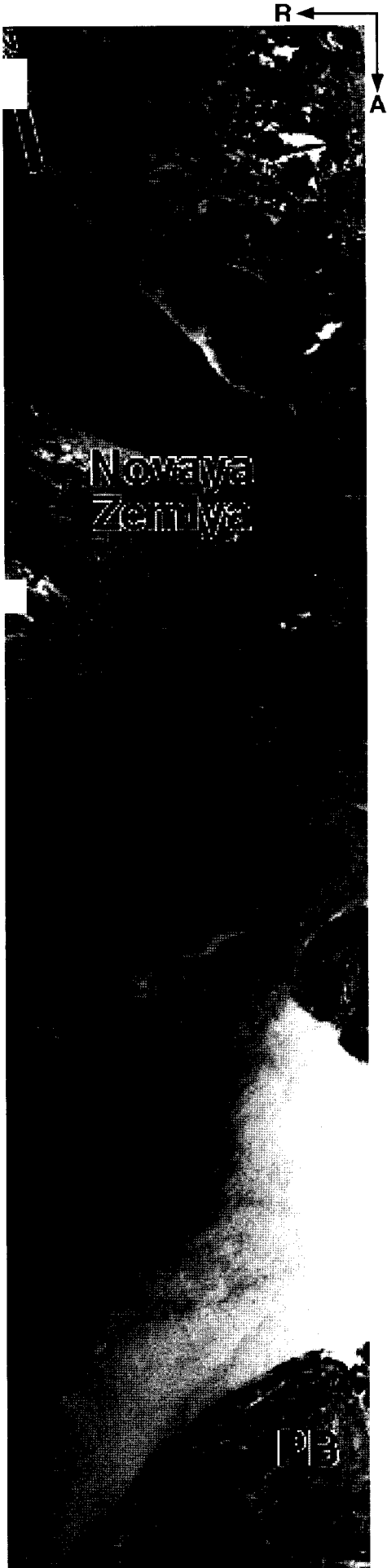
91-08-16

©TSS/ESA

As the first civilian foreign ship since the Maud expedition in 1918-20, the French polar vessel L'Astrolabe was allowed to sail the Northern Sea Route in August 1991. The purpose of the voyage was to reopen the sea route for international merchant shipping and to gain navigational experience along this route for future users. The expedition was organised by Mers Magnétiques, a French association for environmental conservation in the Arctic. The major problem preventing regular shipping through this Northern Sea Route is the cold climate, with large areas of ice-covered seas. Even during the period of minimum ice extent in late summer/early autumn, parts of this Northern Sea Route are covered by sea ice. The L'Astrolabe expedition coincided with the acquisition of the first detailed SAR ice images from the ERS-1 satellite. The satellite was launched on 16 July 1991 and the first SAR images were produced just two weeks later. The image above was obtained a month after the launch and was sent to the L'Astrolabe in near-real time for use in ice navigation. The full image covers 100 x 100 km of the sailing route west of

Vilkitskogo Strait, with a pixel size of 100 m. The enlarged subimage is full-resolution (20 x 16 m pixel size) and covers about 10 x 15 km of the sailing route. The icebreaker's track as well as ice floes and some small islands are visible in the image.

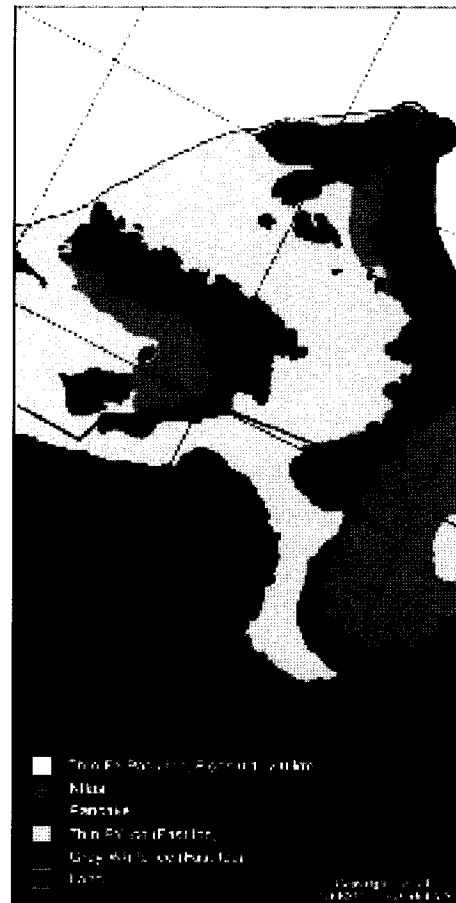
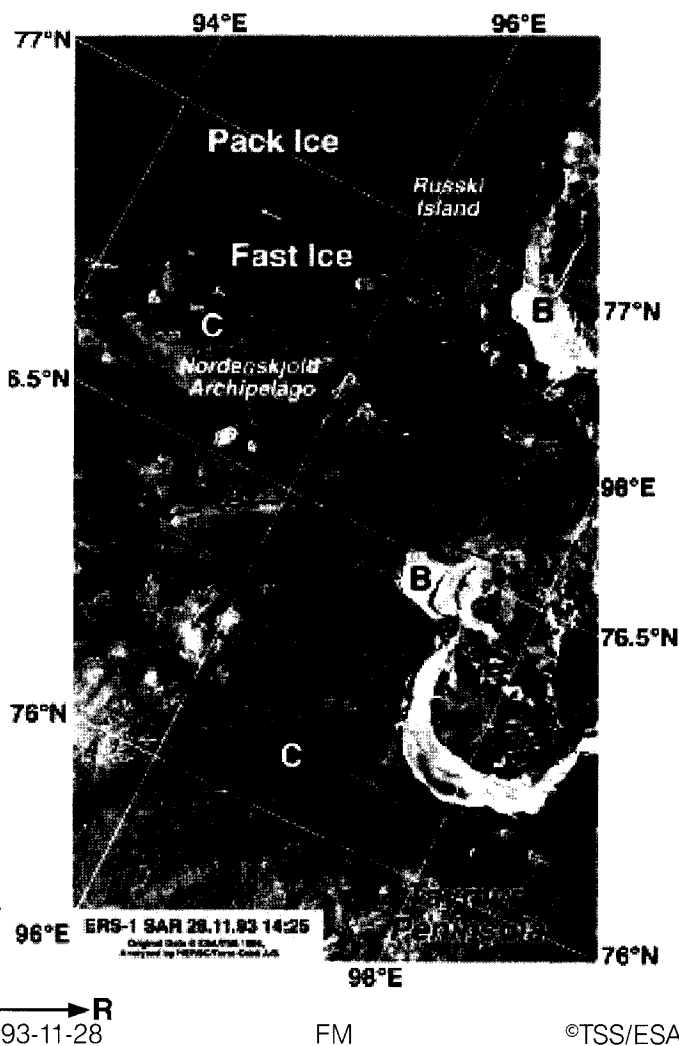
The SAR ice-routing project was set up jointly by NERSC, Mers Magnétiques, ESA, the Norwegian Space Centre and the Alaska SAR Facility (ASF). The purpose of the project was to demonstrate that ERS-1 SAR images, transmitted to icebreakers in near-real time, could be useful for navigation in sea ice. This project was the first in a series of demonstrations in which ERS-1 SAR data were used for ice monitoring in the Kara Sea region.



Eddy Currents in the Pechora Sea

This strip covers 400 x 100 km and includes some of the Kara Sea, the southern part of Novaya Zemlya, a section across the Pechora Sea, and some of the mainland. The image was taken on 12 November 1993 and shows several ice phenomena in the freeze-up period. In the lower part, the Pechora Bay (PB) is covered by young ice, while the southern part of the Pechora Sea is ice-free. Further north, grease ice and pancake ice show a complex pattern of several eddies and meanders which reflect the mesoscale ocean circulation in the area. The ice in the Pechora Sea is not more than two weeks old. In the Kara Sea, however, several ice floes of various sizes can be identified. Some of the ice in this region formed earlier in the season and was subsequently advected southwards along the east coast of Novaya Zemlya.

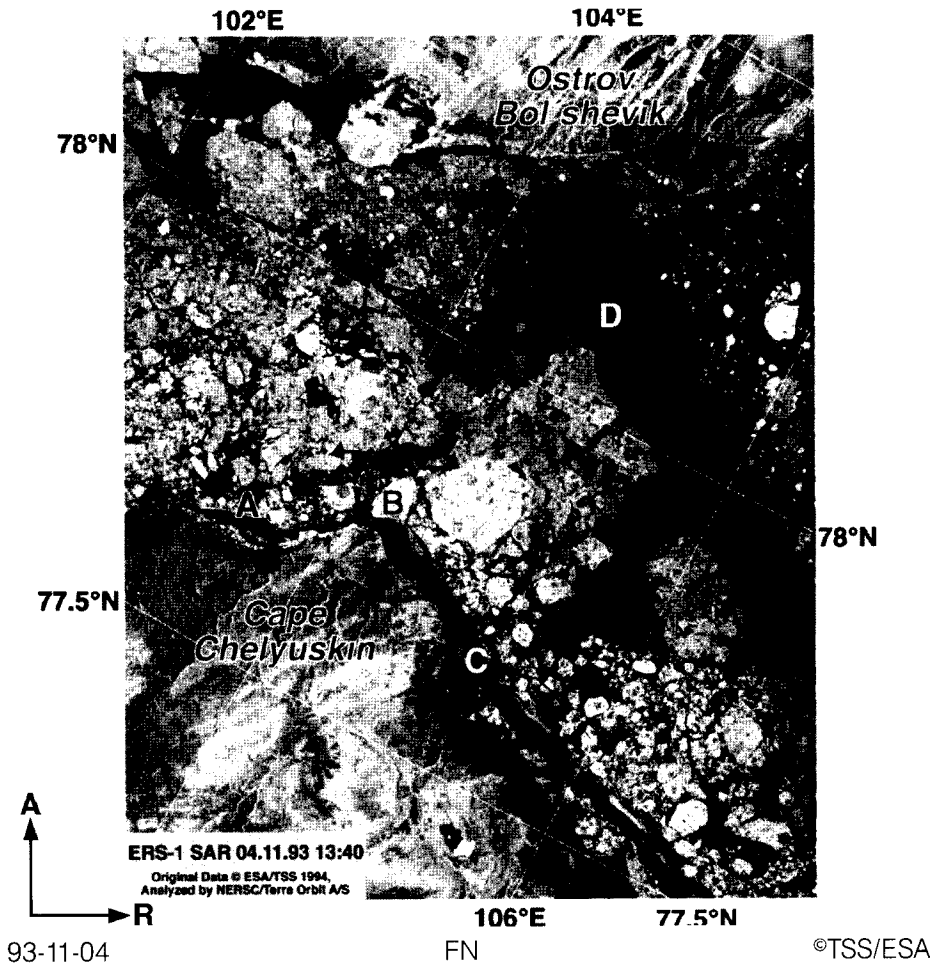
Icebreaker Navigation in the Mathiessen Strait



Land-fast ice, which is common around islands and along the margins of the Kara Sea, has variable thicknesses and can be heavily ridged. Icebreaker navigation in land-fast ice such as in the Mathiessen Strait, between the Nordenskjold Archipelago and the mainland, can therefore be difficult. The varied nature of the ice in this strait can be seen in the SAR image of 28 November 1993. This image was particularly useful because it was received and used by the vessel 'Sovetsky Soyuz' during its westward transit from the East Siberian Sea to the Kara Gate. Ice observations made onboard the "Sovetsky Soyuz" showed that the ice in Mathiessen Strait (site A) consisted of: (i) nilas about 5 cm thick (land-fast ice) with dark SAR signature; (ii) 12 km large mostly smooth, snow-free floes 30–40 cm thick observed near the land-fast ice boundary; and (iii) highly compressed and ridged first-year ice. The SAR signature of the ridged region is a mixture of brighter and darker patches.

The image also shows the track of the "Sovetsky Soyuz" through the ice (indicated by dark arrows). Other characteristic features are regions of 90–100% concentrations of pancake ice causing high backscatter and bright signatures in the SAR image (site B), and new land-fast ice in bays, inlets and estuaries formed during calm weather. This ice is identified as dark homogeneous areas in the SAR image (site C).

The image to the right is a classified ice map based on the SAR image to the left.

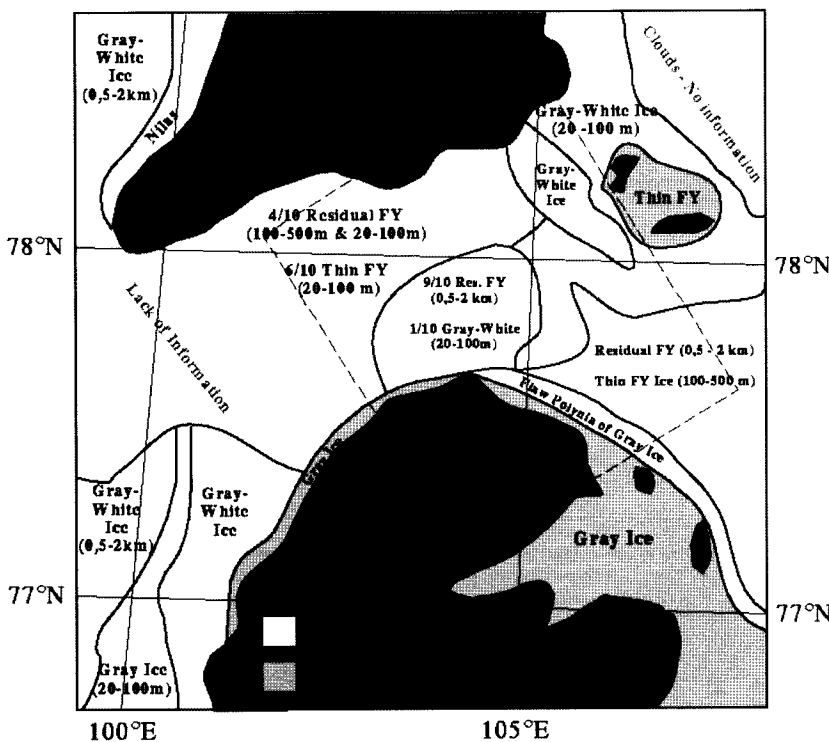


Vilkitskogo Strait – A Difficult Area for Ice Navigation

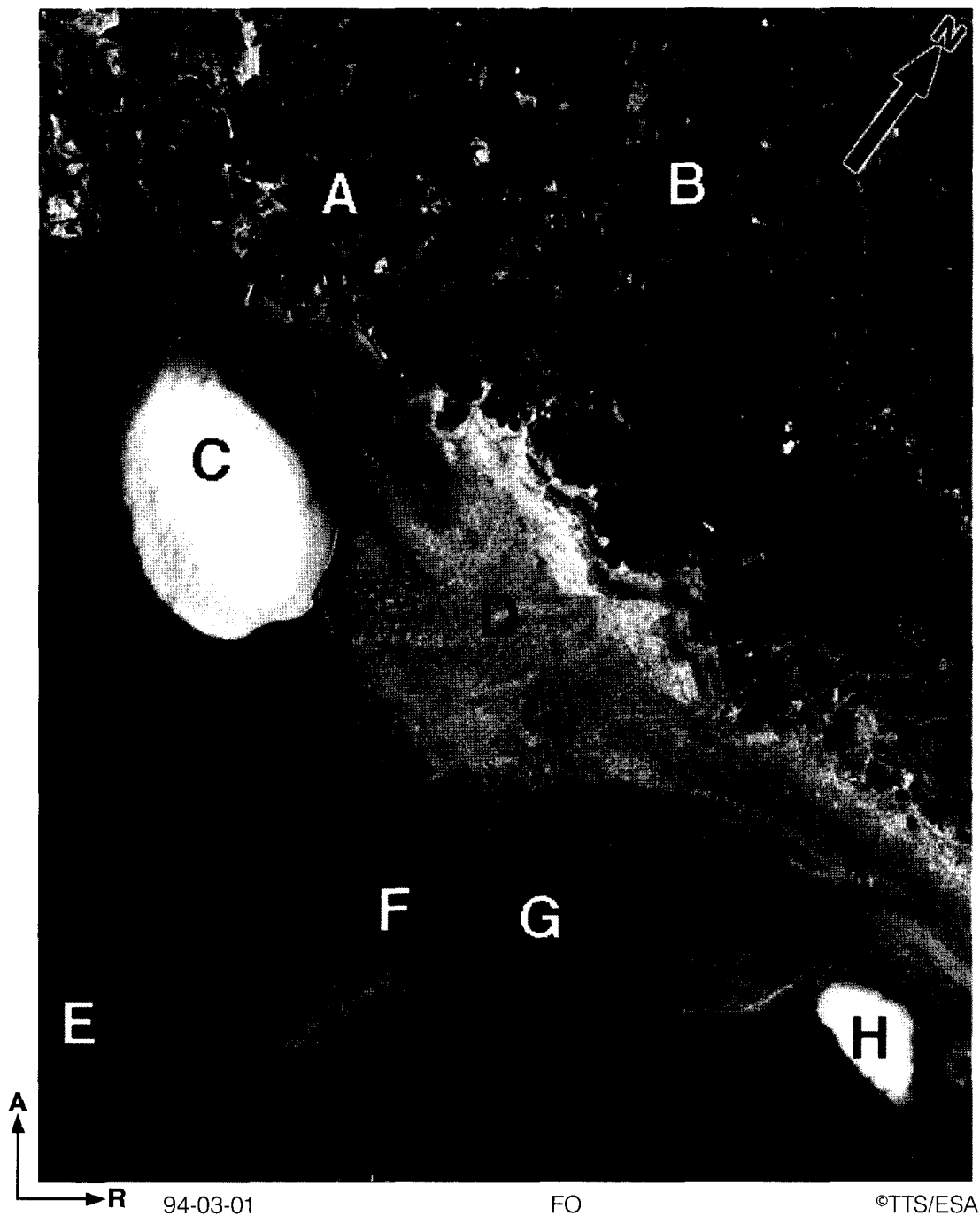
The Vilkitskogo Strait, which is the northernmost part of the Northeast Passage, is a particularly difficult area for ice navigation. Thick residual floes (second- or multi-year ice) often occur in this region where differential ice motion causes heavy compression and ridging of the ice pack. The large thick floes and heavy ridges, as well as land-fast ice, make it difficult to navigate even for the most powerful ice breakers. The SAR image of 4 November 1993 shows examples of the ice types which often occur in the Vilkitskogo Strait.

The "Sovetsky Soyuz" navigated along the Taymyr Coast in the flaw lead denoted A, B, C. The polynya consisted of young ice 15–30 cm thick (dark signature) which was easy to penetrate. Other ice types are thin first-year ice about 40 cm thick (area D) and multi-year ice about 3 m thick. The multi-year ice has a high backscatter, in contrast to the young and first-year ice. Mapping of multi-year ice is very important because navigation through such ice is difficult and should be avoided. The SAR image of 4 November provided useful information for the ice breakers to find the best sailing route. Navigation through the flaw lead along the Taymyr Coast was much faster and less difficult and hazardous than through alternative routes.

The Russian ice map of the same area is shown to the left (original labelling translated into English).



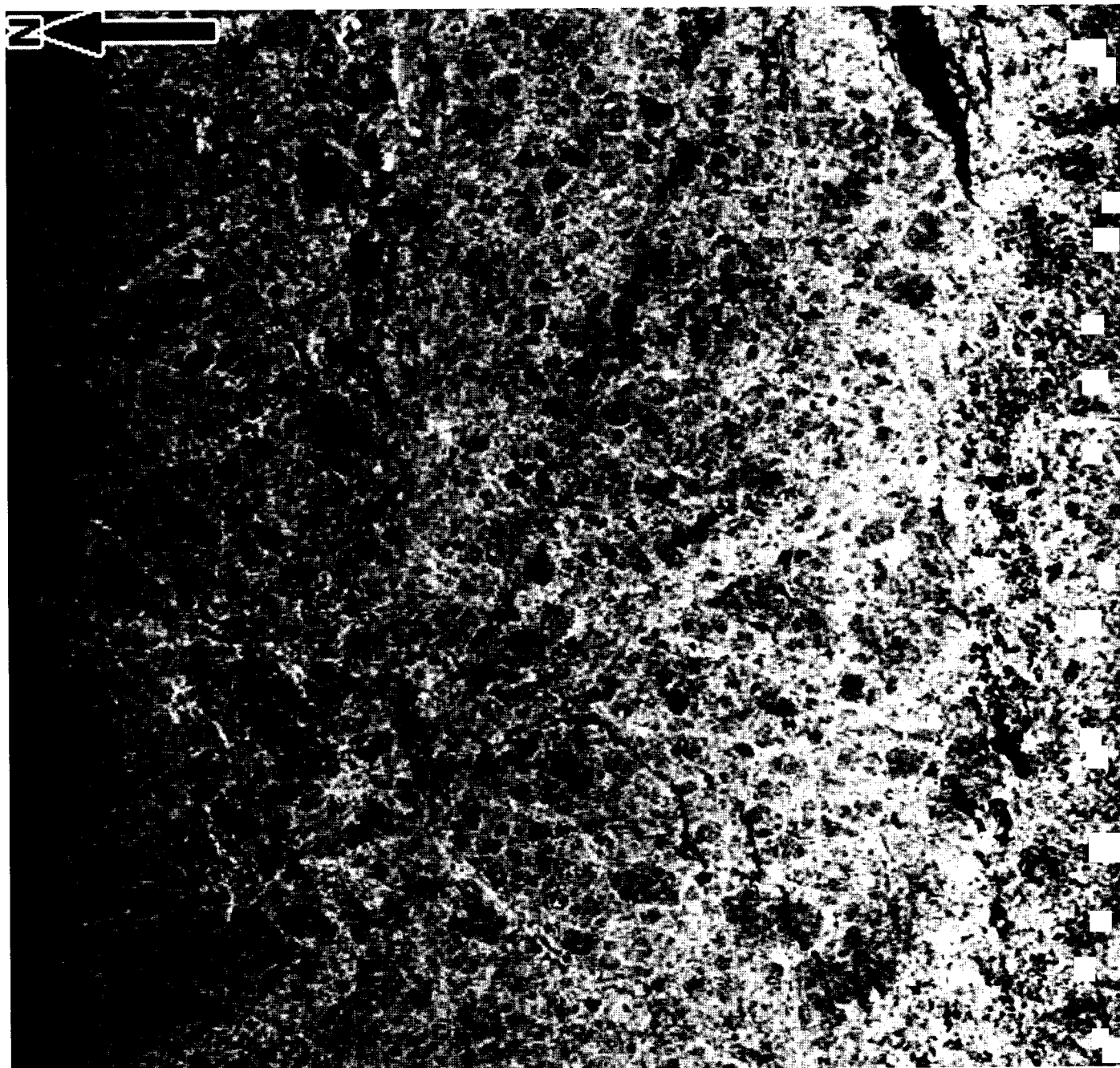
Severnya Zemlya: The Northernmost Islands off the Siberian Coast



- A = Large ice floes and leads
- B = Pack ice
- C = Glacier (Smiths Island)
- D = Open water
- E = Newly frozen ice
- F = Rough new ice
- G = Smooth new ice
- H = Glacier.

This image was used by the Norwegian adventurer Børge Ousland on his ski expedition to the North Pole in March 1994. He set out from the northernmost island (lower right corner) and used information in the SAR image to ascertain the ice conditions and plan his route. He pulled a sled and tried to avoid areas of open water. The upper part of the SAR image shows that the ice pack was dominated by large floes with leads in between, which are shown as bright signatures.

The Interior of the Arctic Pack Ice

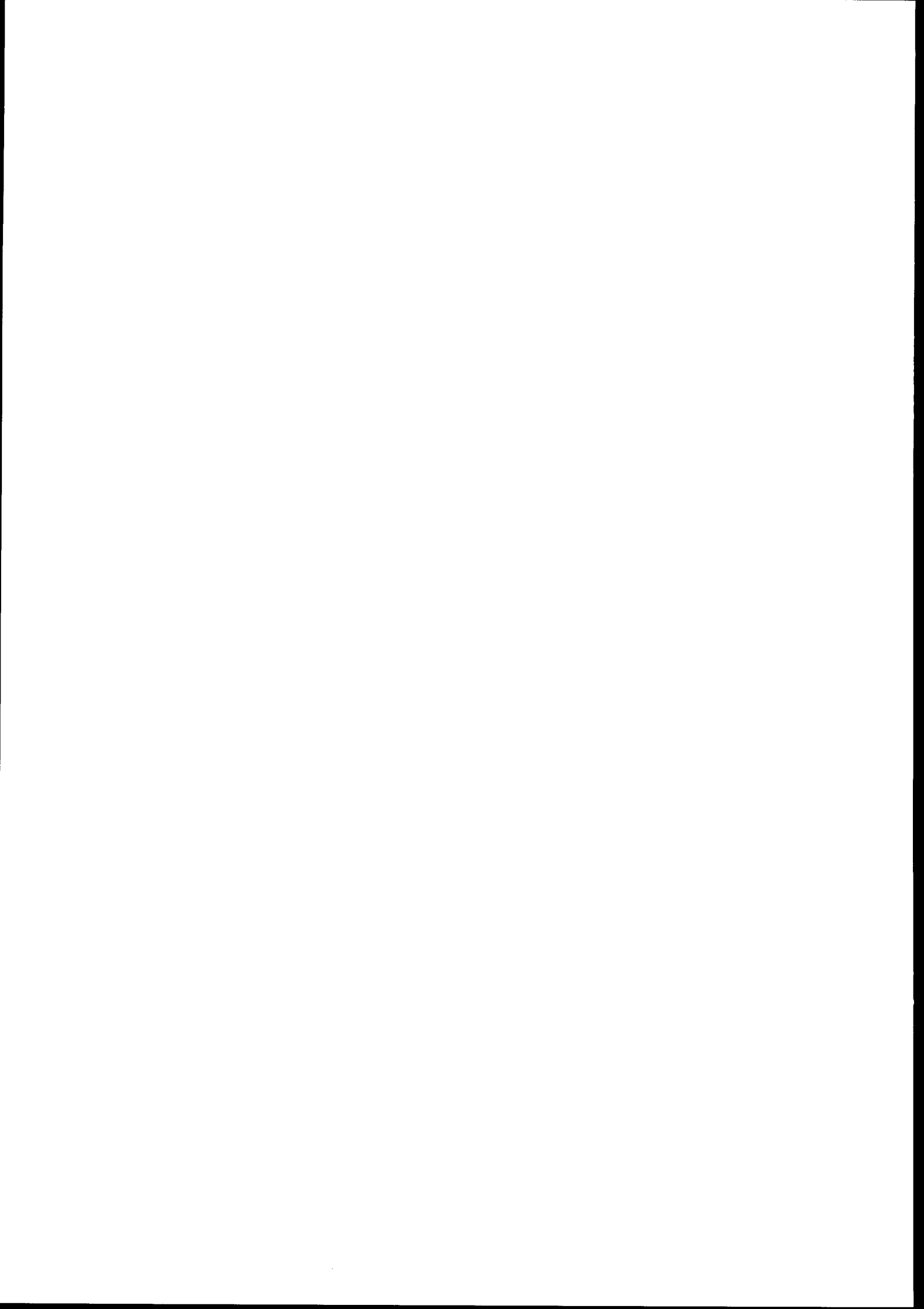


93-09-22

FP

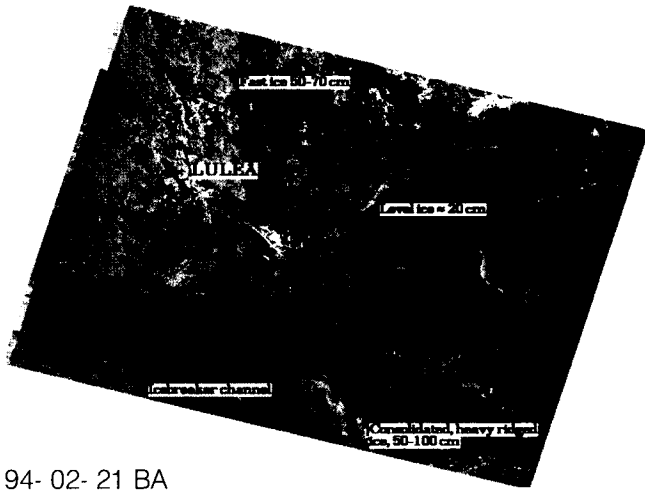
©TSS/ESA

This image is an example of a 95–100 % concentration of multi-year ice combined with some first-year ice and refrozen leads at 84°N and 65°E. This is near the northernmost limit of SAR coverage by ERS-1. The image was obtained in late summer and many of the floes may have been covered with melt water. The SAR signature of multi-year ice is often darker in late summer than in the winter. The dark signatures in the leads indicate young ice with a smooth surface.

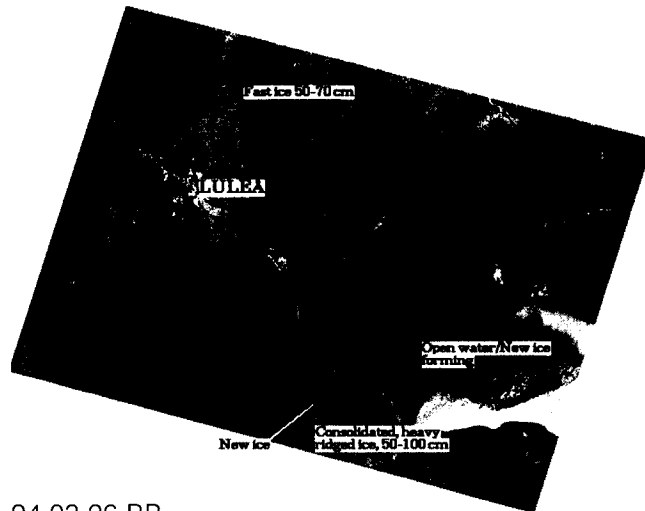


7. Baltic Sea

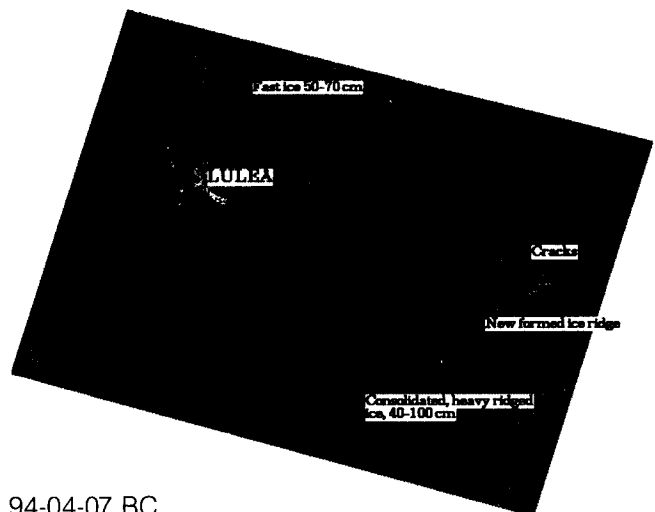
Gulf of Bothnia



94-02-21 BA

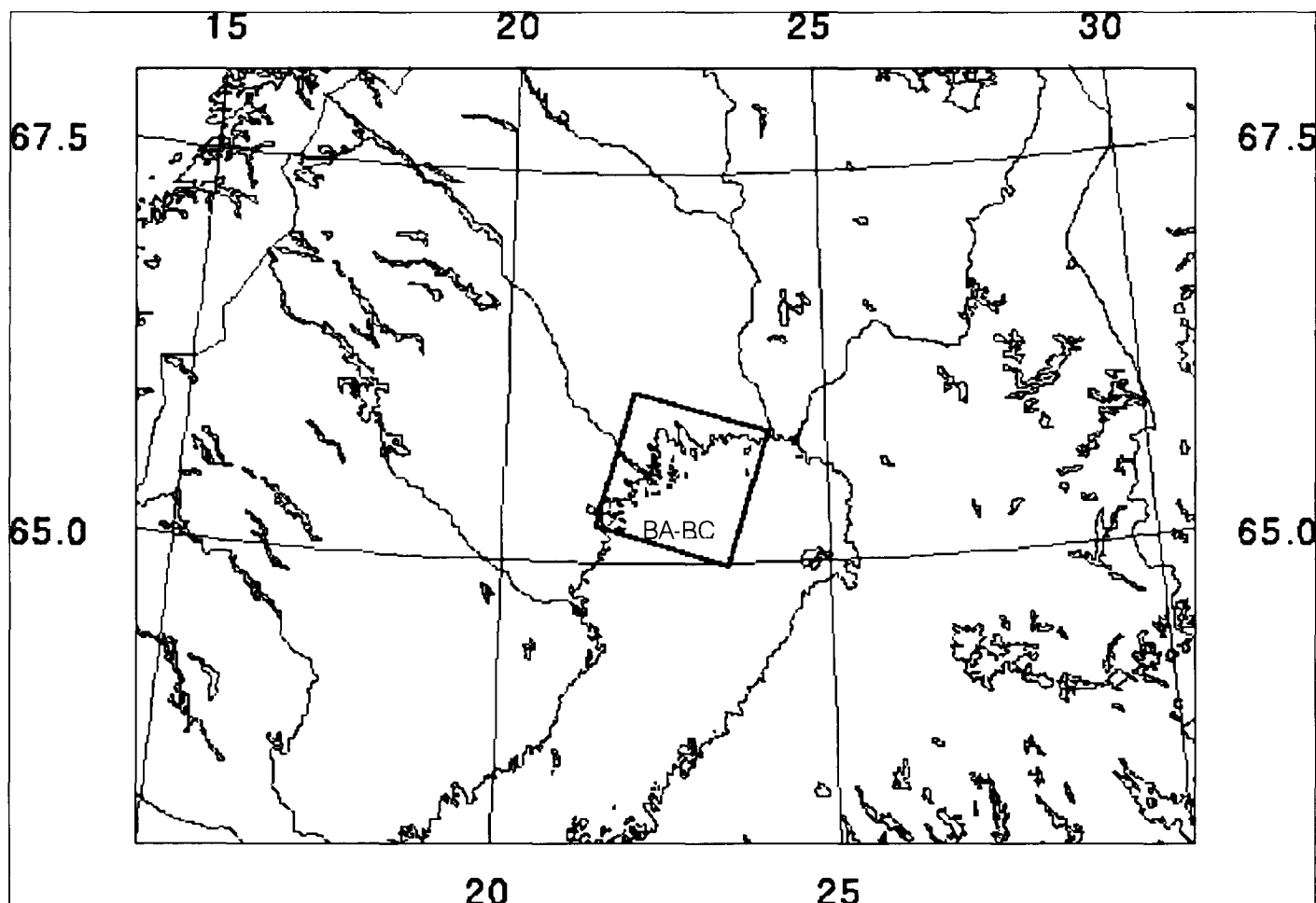


94-03-26 BB



94-04-07 BC

Courtesy of M. Moberg, SMHI, Sweden



Images: 94-02-21 BA, 94-03-26 BB, 94-04-07 BC

The ice season in the Gulf of Bothnia, which is the northernmost part of the Baltic Sea, normally lasts for more than six months, with the maximum ice extent occurring in the January–March period. The maximum ice thickness varies between 50 and 120 cm and severely affects marine traffic in the area. The Finnish Board of Navigation operates nine icebreakers to assist the movement of shipping and keep important harbours open during the ice season. Sweden and Finland have operational ice services which use satellite images to produce ice maps. During the winters of 1992, 1993 and 1994, ERS-1 SAR images were used for demonstrations of real-time ice monitoring. Images are transmitted to icebreakers using the Nordic Mobile Telephone (NMT) system. On board the icebreakers, the SAR images can be analysed by the captain using an image work station.

The three ERS-1 SAR images show the ice conditions on 21 February, 26 March and 7 April, 1994 in the northernmost corner of the Gulf of Bothnia. The fast ice and some of the ship tracks show minor changes, while the drifting ice varies considerably in this period.



8. North America

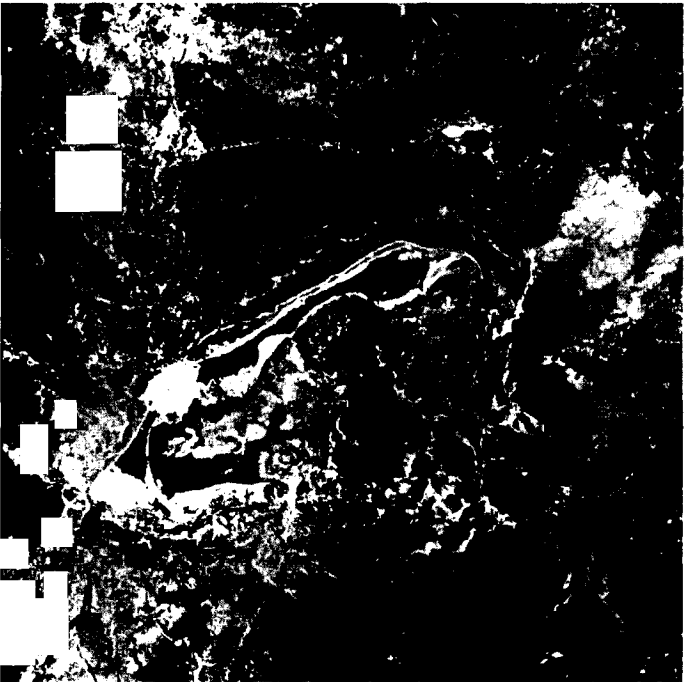
Labrador and the Canadian Arctic Archipelego



92-03-02 DB



94-03-04 DJ

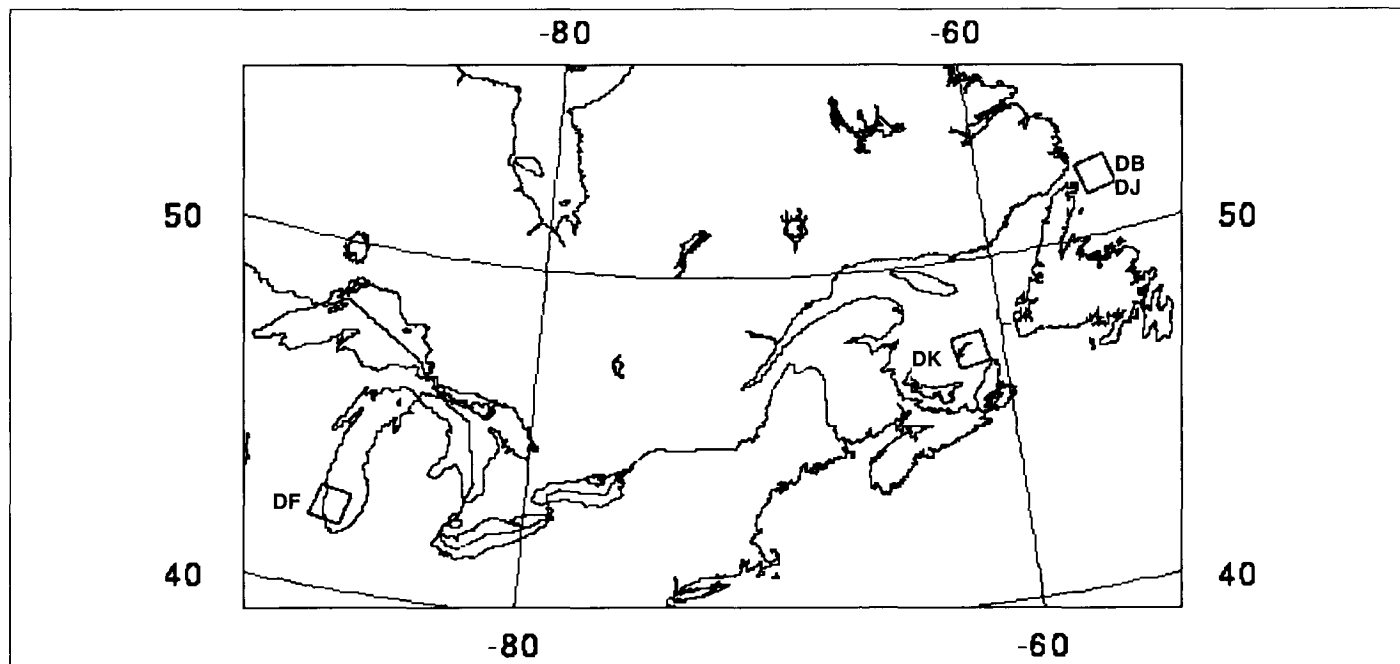


94-01-23 DK



93-04-28 DL

(Courtesy of B. Ramsay, Canadian Ice Centre, Canada)



Images: 92-03-02 DB, 94-03-04 DJ

The two upper scenes, acquired on 2 March 1992 and 4 March 1994, are from the Labrador Sea (52°N, 56°W) near Belle Isle (top left of images). This area is within the pack ice, i.e. far from the ice edge. A northwest wind with a mean speed of 50 km/h prevailed. It pushed most of the ice off the lee side of the island, leaving only small ice strips. This is demonstrated by the bright streaky pattern. The main pack ice had virtually no surface structure and was classified as 'grey-white' ice with a thickness of about 25 cm. Small floes, however, appear at the top left-hand corner, with water filling the space between them.

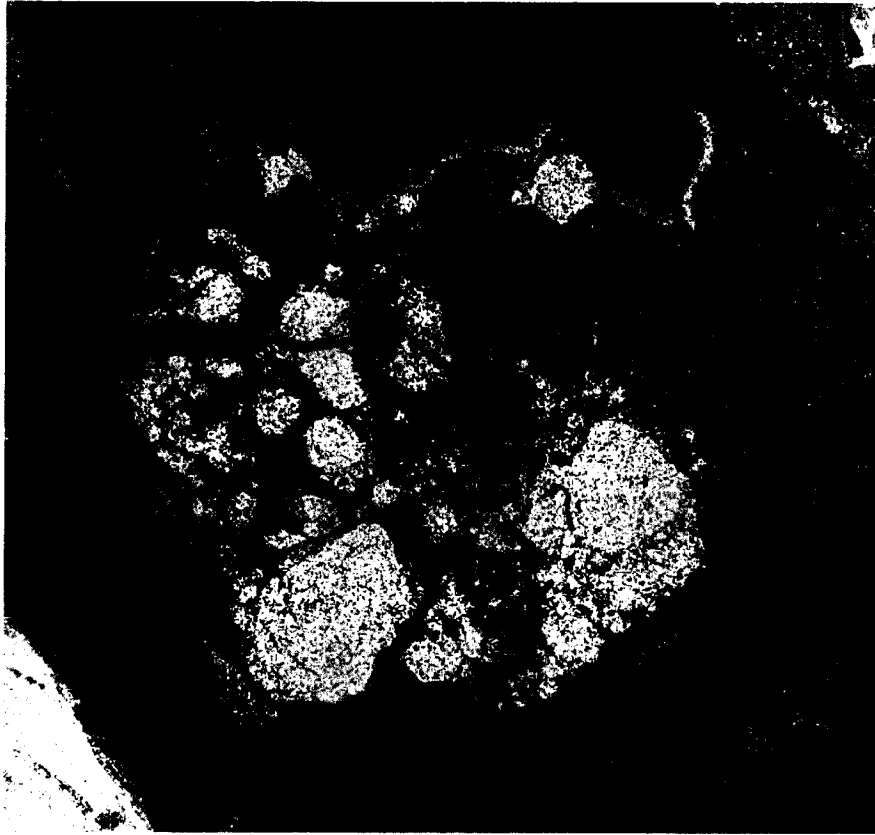
Image: 94-01-23 DK

This image, acquired on 23 January 1994, from the Gulf of St. Lawrence, includes a group of islands known as the Magdalen Islands, which enclose a long strip of sea water that became covered with fast ice (textureless SAR signature). Two capes are shown with bright signatures to the south side of the islands. The scene features first-year thin and medium ice (thickness estimated at between 50 and 100 cm). Refrozen fractures appear as dark strips in the top left-hand section of the image. They are interspersed in a matrix of grey ice (thickness about 15 cm) of bright signature. The floes probably drifted from the ocean as the ice in the gulf does not usually grow in thickness to form this type of floes at that time of year.

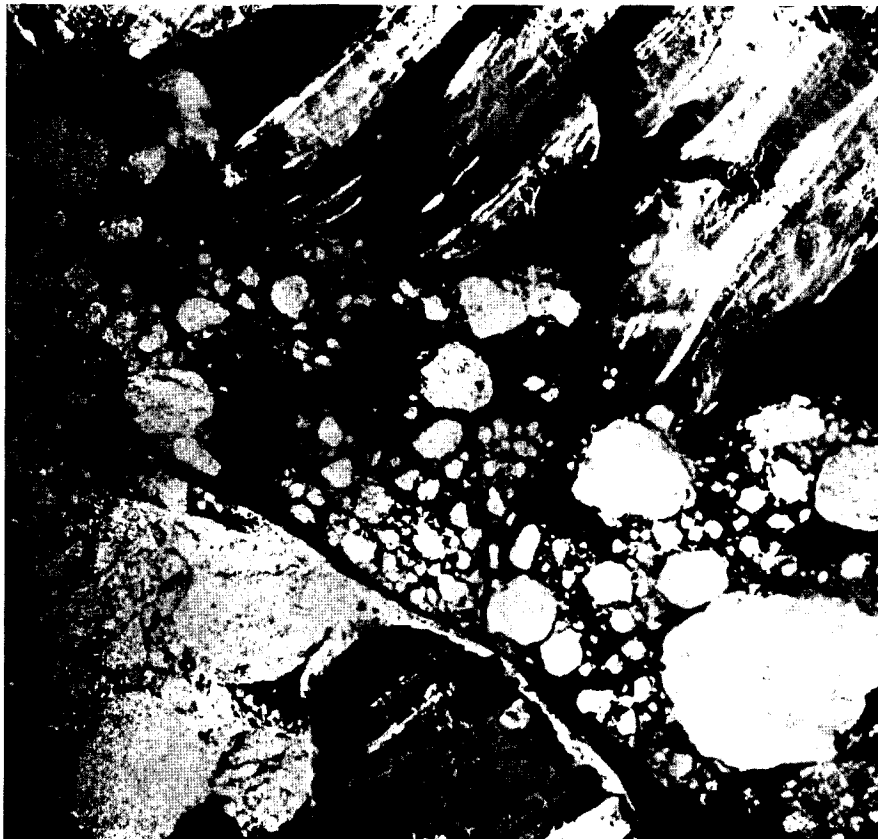
Image: 93-04-23 DL

This image was acquired on 28 April 1993 in the Canadian Arctic Archipelago. The scene shows the southeast corner of Cornwallis Island and Griffith Island. Ice is fully consolidated. Consolidation periods, however, vary as indicated by the shear line in the image. Ice in Resolute Passage was consolidated first in November 1992, and ice in Lancaster Sound was consolidated later in January 1993. Two small multi-year ice floes, with relatively bright signatures, are located in the Passage. Different brightnesses indicate different freezing conditions and consequently different physical properties of the ice.

Canadian Arctic Archipelago



93-05-10 DM



92-05-15 DA

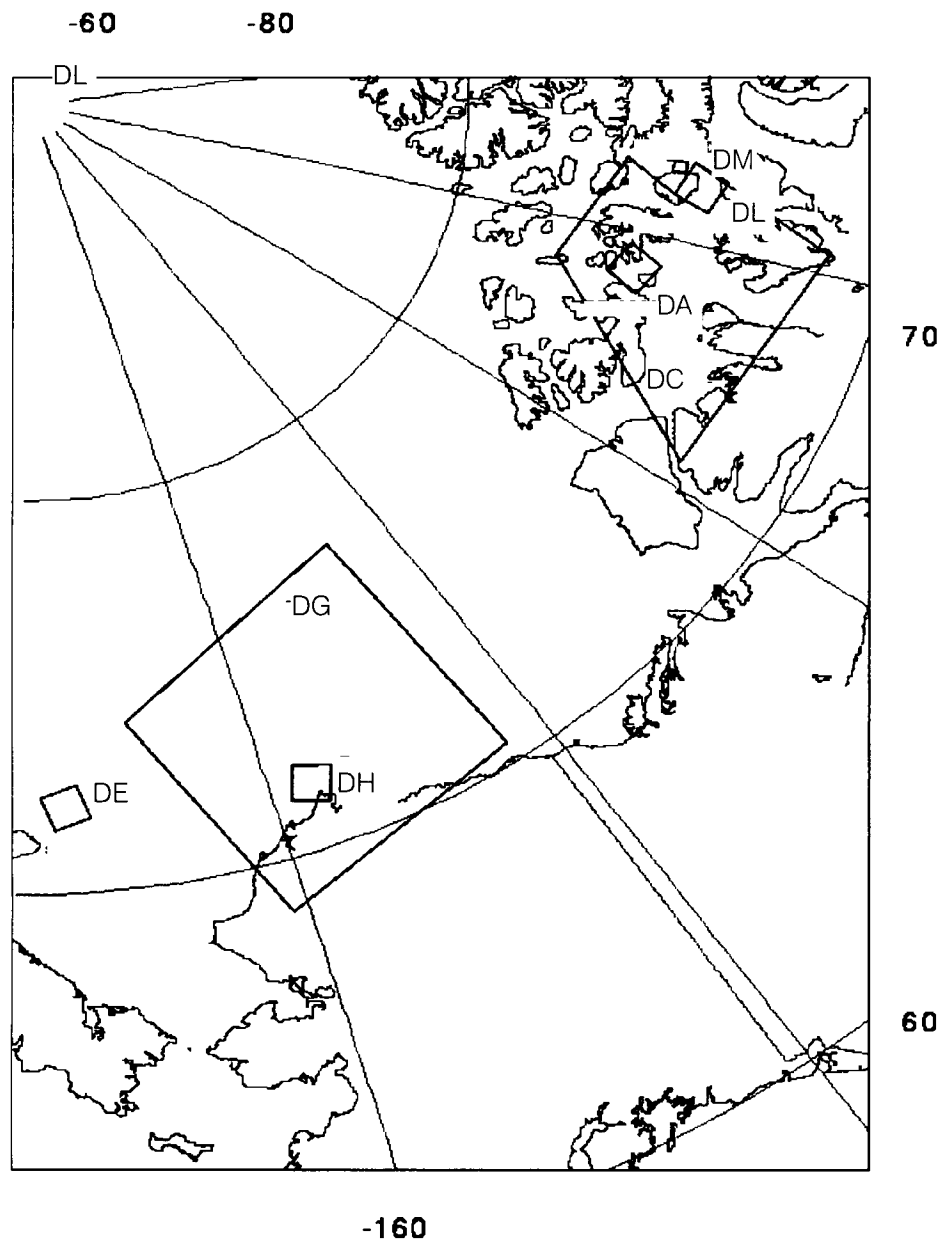
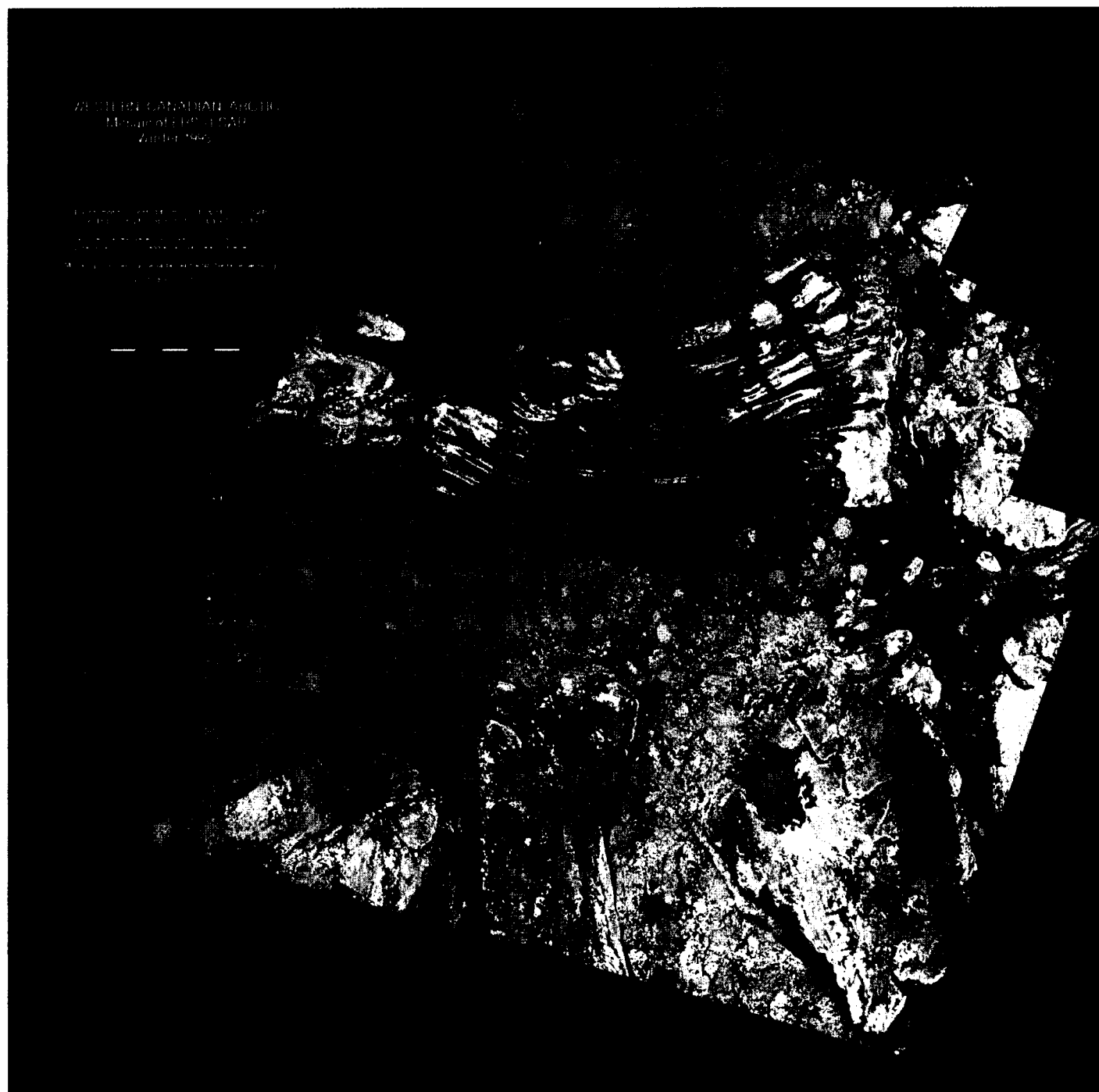


Image: 93-05-10 DM

The image was acquired on 10 May 1993 from Wellington Channel in the Canadian Arctic Archipelago. The scene features a composite multi-year ice floe approximately 4 km² in area. The average relief was between 1 and 2 m. The ERS-1 SAR was able to reveal the composite nature of the floe, which visual and photographic observations had not. Dark streaks in the image represent smooth refrozen leads.

Image: 92-05-15 DA

The image was acquired on 15 May 1992 from the strait between Bathurst Island (upper part of the image) and Melville Island in the Canadian Arctic (73°50' N, 103°W). Multi-year floes from the Arctic drift southwards into Viscount Melville Sound in the Northwest Passage. The ice conditions in this region are important for the transportation of oil by sea from bases such as Bent-Horn.



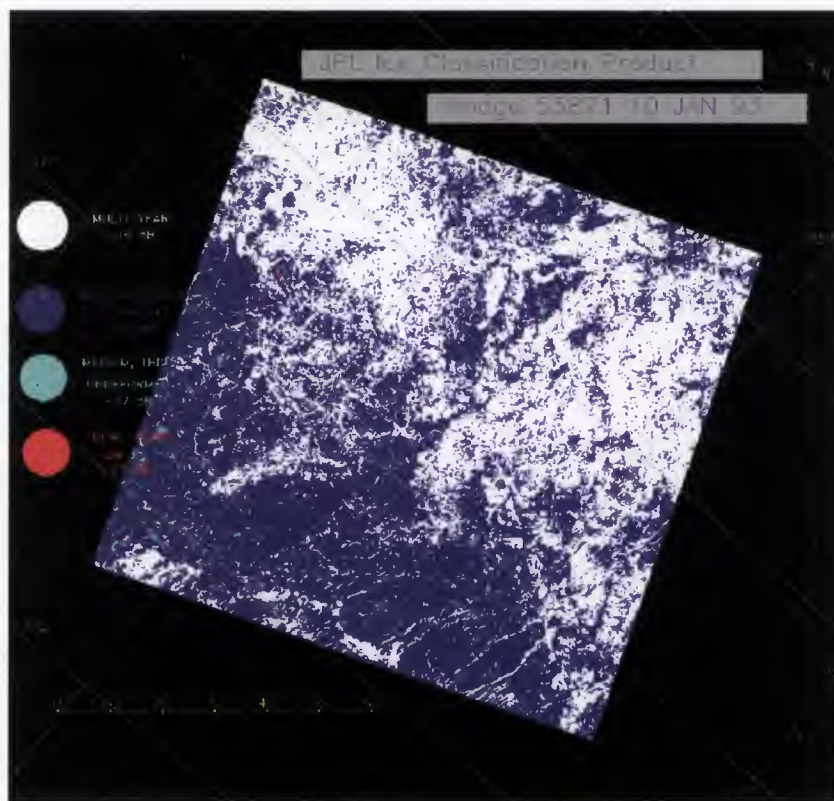
93-02 DC

(Courtesy of M. Manore, CCRS, Canada)

Image: 93-02-DC

The SAR mosaic of the western Canadian Arctic is composed of more than 70 scenes of ERS-1 data covering a 700 km x 700 km area at a 50 m pixel spacing during the period 7–22 February 1993. The mosaicking process, done by the Canada Centre for Remote Sensing, involved data collection, antenna pattern correction, histogram matching, ground control point referencing, image-to-image registration and look-up-table (LUT) enhancements. ERS-1 data were selected to simulate Radarsat products because of their similar orbits and frequencies. The mosaic was then processed with the SARPAC software so that the ERS-1 data could portray the 500 km x 500 km areal extent, 100 m x 100 m spatial resolution, and noise features of the Radarsat satellite. The main use of Radarsat data at the Canadian Ice Centre will be to monitor sea-ice conditions for offshore drilling operations. Radarsat simulation products have proved to be a useful tool for determining the geographical coverage and radiometric quality of the ScanSAR Wide Mode for sea-ice monitoring.

US Ice Center Analyses: Beaufort Sea and Great Lakes



93-01-10 DE



94-03-02 DF

(Courtesy C. Bertoina, National Ice Center, USA)

Image: 93-01-10 DE

The National Ice Center employs software similar to that designed by the Jet Propulsion Laboratory for use at the Geophysical Institute at the University of Alaska for the classification of SAR images. This unsupervised classification software first calibrates the imagery to remove the effects of noise, antenna pattern and system gains. The calibrated data then undergo cluster analysis using the ISODATA clustering technique. The dominant cluster is labelled by comparing the cluster centroid with the backscatter values associated with various ice types from a look-up table:

Multi-year ice	-10 dB
Thick, medium or deformed first-year ice	-14 dB
Medium, thin or undeformed first-year ice	-17 dB
New, young ice or open water	-22 dB

Cluster centroids for other ice types are determined using the expected difference in mean backscatter between each ice type and the dominant ice type as determined by the look-up table. This technique is described in detail in Kwok et al. (1992) and Gineris et al. (1993). Experience has shown that this ice classifier works quite well under certain geographic and seasonal limitations, namely the northern Beaufort Sea under winter conditions. At times, however, as can be seen in this image, areas of heavy ridging are identified as multi-year ice owing to their relatively high backscatter.

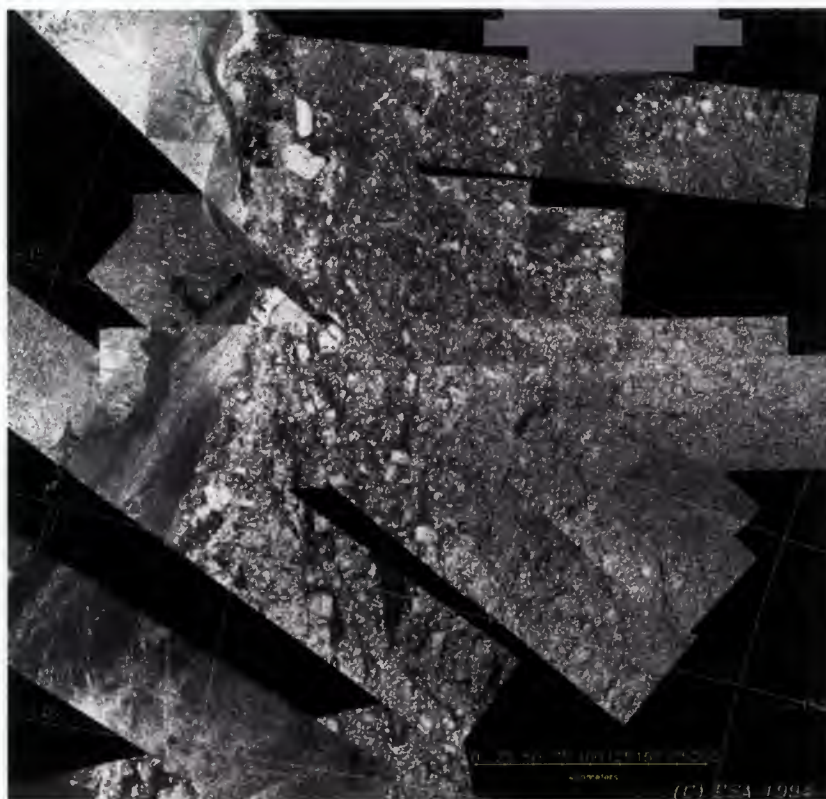
Image: 94-03-02 DF

This ERS-1 SAR image of southern Lake Michigan was received at the National Ice Center (NIC), in Washington DC, from the Gatineau ground station via the North American Ice Link. This link utilises a 56 kbps fraction of a T1 link to transfer ice images and ice products in near-real-time between the US and Canadian National Ice Centers (Bertoia et al., 1994).

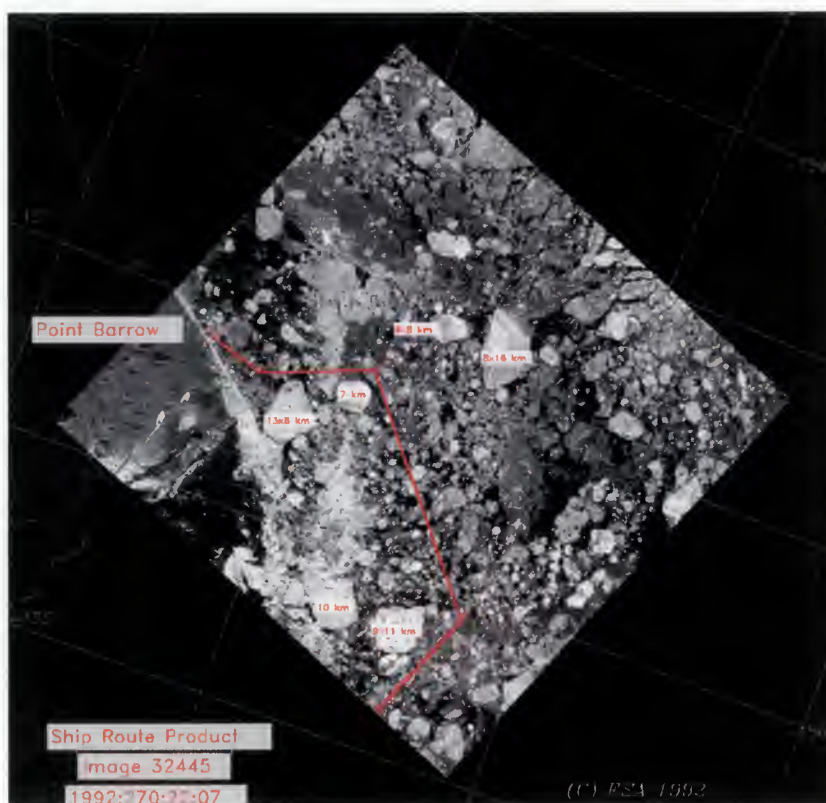
The NIC produces a complete analysis of ice conditions in the Great Lakes three times a week. In previous years, the best routinely available data source was 1km-resolution, visible and infrared imagery from the Advanced Very High Resolution Radiometer (AVHRR) instrument aboard the NOAA Tiros satellites. The routine availability of 100 m-resolution imagery that is not cloud-limited has greatly improved the quality of the Great Lakes analyses.

The image shown here was annotated using World Meteorological Organization standard codes for ice concentration and ice type in a manner typical of that used by NIC analysts on a daily basis.

US Ice Center Analyses: Beaufort Sea



94-05-DG



92-09-26 DH

(Courtesy of C. Bertoina, National Ice Center, USA)

Image: 94-05-DG

This mosaic was created over a period of ten days at the end of May 1994 using the Navy Satellite Image Processing System (NSIPS) PV-Wave-based software package. The mosaic was used to determine the southern limit of the extent of multi-year ice in the Beaufort Sea. Multi-year ice is defined as ice that has survived at least one summer melt season and is considered dangerous to shipping owing to its low salinity and corresponding high tensile strength. The extent of multi-year ice is clearly visible in wintertime SAR imagery; in this image the multi-year ice is bright white and consists primarily of well-shaped rounded floes.

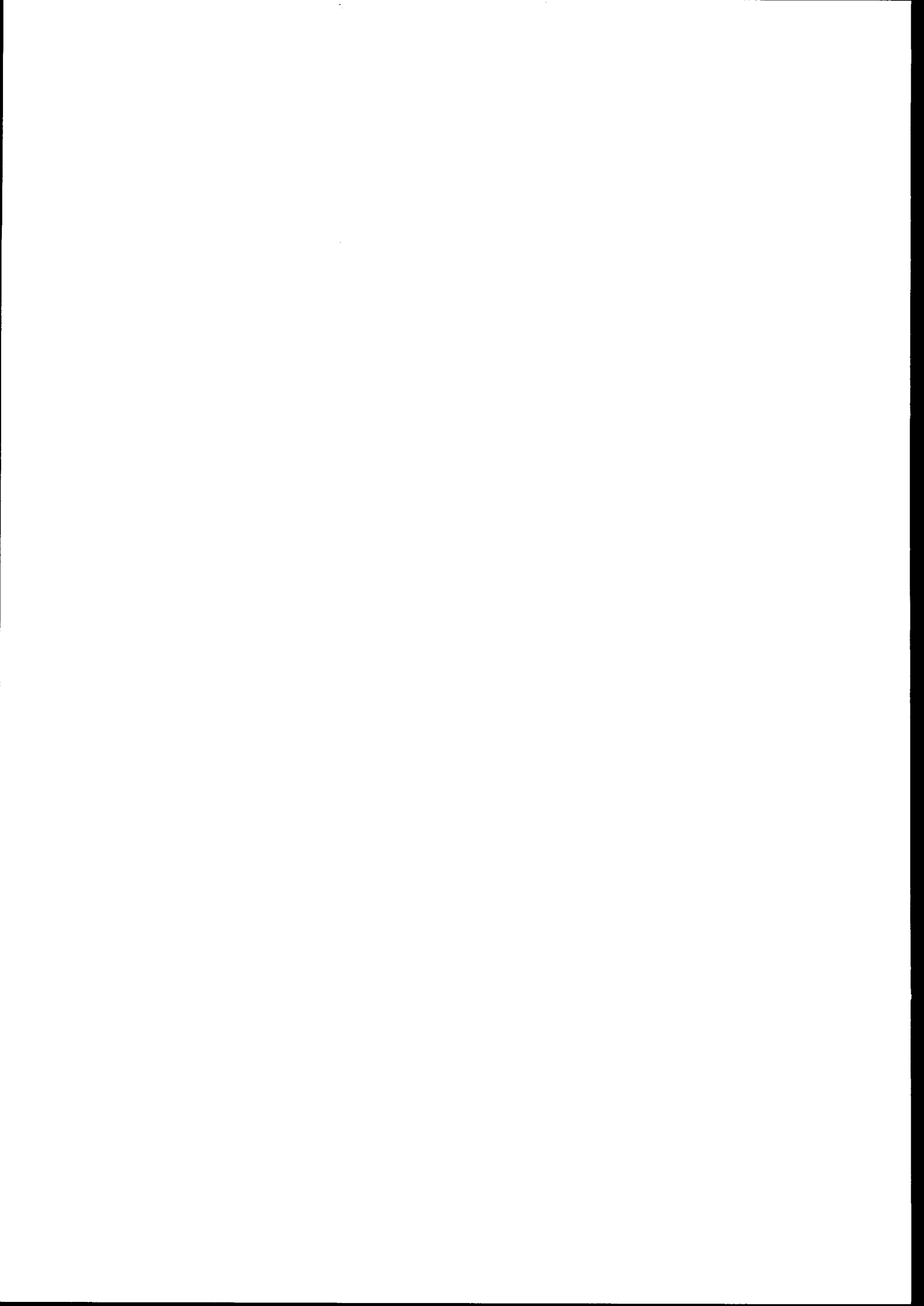
Each spring, the National Ice Center issues a forecast for the break-up of ice along the North Slope of Alaska. The southern limit of multi-year ice is an important input parameter for this forecast. SAR data provide the only high-resolution imagery capable of yielding this valuable information. The two large multi-year floes situated at approximately 72°N, 160°W in this image were tracked from a position near Banks Island in the Canadian Arctic Archipelago in October 1993. They continued their eastward trek towards the Bering Strait and broke into many small pieces in June 1994.

Image: 92-09-26 DH

This image was analysed at the National Ice Center by means of the Navy Satellite Image Processing System (NSIPS). This PV-Wave-based software package was developed at the Naval Research Laboratory at the Stennis Space Center. This particular image was analysed in support of the US Coast Guard ice breaker Polar Star, which at the time was en route to Point Barrow, Alaska, after a ship rendezvous in the Canadian Archipelago. The tools provided by NSIPS allowed the identification of several large multi-year ice floes considered hazards to navigation. The ship route software provides a course and heading for each designated way point on the recommended ship track. The following was generated for the attached image:

Point	Latitude DDD:MM:SS	Longitude DDD:MM:SS	True heading	Distance (km)
A	71:47:50.531	- 155:13:42.653	293	23.93
B	71:52:55.721	- 155:51:44.755	230	51.52
C	71:34:55.876	- 156:59:13.014	156	22.6
D	71:24:00.425	- 156:44:24.591	195	12.20
E	71:17:39.737	- 156:49:49.036		

The National Ice Center has been successful in sending analysed SAR imagery, as well as other ice products, to the USCG polar-class icebreakers via Internet connections.

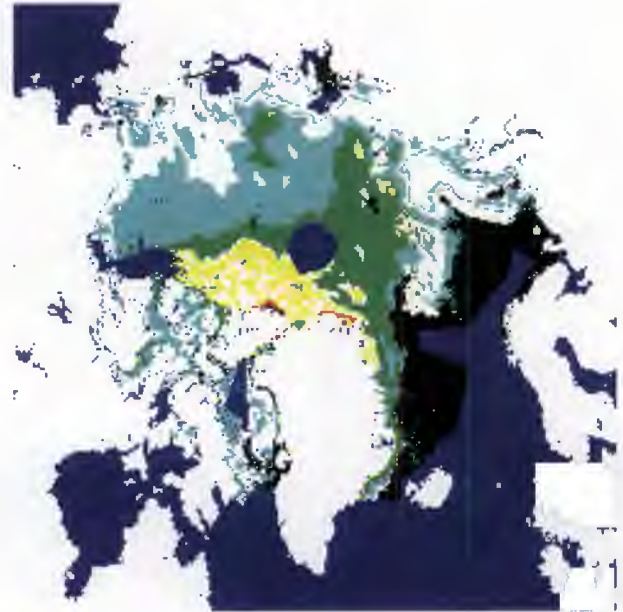


9. Arctic, Scatterometer

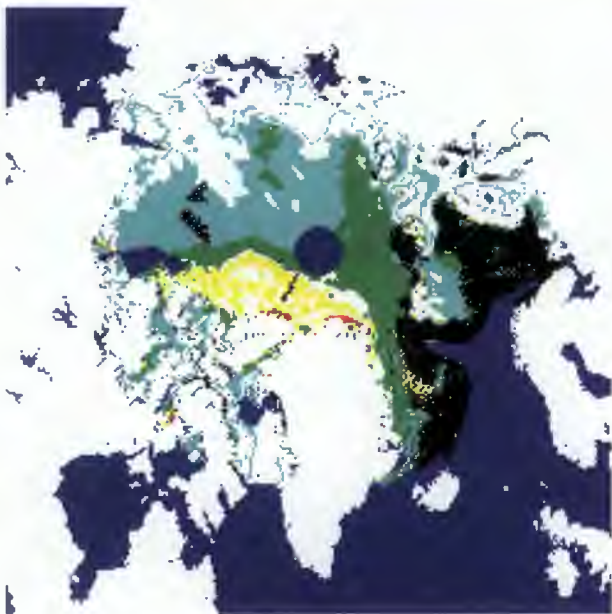
Ice Mapping of the Arctic Ocean with Scatterometer Data



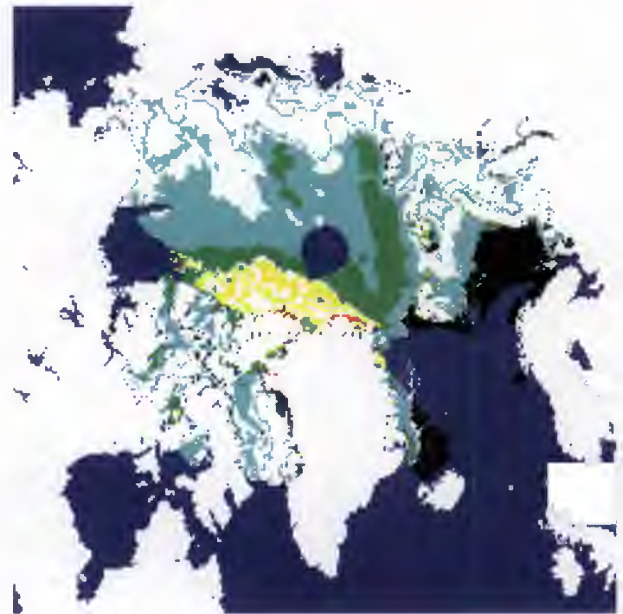
92-10-09



92-12-09



93-02-09



93-04-09

*(Courtesy of
A. Cavanie,
IFREMER, France)*

The scatterometer data from ERS-1, with a resolution of 50 km, provide near-full spatial coverage of the Arctic over a three-day period. The images in these examples are 9 day averages obtained at 2 month intervals from October 1992 to April 1993. In the processing, the backscattering coefficients are brought back to 40° incidence angle by using a linear relationship between the incidence angle and the backscatter over the ice. The scatterometer data provide interesting images of the large-scale variability of ice roughness. On these images, the purple and blue values indicate new ice, while multi-year and rough ice appear in green and yellow. The open water is coloured brown, and areas with no information in marine blue.

10. Antarctica

Icebergs in Antarctic Pack Ice



92-07-13 HA



92-07-13 HB

(Courtesy of T. Viehof, AWI, Germany)

Image: 92-07-13 HA

This image was taken on 13 July 1992 and consists of two frames: 5067 and 5085. The high-backscatter targets with values of -2.3 dB to +0.9 dB represent grounded icebergs. ERS-1 images over the same area from October 1991 show that the locations and sizes of the icebergs hardly varied between October 1991 and July 1992.

Image: 92-07-13 HB

This is a part of 92-07-13 HA. Tracks in the lee (north) of the icebergs can clearly be seen. The mechanism that causes the bands of high backscatter values north of the icebergs is opposite to that of an iceberg drifting through a closed ice cover: because of the difference in velocity of the iceberg (stationary) and the surrounding sea ice cover, the icebergs create a track of open water/brash ice. The icebergs act as a barrier.

Antarctic Sea Ice Types

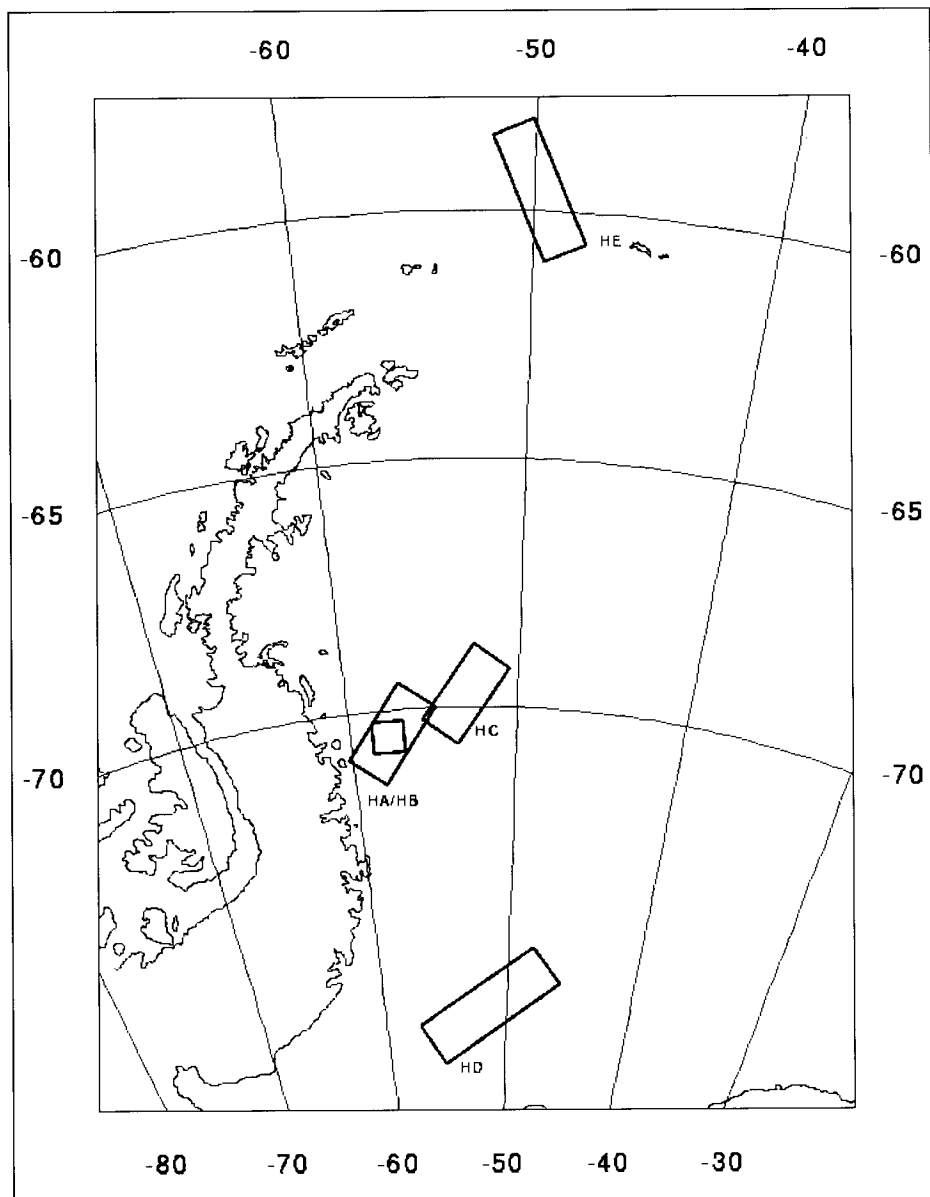


Image: 92-07-07- HC

The figure, which combines image 5106/5049 with 5106/5067 from 7 July 1992, shows the first-year ice fraction on the continental shelf (southern part) as well as multi-year ice fraction over the continental slope (northern part). In the northern part, the backscatter values are about -9 dB. On the other hand, the backscatter values of the first-year ice fraction in the southern part of the figure are only about -13.5 dB. (Courtesy of T. Viehof, AWI, Germany).



92-07-07 HC

Weddel Sea Ice and an Iceberg off the South Orkney Islands



92-07-13 HD



92-07-27 HE

(Courtesy of T. Viehof, AWI, Germany)

Image: 92-07-13 HD

Orbit: 5191 Frames: 5221, 5229 and 5249, taken on 13 July 1992

This figure shows different ice regimes in the southern Weddell Sea off the Ronne Ice Shelf. The Ice Shelf can be seen in the southernmost part of the image. Off the Ice Shelf edge, newly formed ice is visible which has been developed during different ice and wind condition events. In the northern part of the image, relatively smooth first-year ice is visible. This ice was also formed in the offshore regime earlier in the year, as observed from SSM/I time series.

Image: 92-07-27 HE

This image shows the marginal ice zone west of the South Orkney Islands on 27 July 1992. The most remarkable feature in the image is the huge tabular iceberg in the eastern part, and the open-water area that it created to the east of it. The German research icebreaker RV Polarstern passed this area about one day after the image was taken. Ice observations from the bridge as well as by helicopter allowed the general ice conditions to be estimated. The central part of the image consisted mainly of loosely packed fragments of first-year and second-year floes, never more than 50 m in diameter, with up to 45% brash ice in between. Some pieces of ice had more than 2 m of freeboard. Only very few melt puddles or bare ice areas were visible and no pronounced ridges were observed. In the southern part, a smaller iceberg is visible. In the most southerly part, the transition to second-year ice signatures can be seen. The ice edge is very diffuse in the northwestern part, and it consisted of a high percentage of newly formed pancake ice in combination with brash ice and small first-year floes. Only in the northeastern part can a clearly developed edge be seen.

Acknowledgements

We would like to acknowledge the support of the following individuals and organisations who provided images and information included in this catalogue:

Bertoia, Cheryl	National Ice Center,
Cavanie, Alain	USAIFREMER, France
Manore, Mike	Centre for Remote Sensing, Canada
Moberg, Mats	Meteorological and Hydrological Institute, Sweden
Ramsay, Bruce	Ice Centre, Canada
Valeur, Hans	Danish Meteorological Institute, Denmark
Viehoff, Thomas	Alfred Wegener Institute for Polar and Ocean Research, Germany

References

1. Bertoia, C. & T. Carrieres 1994, Operational Use of Satellite Data for Sea Ice Analysis at the US and Canadian National Ice Centers, Proc. International Geoscience and Remote Sensing Symposium, Pasadena, California, Vol. II, pp. 1228–1230.
2. Hansen K.Q. & H.H. Valeur 1994, Satellitter og operationel kortlegging av Groenlands havis, Nordisk romvirksomhet, No. 2, pp. 8–12.
3. Johannessen O.M., 1986, Brief Overview of the Physical Oceanography in the Nordic Seas (Ed. B.G. Hurdle) Springer Verlag, N.Y., pp. 103-127.
4. Johannessen, O.M., J.A. Johannessen, E. Svendsen, R. Schuchman, T. Manley, W.J. Campbell & E.G. Josberger 1987a, Ice-edge Eddies in the Fram Strait Marginal Ice Zone, Science, Vol. 236, p. 427.
5. Johannessen, J.A., O.M. Johannessen, R. Schuchman, T. Manley, W.J. Campbell, E.G. Josberger, S. Sandven, J.C. Garscard, T. Olaussen, K. Davidson & J. van Leer 1987b, Mesoscale Eddies in the Fram Strait Marginal Ice Zone during the 1983 and 1984 Marginal Ice Zone Experiment, J. Geophys., Vol. 92, pp. 6754 - 6772.
6. Johannessen, O.M., W.J. Campbell, R. Schuchman, S. Sandven, P. Gloersen, E.G. Josberger, J.A. Johannessen & P. M. Haugan 1992, in Microwave Remote Sensing of Sea Ice (Ed. F. Carsey), AGU Geophysical Monograph 68, pp. 261–289.
7. Johannessen, O.M., S. Sandven, W.P. Budgell, J.A. Johannessen & R. Schuchman 1994, Observation and Simulation of Ice Tongues and Vortex Pairs in the Marginal Ice Zone, Nansen Centennial Volume, AGU Geophysical Monograph.
8. Onstott, R.G. 1992, SAR and Scatterometer Signatures of Sea Ice, in Microwave Remote Sensing of Sea Ice (Ed. F. Carsey), AGU Geophysical Monograph 68, pp. 73–104.
9. Sandven, S. & O.M. Johannessen 1993, The use of microwave remote sensing for sea ice studies in the Barents Sea, ISPRS Journal of Photogrammetry and Remote Sensing, Vol. 48, No. 1, pp. 2–18.
10. Sandven, S., O.M. Johannessen, R. Schuchman, K. Kloster & M. Miles 1994a, SIZEX 92 ERS-1 SAR ice validation experiment, Proc. Second ERS-1 Symposium, Space at the Service of our Environment, 11–14 October 1993, Hamburg, ESA SP-361, pp. 353–358.
11. Sandven, S., O.M. Johannessen, L.H. Pettersson, M.W. Miles & A. Drottning 1994b, A Pilot Ice Monitoring Service using ERS-1 SAR Images, Proc. First ERS-1 Pilot Project Workshop, Toledo, 22–24 June 1994.
12. Vachon, P., O.M. Johannessen & J.A. Johannessen 1994, An ERS-1 SAR Image of Atmospheric Lee Waves, J. Geophys. Res.
13. Vinje, T. 1985, Drift, composition, morphology and distribution of sea ice fields in the Barents Sea, Norw. Polar Inst. Skr. 179c, pp. 3–26.
14. Wadhams, P. 1981, The ice cover in the Greenland and Norwegian Seas, Rev. Geophys. and Space Physics, Vol. 19, No. 3, pp. 345–393.
15. Wagner, M.J. 1994, Satellite data delights Arctic drillers, Offshore Engineer, February 1994.

Appendix
Ice Glossary

Brash ice

Accumulation of floating ice made up of fragments not more than 2 m across (small ice cakes), the wreckage of other forms of ice.

Break up

A general expression applied to the formation of a large number of fractures through a compact ice cover, followed by a rapid diverging motion of the separate fragments.

Compactness

The ratio of the area of the sea surface actually covered by ice to the total area of the sea surface under consideration; therefore, a compactness of 0 corresponds to ice-free and a compactness of 1 to compact ice.

Concentration

The ratio in tenths of the sea surface actually covered by ice to the total area of the surface, both ice-covered and ice-free at a specific location or over a defined area.

May be expressed in the following terms:

Compact pack ice: Concentration 10/10, no water visible.

Consolidated ice: Concentration 10/10, floes frozen together.

Very close pack ice: Concentration 9/10 to less than 10/10.

Close pack ice: Concentration 7/10 to 8/10, floes mostly in contact.

Open pack ice: Concentration 4/10 to 6/10, many leads and polynyas, floes generally not in contact.

Very open pack ice: Concentration 1/10 to 3/10.

Crack

Any fracture which has not yet parted.

Deformed ice

A general term for ice which has been squeezed together and in places forced upwards (and downwards). Forms of deformation include rafting, ridging and hummocking.

Divergence

Formally defined as $\text{div } \mathbf{V} = du/dx + dv/dy$. The divergence can be considered as the change in area per unit area at a given point. The word is also used to indicate a general diverging motion in the ice.

Draft

The distance, measured normal to the sea surface, between the lower surface of the ice and the water level.

Fast ice

Sea ice of any origin which remains fast (attached with little horizontal motion) along a coast or to some other fixed object.

First-year ice

Sea ice of not more than one winter's growth, developing from young ice. Thickness 0.3–3 m. May be subdivided into thin first-year ice/white ice (0.30–0.7 m), medium first-year ice (0.7–1.2 m) and thick first-year ice (over 1.2 m).

Flaw

A narrow separation zone between pack ice and fast ice, where the pieces of ice are in a chaotic state, that forms when pack ice shears under the effect of a strong wind or current along the fast ice boundary.

Flaw lead

A lead between pack ice and fast ice.

Floe

Any relatively flat piece of sea ice 20 m or more across. Floes are subdivided according to horizontal extent:

Giant floe: more than 10 km across

Vast floe: 2–10 km across

Big floe: 0.5–2 km across

Medium floe: 100–500 m across

Small floe: 20–100 m across.

Fracture

Any break or rupture through very close, compact or consolidated pack ice, fast ice or a single floe resulting from deformation processes (cf. lead). Fractures may contain brash ice and be covered with nilas or young ice. The length may be a few metres or many kilometres.

Frazil ice

Fine spicules or plates of ice, suspended in water.

Freeboard

The distance, measured normal to the surface, between the upper surface of the ice and the water level.

Grease ice

A stage of freezing, in which the crystals have coagulated to form a soupy layer on the surface. Grease ice reflects little light, giving the sea a matt appearance.

Grey ice

Young ice, 10–15 cm thick, less elastic than nilas, usually rafts under pressure.

Grey-white ice

Young ice, 15–30 cm thick. Under pressure, it is more likely to ridge than to raft.

Grounded ice

Floating ice (e.g. ridge, hummock and ice island) which is aground (stranded) in shoal water.

Hummock

The raised area of multi-year ice formed by the ablation of the surrounding ice. Also, a hillock of broken ice which has been forced upwards by pressure. May be fresh or weathered. The submerged volume of ice under the hummock is called a bummock.

Iceberg

A massive piece of ice of greatly varying shape with a freeboard of more than 5 m, which has broken away from a glacier and may be afloat or aground.

Ice boundary

The demarcation at any given time between fast ice and pack ice or between areas of pack ice of different concentrations (cf. ice edge).

Ice cake

Any relatively flat piece of sea ice less than 20 m across (cf. floe). If less than 2 m across, it is a small ice cake.

Ice cover

The ratio of an area of ice of any concentration to the total area of sea surface within some large geographic locale; this locale may be global, hemispheric, or prescribed by a specific oceanographic entity, such as Baffin Bay or the Barents Sea.

Ice edge

The demarcation at any given time between the open sea and sea ice of any kind, whether fast or drifting.

Ice field

Area of pack ice greater than 10 km across (cf. ice patch), consisting of floes of any size. Subdivided as follows:

Large ice field: more than 20 km across

Medium ice field: 15–20 km across

Small ice field: 10–15 km across.

Ice free

No sea ice present. There may, however, be some icebergs present (see also open water).

Ice limit

Climatological term referring to the extreme minimum or extreme maximum extent of the ice edge in any given month or period, based on observations over a number of years.

Ice shelf

A floating ice sheet of considerable thickness, showing 2–50 m or more above sea level, attached to the coast. Usually of great horizontal extent and with a level or gently undulating surface. Nourished by annual snow accumulation and often by the seaward extension of land glaciers. Parts of it may be aground. The seaward edge is called an ice front.

Keel

The underside of a ridge that projects downwards below the lower surface of the surrounding sea ice.

Lead

Any fracture or passage through sea ice that is generally too wide to jump across. A lead may contain open water (open lead) or be ice-covered (frozen lead).

Level ice

Sea ice which has been unaffected by deformation.

Melt pond

An accumulation of melt water on the surface, or sea ice that, because of appreciable melting of the ice surface, exceeds 20 cm in depth, is embedded in the ice (has distinct banks of ice), and may reach several tens of metres in diameter.

Multi-year ice

Old ice 3 m or more thick, which has survived at least two summers' melt. The hummocks are even smoother than in second-year ice, and the ice is almost salt-free. The colour, where bare, is usually blue. The melt pattern consists of large interconnecting irregular puddles and melt ponds, and a well-developed drainage system.

New ice

A general term for recently formed ice, which includes frazil ice, grease ice, slush and shuga. These types of ice are composed of ice crystals which are only weakly frozen together (if at all) and have a definite form only while they are afloat.

Nilas

A thin elastic crust of ice up to 10 cm thick, with a matt surface. Bends easily under pressure, thrusting in a pattern of interlocking 'fingers' (finger rafting). Dark nilas, up to 5 cm thick, is very dark in colour; light nilas, 5–10 cm thick, is rather lighter in colour (cf. ice rind).

Old ice

Sea ice which has survived at least one summer's melt. Most topographic features are smoother than for first-year ice. May be subdivided into second-year and multi-year ice.

Open water

A large area of freely navigable water in which sea ice is present in less than 1/10 concentration (see also ice free).

Pack ice

Any accumulation of sea ice, other than fast ice, no matter what form it takes or how it is disposed (see also concentration).

Pancake ice

Predominantly circular pieces of ice from 0.3–3 m in diameter, and up to about 10 cm in thickness, with raised rims due to the pieces striking against one another. It may be formed on a slight swell from grease ice, shuga or slush, or as a result of the breaking up of ice rind, nilas, or under severe conditions of swell or waves, grey ice. It also sometimes forms at some depth, at an interface between water bodies of different physical characteristics, and floats to the surface. It may rapidly cover wide areas of water.

Polynya

Any nonlinear-shaped opening enclosed in ice. Polynyas may contain brash ice or be covered with new ice, nilas or young ice. If it is limited on one side by the coast, it is called a 'shore polynya'; if it is limited by fast ice, it is called a 'flaw polynya'. If it is found in the same place every year, it is called a 'recurring polynya'.

Pressure ridge

A general expression for any elongated (in plain view) ridge-like accumulation of broken ice caused by ice deformation.

Rafting

Process whereby one piece of ice overrides another. Most obvious in new and young ice, but common in ice of all thicknesses.

Ridging

The process whereby ice is deformed into ridges.

Rubble field

An area of sea ice that has essentially all been deformed. Unlike hummock field, does not imply any specific form of the upper or lower surface or the deformed ice.

Second-year ice

Ice which has survived only one summer's melt. Because it is thicker and less dense than first-year ice, it stands higher in the water. In contrast to multi-year ice, second-year ice during the summer melt shows a regular pattern of numerous small puddles. Bare patches and puddles are usually greenish blue.

Shear zone

An area in which a large amount of shearing deformation has been concentrated.

Shore lead

A lead between pack ice and the shore or between pack ice and an ice shelf or a glacier.

Shuga

An accumulation of spongy white ice lumps a few centimetres across, formed from grease ice or slush and sometimes from anchor ice rising to the surface.

Slush

Snow which is saturated and mixed with water on land or ice surfaces, or forms as a viscous mass floating in water after a heavy snowfall.

Snow ice

The equi-granular ice that is produced when slush freezes completely.

Young ice

Ice in the transition stage between nilas and first-year ice, 10–30 cm thick. May be subdivided into grey ice and grey-white ice. The expression young ice is also commonly used in a more general way to indicate the complete range of ice thicknesses between 0 and 30 cm (as in 'the formation and growth of young ice'). Usually, these differences in meaning are clear from the context of the discussion.

